Establishment of a CRISPR-Cas9 System for Promoter Recombination in *Cryptococcus deneoformans*

A thesis presented to the Faculty of the Graduate School of Western Carolina University in partial fulfillment of the requirements for the degree of Master of Science in Biology

By

Jack S. Evans II

Director: Dr. Indrani Bose

Associate Professor of Biology

Biology Department

Committee Members: Dr. Amanda Storm, Biology

Dr. Robert Youker, Biology

TABLE OF CONTENTS

LIST OF TABLES……IV
LIST OF FIGURES ……..……....V
LIST OF TERMS/ABBREVIATIONS……VII
LIST OF ABBREVIATED GENES……...……VIII
ABSTRACT……..……IX
Chapter I. INTRODUCTION ……...……..1
1. *Cryptococcus neoformans* – Description and significance……1
2. Gene manipulation in *Cryptococcus* – Transformation and genetic functionalization……3
3. *Cryptococcus* and CRISPR-Cas9 – Description and significance……7
Chapter II. MATERIALS AND METHODS ……...13
1. Fungal cultures used and growth conditions ……13
2. Bacterial cultures used and growth conditions ……...…..13
3. Plasmid 'MiniPrep' extraction and purifications. ……....14
4. *Cryptococcus* genomic sequence acquisition……...…..14
5. Genomic DNA extraction from *Cryptococcus*……....14
6. PCR amplification and purification of modular gene expression cassette reagents……..15
a. Amplification of *CTR4p*, *NEO*^{R}, and *GFP*……15
b. Amplification of *CnMIP1* MLS*, CnCYC1t, CnURA5t, and CdMIP1 fragments* …….16
7. Ligation of modular gene expression cassettes using T4 DNA ligase……...17
8. Sanger sequencing……...……..18
9. sgDNA crRNA sequence acquisition and *in silico* evaluation……..19
10. Acquisition of *GDP-CAS9* and sgDNA scaffold vectors……19
11. PCR amplification and purification of sgDNA scaffold, *CdU6p*, sgDNA, and *CAS9*……20
12. PCR assembly of *C. deneoformans* HDR templates……21
a. Amplification of homology arms for HDR templates……...22
b. Amplification of cassettes for HDR templates…….……23
c. Overlap PCR to assemble HDR templates……24
13. Transformation of *C. deneoformans* via electroporation……26
14. PCR Assays of *URA5* and *MIP1*……27
15. *GFP* expression tracking with EVOS Widefield fluorescent microscopy……..29
Chapter III. RESULTS……..….31
1. Construction of a series of modular gene cassettes for *Cryptococcus*……...31
a. Design and assembly of a modular gene cassette for homology-driven recombination…31
b. Addition of a putative MLS from *CnMIP1* into SpeI site of the modular gene cassette...35
c. Creating modular gene cassettes with terminator fragments……37
d. Creating a *NEO*^{R}*-CTR4p-CdMIP1* N-terminal fragment cassette……42
2. CRISPR-Cas9 in the yeast, *C. deneoformans*……..45
a. Design and assembly of cryptococcal *CAS9* and *URA5*-targeting sgDNAs……45
b. Disruption of *URA5* with CRISPR-Cas9 mediated NHEJ……49
c. Insertion of the modular gene cassette into *URA5* with CRISPR-Cas9 by using sequence homology……..57
3. Conditional regulation of *CdMIP1* via CRISPR-Cas9-mediated promoter replacement…….63
a. Design and assembly of CRISPR-Cas9 sgDNAs targeting the *MIP1* 5' UTR……64
b. Insertion of a modular gene cassette into the *MIP1* 5' UTR……65
Chapter IV. DISCUSSION AND FUTURE DIRECTIONS……71

1. The *URA5* gene was edited *in vivo* via CRISPR-Cas9 induced damage followed by NHEJ mutagenesis and HDR-mediated recombination……...71
2. CRISPR-Cas9 crDNAs must be 20nt and not have complement covering targeted PAM……...74
3. A modular gene cassette was assembled and tested……..…76
4. *MIP1* might not be a necessary gene or the *CnCTR4p* construct may be 'leaky.'……....77
REFERENCES ……..…80
APPENDIX ……...87
1. Primers used in project……...87
2. Plasmids used in project…….89
3. Alignment data……...90
   a. sg265 BLO260 F……..90
   b. pIBB326 *NEO*^{R} BLO291 F ……...91
   c. pIBB326 *NEO*^{R} BLO292 R..……92
   d. pIBB326 *CTR4p* BLO293 F……93
   e. pIBB326 *CTR4p* BLO294 R ……94
   f. pIBB326 GFP BLO295 F ……95
   g. pIBB326 GFP BLO296 R……96
   h. +MLS pIBB327 BLO318 R……97
   i. +MLS pIBB327 BLO311 F……97
4. Design and assembly of telomeric cassette-terminator constructs…….98
5. CRISPR-Cas9 targeting *URA5* with *NEO*^{R} cassette; trial experiment……99
   a. Design and assembly of *NEO*^{R} HDR reagents ……99
   b. HDR disruption of *URA5* with CRISPR-Cas9……100
6. Fluorescent microscopy of transformed *C. deneoformans*……..105
   a. Screening for episomal *GFP* expression……105
   b. Screening for chromosomal *GFP* expression……106
   c. Screening for episomal telomeric *GFP* expression……107

LIST OF TABLES

Table 1. Phenotypes of *URA5* NHEJ CRISPR.……52
Table 2. Phenotypes of *URA5* excision HDR CRISPR…….61
Table 3. Genotypes of *URA5* excision HDR CRISPR……...63
Table 4. Phenotypes of *MIP1p* replacement HDR CRISPR……..67
Table 5. Genotypes of *MIP1p* replacement CRISPR…….70
Table 6. Phenotypes of *URA5* preliminary HDR CRISPR trial ……..102
Table 7. Genotypes of *URA5* preliminary HDR CRISPR trial ……...103

LIST OF FIGURES

Figure 1. CRISPR locus from *S. pyogenes*……7
Figure 2. Base schematic for modular gene expression cassettes designed in this project.…..…31
Figure 3. Schematic for synthesized modular gene cassette ….……32
Figure 4. Purified *CTR4p*, *NEO*^{R}, and GFP……...33
Figure 5. Double digests of pIBB326 vectors. (A) HindIII-XbaI. (B). HindIII-BamHI. (C) BamHI-SpeI. (D) SpeI-XbaI. …….……...33
Figure 6. Plasmid map of the cassette plasmid pIBB326……..34
Figure 7. Plasmid map of the +MLS cassette plasmid pIBB327……...35
Figure 8. MLS orientation PCR assays. (A) MLS-GFP assay. (B) *CTR4p*-MLS assay……...36
Figure 9. Plasmid maps of terminator-containing cassette plasmids. (A) +MLS,+*URA5t* pIBB328. (B) +MLS,+*CYC1t* pIBB329. (C) +*URA5t* pIBB331. (D) + *CYC1t* pIBB332….……38
Figure 10. NdeI digests of pIBB329 and pIBB332 (A) Cassette schematics (B) Digest assays...39
Figure 11. PCR assay for +MLS,+terminator cassette orientation. (A) Schematics. (B) PCR assays…….40
Figure 12. Confirming constructs pIBB331 and pIBB332. (A) Schematics. (B) NdeI-SalI digest assay. (C) PCR Assays……..41
Figure 13. Plasmid map of the +*MIP1 Nterm* cassette plasmid pIBB333/334……..43
Figure 14. Confirming construct pIBB333/334. (A) Schematics. (B) ScaI digest assay. (C) PCR Assay…….44
Figure 15. *URA5* CRISPR-Cas9 system used in this project. (A) Diagram of *URA5* with annotated cut sites. (B) Schematic of cryptococcal sgDNA sequence. (C) pXL1 plasmid map with annotated *CAS9* gene and gel. …….……47
Figure 16. Sequence comparison of sg265 and 328 crDNAs ……..…….……48
Figure 17. *URA5* NHEJ CRISPR electroporation. (A) NEO initial selection plates. (B) Dual phenotype assays ……..……..…..51
Figure 18. *URA5* CRISPR cut-site PCRs. ……53
Figure 19. *URA5* CRISPR cut-site sequencing alignment data…….54
Figure 20. NHEJ CRISPR *URA5* size assays. (A) Schematics. (B)Whole locus. (C). CDS. (D) Cutsite……56
Figure 21. *URA5* excision HDR template assembly. (A) Schematics. (B) Arm synthesis. (C) cassette synthesis. (D) Purified product…….58
Figure 22 *URA5* excision HDR CRISPR electroporation. (A) NEO vs. 5-FOA initial selection plates. (B) Dual phenotype assay…….……60
Figure 23. Cassette insertion assays. (A) PCR assay of *URA5* locus. (B) PCR assay for *CTR4p* insertion……..62
Figure 24. Homology-driven recombination between a replacement promoter cassette and *MIP1*. (A) Schematic. (B) crDNA sequences.……..65
Figure 25. *MIP1p* replacement HDR CRISPR electroporation. (A) Initial selection plates. (B) Dual phenotyping assays. (C) Irregular colony v. WT..……67
Figure 26. *MIP1* genotype assays. (A) Schematics. (B) Locus size assay. (C) *CTR4p* insertion assay.……69
Figure 27. Digests assays of the pIBB207-cassette-terminator constructs. (A) SalI digests. (B) KpnI digests……...…98
Figure 28. *NEO*^{R} preliminary *URA5* HDR trial reagents. (A) Schematics. (B) Reagent PCRs and template assembly.……..…100

Figure 29. *NEO*^{R} preliminary *URA5* HDR trial electroporation ……102
Figure 30. *URA5* preliminary HDR trial PCR screening for recombination. (A) Recombination schematic. (B) Locus amplicon size assay. ……104
Figure 31. Epsiomal GFP assay with +*CYC1t* and +MLS,+*CYC1t* vectors ……106
Figure 32. Telomeric GFP assay with +*CYC1t* and +MLS,+*CYC1t* vectors ……107

LIST OF TERMS/ABBREVIATIONS

dNTP	Deoxynucleotide triphosphate
gDNA	Genomic DNA
JEC21 matα	*C. deneoformans* Serotype D strain, mating type alpha
KN99 matα	*C. neoformans* Serotype A strain, mating type alpha
mpH2O	Millipore ultra-purified water
DTT	Dithiothreitol
YPD	Yeast Extract, Peptone, Dextrose
LB	Lysogeny Broth
LA	Lysogeny Agar
SDS	Sodium Dodecyl Sulfate
EDTA	Ethyleneidaminetetraacetic acid
BCS	Bathocuproine disulfonate disodium salt
$CuSO_4$	Cupric sulfate
G418/NEO	Geneticin, AKA neomycin
5-FOA	5-fluoroorotic acid
KAN	Kanamycin
AMP	Ampicillin
DSB	Double-stranded DNA break
ORF	Open-reading frame
CDS	Coding sequence
UTR	Untranslated region
MLS	Mitochondrial Localization Signal
NLS	Nuclear Localization Signal
TEL	Telomeric construct

LIST OF ABBREVIATED GENES

MIP1	DNA polymerase Gamma gene
CTR4	Copper Transporter 4 gene
GFP	Green Fluorescent Protein
mCherry	Monomeric Cherry
URA5	Orotodine 5' phosphate decarboxylase gene
MAT	*C. neoformans* Mating Type
GPD	Glyceraldehyde-3-phosphate dehydrogenase
U6	U6 RNA gene
TPS	Trehalose-6-phosphate synthase
SV40	Simian Virus 40 T-antigen gene

ABSTRACT

ESTABLISHMENT OF A CRISPR-CAS9 SYSTEM FOR PROMOTER RECOMBINATION IN *CRYPTOCOCCUS DENEOFORMANS*
Jack Slade Evans II, Master of Science in Biology
Western Carolina University (Date 07/20/21)
Director: Dr. Indrani Bose

Cryptococcus deneoformans is a basidiomycetous yeast found in multiple habitats across the globe. The species is a causative agent of cryptococcosis, a disease in which the inhalation of spores leads to fungal colonization of the lungs in various hosts. Cryptococcosis may also progress to other organs, notably the brain, which can result in cryptococcal meningoencephalitis. Unchecked cryptococcal disease is invasive, disruptive, and highly lethal, resulting in 13%-73% mortality rates despite treatment and 100% mortality when left untreated. Treatment options for cryptococcal disease are limited, especially in underdeveloped countries bearing the brunt of cryptococcal mortality due to lack of effective antifungal drugs.

The search for drug targets in the *C. neoformans* species complex is being driven by molecular research into conserved proteins, many of which play key roles in cell survival and/or virulent processes. Studying the function of such proteins often requires complex genetic manipulations either *in vitro* or *in vivo*. This thesis aimed to test a CRISPR-Cas9 gene editing system in *C. deneoformans* that could be used to induce damage in precise gene targets, and also design a modular gene cassette that could recombine at those damaged sites by manipulating the endogenous DNA repair mechanisms of the cell. Editing was successfully accomplished in the *URA5* gene by disrupting and later excising the coding region by homology-driven recombination with a modular gene cassette. In addition, the promoter region of the DNA polymerase gamma gene, *MIP1,* a putative essential gene, was replaced with a copper-repressible promoter*, CTR4p*, to attempt to convey evidence for its necessity and suitability as a drug target.

CHAPTER I. INTRODUCTION

1. *Cryptococcus deneoformans* – Description and significance

The *Cryptococcus neoformans* species complex comprises seven species of basidiomycetous, medically relevant yeast.[1,2] These species are the flagbearers for the *Cryptococcus* genus, which contains more than 30 species.[3] The most clinically significant species of the complex are *C. deneoformans, C. neoformans,* and *C. gatti*. These organisms typically exist as single-celled, budding yeasts and are obligate aerobes. Under certain conditions, they can enter a sexual state in which hyphal structures and basidospores form.[4] These species have two mating archetypes (*MAT*), a and α; each operating in the fungus akin to opposing 'sexes.' Mating type is determined by approximately 20 genes and restricts sexual recombination to mutually exclusive *MAT* strains. These yeasts also exude a polysaccharide capsule that can vary in glycan content such that they can be classified into five distinct antibody response types, or serotypes – A, AD, B, C, and D.[5] These serotypes were previously used to distinguish different subvarieties of *C. neoformans* that have now been segregated into seven species. Those serotypes largely coincide with some species: A and AD are found predominantly in *C. neoformans*, D in *C. deneoformans*, and B and C in *C. gatti.*[1]

C. deneoformans (and also *C. gatti* and *C. neoformans*) have a series of notable characteristics that contribute to an opportunistic virulence in a variety of mammals, humans included.[3] Some of these major characteristics include: the potential for melanin production, the capacity to survive at 37°C, and the presence of a complex extracellular polysaccharide capsule. *C. deneoformans* and its sister species induce Cryptococcosis, which manifests as a respiratory infection wrought by inhalation of cryptococcal basidiospores and/or heavily desiccated cells.[6] This tends to be an asymptomatic infection following exposure to guano-contaminated

environments and/or flora. In most cases, the disease is either cleared by the host adaptive immune response or becomes asymptomatically latent. However, in the immunocompromised, this disease induces pulmonary symptoms as the yeast population goes unchecked. Most concerningly, this may lead to fungal sepsis as the yeast disseminates into the bloodstream from the lungs. Once systemic, cryptococcosis can manifest in various organs – notably the central nervous system. While the yeast cannot normally cross the blood-brain-barrier, *MATα* strains can manipulate endothelial cells to enter the brain, inducing a unique, highly lethal neurological disease, cryptococcal meningoencephalitis.[3,7]

Cryptococcal diseases are concerning due to poor patient outlook and limited treatment options. Without proper care, prognosis is dire. Non-treatment mortality rates of 100% have been observed within two weeks of clinical presentation. Primary chemotherapeutic regimens typically involve amphotericin B deoxycholate, fluconazole, flucytosine, and intraconazole. These drugs reliably reduce patient cryptococcal load; however, the treatments have few alternatives and can cause severe complications. Novel therapeutic options are needed given the risk of emerging, resistant cryptococcal strains and the complications posed by current treatments.[8] Antimicrobial design revolves around the discovery of 'drug targets', which are typically gene products that are essential to the microbe's survival and/or virulence in the host. Such cellular components are usually unique elements that distinguish it from humans. Essential genes can sometimes be difficult to delete for experimental study due to the important roles they play in the life of the microbe. An example of a drug target is ergosterol, a unique fungal sterol that integrates into fungal membranes and is required for proper fungal growth. The molecule and its underlying biosynthetic pathway are essential for fungal virulence trans-taxa, and as such, both the sterol and the underlying synthase enzymes can be considered drug targets.[9]

Amphotericin B is a drug that binds ergosterol and induces perforation of the fungal plasma membranes, ultimately killing the cell via cytoplasmic exsanguination. While it is effective against fungal pathogens like *C. deneoformans*, the similarity of the structure of ergosterol to mammalian sterols presumably contributes to the severe side-effects it causes in humans.[10, 11] Amphotericin B is, consequently, far from an ideal drug and is reserved for critical scenarios. However, as mentioned above, there are few alternatives for culling fungal pathogens in humans; hence the need for new drugs and drug targets. One method of studying a gene products's candidacy as a drug target is by silencing the underlying gene's expression by repressing its promoter in a conditional manner. For some drug targets, this can be the only method of showing essentiality due to the deleterious effects caused by lacking the gene product.[3] Accordingly, promoter replacement is a useful technique to show the essentiality of a gene. That being said, gene necessity does not universally correlate to drug target candidacy. A drug target must be sufficiently different from any orthologous gene products in the host to minimize side-effects posed to the host. An ideal drug target is one that is necessary and has no similar components in humans. In order to probe for said drug targets, genetic manipulation is a primary method.

2. Gene manipulation in *Cryptococcus* – Transformation and genetic functionalization

The *C. neoformans* species complex has been extensively researched over the last century, establishing these yeasts as robust model organisms for molecular study.[4, 6] Genomic data on *C. neoformans* and *C. deneoformans* is readily available due to whole-genome sequencing. Significant study into virulence mechanisms and mating types has additionally contributed to a rich literature on cryptococcal biology.[4] The richness in literature alongside the

ease of culturing these free-living haploid yeasts gives researchers plentiful opportunities to probe cryptococcal genes for clinical relevance at both the *in vitro* and *in vivo* level. *In vivo* studies on cryptococcal gene function have been spearheaded by site-specific mutagenesis techniques.[12, 13] To accomplish this, two transformation approaches – biolistics and electroporation – have been the primary methods to introduce gene editing systems into the yeasts.[13, 14, 15] These systems typically insert exogenous DNAs by inducing damage in the genome that then activates the cell's DNA repair mechanisms. This helps integrate the sequences into chromosomes in a relatively predictable, replicable manner. Such systems can be used to facilitate both gene knock-out or gene knock-in, allowing for a gene's role in the fungal phenotype to be assayed by the presence or absence of the encoded protein or RNA.[13]

Biolistic techniques have, until recently, been the go-to transformation method for *Cryptococcus* when seeking genomic integration of constructs.[13] It features a combined exogenous DNA-delivery and endogenous DNA-damaging mechanism whereby DNA-coated microparticles are ballistically projected into living cells. These microparticles penetrate the yeast's nucleus and induce chromosomal damage via the force of the collision.[15] Although a reliable means of delivering DNA-based editing systems, transformation via biolistics carries a risk of producing unstable transformant strains. The instability is likely caused by a randomness of damage sites and high rates of episomal DNA expression.[4,13] Further, biolistic approaches also tend to be hampered by the need for expensive equipment that is not readily available to most institutions.[16]

Electroporation protocols were developed at a similar time to biolistics and posed themselves as relatively low cost transformation systems with comparable potential for *en masse* DNA delivery.[17] Both systems can introduce large amounts of DNA into cryptococcal cells and

induce a variety of phenotypes. However, electroporation has a significantly reduced recombination efficiency relative to biolistics. Biolistic transformations across the *C. neoformans* species complex typically have a 1-10% recombination efficiency, with the rate increasing to a range of 2-50% in the *C. neoformans* species specifically. Electroporation on the other hand produced a 10^{-5} – 10^{-3}% frequency when using similar systems, presumably caused by not inducing DNA damage during transformation.[13] Despite the general inefficiency of electroporation in facilitating genomic integration, the ability to pair this with methods that can cause DNA damage by more precise mechanisms than biolistics have revitalized the technique. Targeted DNA damaging systems can be used to improve recombination rates, thereby alleviating electroporation's aforementioned shortcomings. One method of creating site-specific DNA damage is via the use of Clustered Regularly Interspaced Short Palindromic Repeats (CRISPR)-Cas9.[13, 14]

Gene knockout and modification are reliable molecular methods to ascertain gene function in organisms. However, a problem associated with gene knockout studies is the deleterious effect caused by the disruption of an essential gene. One common technique used to get around this problem is the replacement of endogenous promoters by a regulatable promoter. Promoter replacement usually leaves the coding sequence (CDS) of a gene of interest untouched while the upstream regulatory elements are excised and regulatable replacements introduced. This has traditionally been done by assembling an *in vitro* construct that contained the CDS of a gene of interest fused with the 5' untranslated region (UTR) of a regulatable gene, transforming it in, and then screening for gene product activity.[18, 19, 20] However, the development of CRISPR-Cas9 has allowed for promoter manipulation at the chromosomal level *in vivo*.[14, 21] A number of regulatable promoter elements, such as *GAL7p*, *MFA1p*, have been previously identified in *C.*

neoformans and *C. deneoformans* genes. These promoters have been used in various *in vivo* promoter replacement studies.[18,19,20] Of the known conditional cryptococcal promoters, the one used in this study is the promoter of *CTR4* gene (*CTR4p*).

The *CTR4* gene encodes a copper-specific transporter involved in cryptococcal virulence and copper homeostasis.[22,23] The gene's expression is regulated akin to the *CTR4p* mechanism studied in the fission yeast, *Schizosaccharomyces pombe*.[24] In *S. pombe*, *CTR4* transcription is regulated by upstream interactions with Cuf1, an innate transcription factor and sensor for intracellular copper concentrations.[25] When intracellular copper ion concentrations are high, Cuf1 binds the ions and becomes conformationally inactive. When copper concentrations are low, Cuf1 becomes conformationally active and binds to copper-sensing elements (CuSE) in the genome. When Cuf1 interacts with a CuSE, downstream genes like *CTR4* become upregulated, presumably as a long-term response to low copper in the cytosol.[24,25] Ory *et al*. found that *CnCTR4p* also contain CuSE-like sequences and can be used to manipulate recombinant gene expression in *C. neoformans.*[18] Waterman *et al.* demonstrated that a series of virulent *C. neoformans* Serotype A strains contained a Cuf1 homolog that manipulates *CTR4* expression based on copper availability.[24] This homolog effectively regulates the gene akin to *SpCTR4*. Ory *et al.* further demonstrated that *CnCTR4p* can induce altered regulation via a copper-dependent mechanism in modified genes transformed into *C. neoformans* and *C. deneoformans.* However, transcriptional expression from the *CnCTR4p* constructs was unstable as the plasmids lacked a cryptococcal origin of replication, ultimately meaning the plasmids were not maintained *in vivo*. Integrating the construct in the genome could rectify this problem. Therefore, *CnCTR4p* could be used to control chromosomal genes in a regulatable manner when used with recombination-inducing gene editing systems. This would allow for the knocking-down of genes by

manipulating the environmental conditions of the cell, which facilitates the investigation of gene essentiality without having to rely on plasmid constructs. CRISPR-Cas9 is one such tool that can be used to facilitate recombination in the cryptococcal genome.

3. *Cryptococcus* and CRISPR-Cas9 – Description and significance

CRISPR-Cas9 is a relatively simple, programmable gene editing system derived from an adaptive immune response in the bacterium *Streptococcus pyogenes*.[26] In its original form, CRISPR-Cas9 recognizes and damages invading bacteriophage DNA by using an RNA guidance system. This system is produced from a genetic array of partial gene sequences derived from viral DNA. Those arrays arise from prior bacteriophage attacks and get transcribed into CRISPR RNAs (crRNA) that are complementary to a sequence in the injected viral genome. The locus also contains a gene for CRISPR-associated protein 9 (*CAS9*), an endonuclease capable of inducing double-stranded DNA (dsDNA) breaks some three or four base pairs away from an NGG sequence called a Protospacer Adjacent Motif (PAM). Cas9 does not bind to DNA on its own and requires a conserved trans-activating RNA (tracrRNA) to activate and guide the enzyme to it crRNA-designated target.

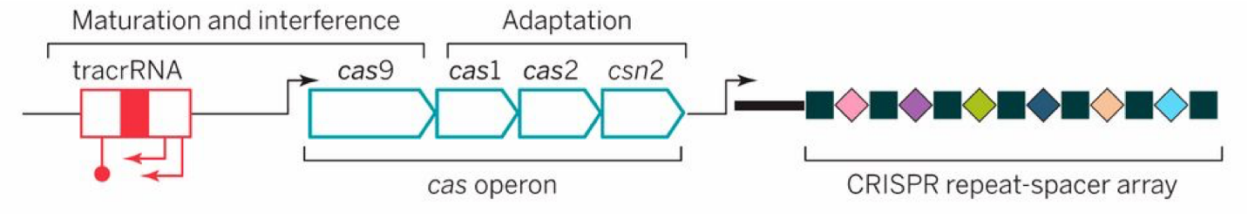

Figure 1 – CRISPR locus from *S. pyogenes*. The tracrRNA is produced from a single gene upstream of the *cas* operon, which itself is upstream of the crDNA array. Each repeat in the array is derived from partial viral DNA sequences and conveys a form of adaptive immunity against previously encountered bacteriophage invasions. (From Doudna and Charpentier (2014))[16]

The tracrRNA acts as a bridge between the Cas9 endonuclease and the crRNA-DNA complex. To facilitate the formation of a protein-RNA-DNA complex, the tracrRNA contains a Cas9 binding sequence and also a complementary stretch to the crRNA. This complementation allows the two RNAs to bind together and form a RNA-protein complex with Cas9. Thereby, the crRNA-viral DNA complex is bridged to the RNA-Cas9 complex via the tracrRNA. The fully assembled DNA-RNA-protein complex induces dsDNA breaks in the viral DNA and adaptively switches guides to target different sequences in the viral genome. The crRNAs target DNAs that have a PAM just off its 5' end of the complementary sequence; this is because the PAM is absolutely necessary for appropriate Cas9 activity. Therefore, crRNAs must target sequences with an adjacent PAM in order to be effective. Ultimately, the CRISPR activity results in degradation of the infecting DNA, averting lytic or latent bacteriophage infection cycles. [26,27]

CRISPR-Cas9 has been adapted for eukaryotic use by expressing the *CAS9* gene using species-specific promoters.[27] Synthetic tracrRNA-crRNA fusions, acting as single guide RNA sequences (sgRNAs), can then be supplied – typically co-transformed alongside the modified *CAS9*, such that precise DNA damage can be induced by the translation products. Accordingly, only those two genes are then needed for CRISPR-Cas9 activity. This system is easy to program, easy to transform, and capable of multiplexed targeting of PAM-adjacent DNA sequences in *in vivo* experiments.[28]

CRISPR-Cas9 has become a recent utility in cryptococcal gene manipulation thanks to its ability to drive homology-directed DNA repair. In other yeasts such as *Saccharomyces cerevisiae*, vector systems have been developed whereby exogenous DNA can be cloned and propagated in the yeast using plasmids with an inserted origin of replication.[29] These plasmids avoid the expression instability exhibited by plasmids transformed into the *C. neoformans*

species complex presumably because they are maintained in *S. cerevisiae* and not *C. neoformans*. At present, inserting a cryptococcal origin of replication into a plasmid is unfeasible given its large size.[30] As such, a stable plasmid system in cryptococcal species is not yet viable. Consequently, the best means of improving expression stability is by inserting exogenous DNA into the cryptococcal genome. This has traditionally been done by homology-driven recombination using homologous repair templates and biolistics.

The *C. deneoformans* and its sister species do not readily uptake foreign DNA like *S. cerevisiae*. Insertion of DNA in *Cryptococcus* requires the manipulation of the organisms' DNA repair mechanisms to facilitate chromosomal recombination. That being said, it has been found that there is a chance for off-target recombinations between the chromosomes and nonhomologous DNAs. These tend to occur when using biolistic transformations, which carries a risk of random genomic damage due to the violence of the mechanism. There is some debate as to how extensive this is but the risk is present none-the-less.[31] To achieve targeted recombination in cryptococcal cells, homologous sequences can be attached to the flanks of a recombinant DNA fragments to facilitate homology-driven recombination.[14] To further improve targeted recombination between the cryptococcal genome and exogenous DNA, it was found that disabling the organism's non-homologous end joining (NHEJ) repair mechanism improves faithful insertion. NHEJ knockout strains were created by knocking out Ku70 and Ku80 gene function, thereby forcing the yeast to rely on homology-driven repair alternatives.[32] Homology-driven DNA repair is highly accurate and site-specific due to the system's reliance on repair templates with significant homology to the damaged site. Accordingly, targeted DNA damage, such as that derived from CRISPR-Cas9, can be used to drive DNA repair in *Cryptococcus*.

As an alternative to Ku-knock out and artificial chromosome engineering, CRISPR-Cas9 has been used to facilitate site-specific recombinations without using biolistic transformation. DNA breakage has been found to correlate to the insertion of exogenous DNA into the cryptococcal genome, meaning that targeted damage can be used to improve genomic recombination.[31] CRISPR-Cas9 is an adaptive DNA damaging system that can precisely damage chromosomes at specific sites. The damage necessitates repair, which researchers can manipulate to insert DNA into the chromosome.[14,27] Thereby, CRISPR-Cas9 is being used to improve recombination in *C. deneoformans* by allowing researchers to take advantage of non-homologous and homology-driven DNA repair.[14,33]

CRISPR-Cas9 has been shown to be a novel, precise technique for targeted DNA damage in *Cryptococcus* while also revitalizing electroporation. By pairing electroporation with a 'programmable' DNA damaging system, homology-drive recombination with exogenous constructs has been shown by Fan and Lin (2018) to be more efficient than biolistics across *C. neoformans* and *C. deneoformans*.[14] Recombination efficiencies targeting *CnADE2* have reached nearly 50% in wildtype strains, matching the effectiveness of contemporary biolistic techniques.[13,14] The procedure, Transient CRISPR-Cas9 Coupled with Electroporation (TRACE), was a modification of a transient CRISPR-Cas9 system developed for *Candida albicans*.[34] TRACE induces homology-driven recombination by co-transforming CRISPR constructs that are unstably expressed alongside a recombination template for a gene of interest. NHEJ still occurs in this system, though homology-directed DNA repair becomes the predominant mechanism of cryptococcal DNA repair. Thus, NHEJ knock-out is not required and recombination between the chromosome and construct(s) readily occurs. The CRISPR-system is presumed to quickly degrade due to lack of replicative origins and telomeres in the transformed constructs.[13,16,35] This

degradation prevents long-term expression of the CRISPR-Cas9 DNAs, which is thought to confer a risk of off-target DNA damage.[14,16] Accordingly, these transient CRISPR systems may mitigate potential off-target DNA damage caused by constitutive over-expression. The extra-chromosomal nature of the aforementioned constructs is, in theory, unable to recombine with the genome, thereby allowing the instability of the episomal DNAs to work in the method's favor. Transient CRISPR systems can be used to induce high rates of chromosomal integration of co-transformed homologous constructs.[13,16] Fan and Lin used a single gene disruption to test their constructs.[14] In this project, I have used a modified version of their TRACE system to target other genes in *C. deneoformans* to test the validity of the system, and to expand its utility by integrating a promoter replacement mechanism along with a fluorescent tag.

The aims of this project were as follows:

(I) Construct a series of modular gene cassettes that may be used episomally or for chromosomal insertion.

(II) Establish a transient CRISPR-Cas9 system capable of disruption of the *URA5* gene.

(III) Use the transient CRISPR-Cas9 system developed in (II) to replace the endogenous *MIP1* promoter with a conditional alternative.

Aim I sought to design and assemble a series of constructs containing a regulatable promoter and a fluorescent tag that could be modified easily to control various aspects of the expression of a gene of choice. Aim II sought to establish a DNA editing system that can reliably and cheaply induce targeted DNA damage in *C. deneoformans* such that constructs like those assembled in Aim I can be recombined with chromosomal targets. Aim III sought to modify the presumably constitutive expression of *MIP1* such that its putative essentiality could be demonstrated while

also demonstrating that the DNA editing system developed in Aim II could be used to modify the regulatory elements outside of genes. The CRISPR-Cas9 system developed in Aim II will be used in future studies of gene function via the aforementioned recombination of chromosomal targets by modifying the constructs derived from Aim I with flanking sequences homologous to various portions of targeted loci to induce gene disruption, excision, or knock-in.

CHAPTER II. MATERIALS AND METHODS

1. *Fungal cultures used and growth conditions.* *Cryptococcus deneoformans* JEC21 MAT-α (Serotype D, IBCN43) was used for CRISPR-Cas9 validation in Aim II and III experiments. *C. neoformans var. grubii* KN99 MAT-α (Serotype A, IBCN2) was used as a genomic source for fragments in Aim I experiments. Stock strains were cultivated on Yeast Extract-Peptone-Dextrose (YPD) agar and in broth cultures (Yeast Extract 10g/L, Tryptone 20g/L, Dextrose 20g/L) at 30°C with 1-2 and 2-3 day incubation times respectively. Broth cultures were incubated at 30°C using a shaking incubator at 200RPM. Cultures were supplemented with 100mg/mL ampicillin to select for fungal growth. Cultures transformed in Aim II were supplemented with 100mg/mL G418 to select for NEO^R expression and then restreaked onto 5-fluoroorotic acid (5-FOA). 5-FOA plates were comprised of: 50mL Yeast Nitrogen Base w/o amino acids (BD 291940) (Base 6.7g/0.1L), 5µg/mL adenine (1mL of 5mg/mL per 100mL), and 1.2µg/mL uracil (600µL of 2mg/mL per 100mL) agar supplemented with 50mL 1mg/1mL 5-fluoroortic acid (100mg/100mL), 4% dextrose (Mallinckrodt 3908-04), and 5µM sodium hydroxide (Fisher S320-500). Cultures transformed in Aim III were supplemented with 100mg/mL G418 and 400mg/mL BCS (Fisher Scientific AC164060010) but then restreaked onto YPD with 25µM $CuSO_4$ (Thermofisher BP346) and 1mM ascorbic acid (Sigma-Aldrich A7506).

2. *Bacterial cultures used and growth conditions.* *Escherichia coli* NEB 5- α High Efficiency Competent cells (New England Biolabs [NEB] C2987I) were used for most Aim I cassette cloning transformations. The NEO^R-*CTR4p-MIP1 Nterm* plasmid; that construct was transformed into NEB Turbo Competent *E. coli* (NEB C2984I). All strains were cultivated on Lysogeny agar (LA) and broth (LB) cultures (Yeast Extract 5g/L, Tryptone 10g/L, NaCl 10g/L) at 37°C with ~24-hour incubation times. Broth cultures were incubated at 37°C using a shaking

incubator at 225RPM. Cultures transformed in Aim I were supplemented with 100µg/mL ampicillin and or kanamycin to select for constructs being cloned.

3. *Plasmid 'MiniPrep' extraction and purification.* Propagated plasmids were extracted from *E. coli* hosts via the WizardPlus SV Minipreps DNA Purification System using a Quick Centrifugation Protocol.[36] Success was gauged by 0.8% TAE-agarose ethidium bromide gel electrophoresis and purifications were stored at -20°C.

4. *Cryptococcus genomic sequence acquisition.* Gene sequences for *CdURA5*, *CdMIP1*, *CnCTR4p* were obtained using the FungiDB Sequence Retrieval tool. Sequence IDs were CNG03730, CNB00310, and CKF44_00979 respectively. FungiDB Releases 51 and 52 were used over the course of the project.

5. *Genomic DNA extraction from Cryptococcus.* A modified version of the extraction method from Boggs (2017), which was originally described by Bose and Doering (2011), was used for genomic DNA extraction.[37,38] Approximately 3mL of broth culture was inoculated from YPD plates followed by an overnight incubation (~17-20hr) for harvest the next day. Cells were pelleted via centrifugation and resuspended in 0.5mL of Extraction Buffer (500mM Tris-HCl pH8, 20mM EDTA, 1% SDS). 0.5mL of sterile 425-600µm glass beads were then added. The mixtures were agitated for 10 min. at room temperature followed by 3-5 min. intervals until 50-80% cellular lysis was confirmed by compound microscopy. The lysed cells were incubated at 70°C for 10 min., buffered with 0.2mL of 5M potassium acetate and 0.15mL of 5M sodium chloride, and centrifuged for 20 min. at top speed in a microcentrifuge. The supernatant was

removed and mixed with 0.45mL of 99% HPLC-grade chloroform followed by ten minutes of 14.5rpm centrifugation. The aqueous phase was transferred to a separate tube, supplemented with 0.2mL of 30% PEG8000 in 1.5M sodium chloride solution, and incubated on ice for 10 min. The resultant nucleic acid pellet was resuspended in 50µL of ~65°C ultrapure H2O. Successful extractions were confirmed with ethidium bromide 0.8% TAE-agarose gel electrophoresis at 100V for 30 minutes. Extracts were then stored at -20°C.

6. *PCR amplification and purification of modular gene expression cassette reagents.* 1.816kb *NEO*^{R}, 0.650kb *CnCTR4p*, 0.771kb GFP, 0.108kb *MIP1* predicted MLS, and 1.105kb *MIP1* N-terminal fragment sequences were amplified for use as reagents in Methods 7. Primers were used in such a way to insert complementary restriction enzyme sites on each sequence flank. All amplicons were visualized on appropriate TAE-agarose ethidium bromide gel electrophoresis with corresponding DNA ladders. All PCR reactions had a 5µL negative control sample taken from the reaction mixture before template DNA(s) were added. All PCR products were purified using the Wizard Plus SV Gel and PCR Clean-Up System Centrifugation Quick protocol.[39]

6. a. *PCR amplification of CTR4p, NEO*^{R}*, and GFP.* PCR fragments were amplified using either Q5 or Phusion proof-reading (NEB M0530S) polymerases and 2µM dNTPs. The *NEO*^{R}, *CnCTR4p*, and GFP sequences were amplified with 450µM primer concentration and ~2.5-10ng pIBB236 and pIBB314 as templates for *CnCTR4p* and *NEO*^{R}*/GFP* respectively. PCR conditions and primers used were as follows:

Amplicon	Polymerase	Forward and reverse primers (#µM)	Template (2.5 - 10ng)	Conditions
CTR4p	Q5	BLO293/294 (450µM)	pIBB236	98°C for 30s, [98°C for 10s, 63°C for 15s, 72°C for 60s]x28, 72°C for 2', hold at 4°C
NEO^{R}	Q5	BLO291/292 (450µM)	pIBB314	As above
GFP	Phusion	BLO295/296 (450µM)	pIBB314	98°C for 15s, [98°C for 10s, 65°C for 10s, 72°C for 30s]x28, 72°C for 2', hold at 4°C

6. b. *PCR amplifications of CnMIP1 MLS, CnCYC1t, CnURA5t, and CdMIP1 fragments.*

PCR fragments were amplified using Phusion proof-reading polymerases and 2µM dNTPs. The *MIP1* predicted MLS, *URA5t*, *CYC1*t, and *MIP1* 1.105kb N-terminus sequence PCRs used 100-200µM primer concentration and~10-20ng *C. neoformans* KN99 genomic DNA extract as a template. PCR conditions and primers used were as follows:

Amplicon	1M Betaine + 5% DMSO	Forward and reverse primers (#µM)	Conditions

MIP1 MLS	X	BLO311/318 (200µM)	98°C for 30s, [98°C for 10s, 67.2°C [62-69°C Gradient] for 10s, 72°C for 15s]x28, 72°C for 2', hold at 4°C
URA5t	X	BLO319/320 (100µM)	98°C for 30s, [98°C for 15s, 60.4°C [54-62°C Gradient] for 10s, 72°C for 15s]x28, 72°C for 2', hold at 4°C
CYC1t	X	BLO321/322 (100µM)	Same as *URA5t*
MIP1 Nterm	√	BLO337/338 (200µM)	95°C for 30s, [95°C for 15s, 61.3°C [57-62°C Gradient] for 20s, 72°C for 45s]x34, 72°C for 4', hold at 4°C
MIP1 5' UTR arm	√	BLO339/341 (200µM)	Same as *MIP1* Nterm

7. *Ligation of modular gene expression cassettes using T4 DNA ligase.* *C. deneoformans* cassette constructs and modified variants were assembled *in vitro* using T4 DNA ligation. The reagent fragments were assembled into a 3.261kb core cassette that was modified with a variety of modular fragments. Modifications were made in the form of: The putative *CnMIP1* MLS being added just 5' of *GFP*, a STOP-229bp *CnCYC1* terminator (*CnCYC1t*) just 3' of *GFP*, an 215bp STOP-*CnURA5* terminator (*CnURA5t*) just 3' of GFP, and a 1.105kb *MIP1* N-terminal fragment replacing the *GFP* CDS. All ligations were incubated overnight at 16°C.

A 3.261kb *NEO*^{R}*-CTR4p-GFP* gene expression cassette was assembled in a multifragment pCR2.1 TOPO ligation containing a series of double-digested reagents: a HindIII-

BamHI digested 1.817kb *NEO*^{R} gene, a BamHI-SpeI digested 0.650kb cryptococcal *CTR4* promoter (*CTR4p*), and a 0.771kb *GFP* coding frame. Purified sequences were ligated in 1:1 and 1:3 molar vector-to-insert conditions using ~50ng of HindIII-XbaI digested vector alongside a negative control in 20µL reactions detailed below.

To create pIBB327, a SpeI digested 108bp *CnMIP1* predicted MLS fragment was ligated into a Shrimp Alkaline Phosphatase-treated [30min. 37°C; 65°C heat-inactivation for 20min.] pIBB326 construct. Purified sequences were ligated in 1:2 and 1:4 molar vector-to-insert conditions using ~50ng SpeI digested vector.

Two different terminator fragments, *URA5t* (212bp) and *CYC1t* (226bp), were added to the SAP-treated (as above) XbaI site of pIBB327. 1:2 and 1:4 molar vector-to-insert ratios using ~50ng of the digested vector were used. The final plasmids were named pIBB328 and pIBB329/330 respectively.

pIBB331 and pIBB332 respectively contained the No-MLS,+*URA5t* and +*CYC1t* cassettes. They were constructed by removing the MLS fragments from plasmids pIBB328 and pIBB329, which were digested with SpeI such that the MLS was separated from the gel purified vector fragment. ~50ng of the SpeI-digested vectors were self-ligated.

Four plasmids containing an MLS and a terminator were created (pIBB333, 334, 335, and 336) using pIBB207 as template, using the conditions described above.

The *MIP1* N-terminal 1.105kb fragment was inserted into the SpeI and XbaI sites of the pIBB326 plasmid using 1:1 and 1:3 vector to insert molar ratios using ~10ng of digested vector.

8. *Sanger sequencing.* DNA samples were sent to Genewiz for Sanger sequencing. All samples totaled 15µL in volume and were prepared in 8-count PCR tube strips. All DNA for sequencing

was purified and quantified such that 2ng/μL/kb was added to each sample. 25μM primer concentrations were included in all samples.

9. *sgDNA crRNA sequence acquisition and in silico evaluation.* CRISPR-Cas9 sgDNA targets for *URA5* and *MIP1* were found and evaluated for off-target potential, cutting efficiency, and potential problems using the Eukaryotic Pathogen CRISPR guide RNA/DNA Design Tool.[40] All sgDNA search parameters were left default and are as follows: SpCas9 RNA Guided Nuclease (SpCas9: 20nt gRNA, NGG PAM on 3' end selection), microhomology search off, conserved region search off, guide RNA search left default, on-target search parameters left default, off-target search parameters left default, HDR repair template parameters left default, *C. deneoformans* genome selected (Fungi>*C. neoformans* JEC21 FungiDB-26), and *URA5*/*MIP1* FASTA sequences put into the Sequence box. crDNA sequences/candidates were generated and candidates with the highest relative CRISPR efficiency scores used. All generated crDNA sequences are listed by the tool with their targeted PAM included; for sgDNAs made using the BLO264 and 265 bridge primers, this PAM was left in the sequence to generate a 23bp crDNA fragment, for all other sgDNA bridge primers, the PAM was excised/not added into the bridge primer sequence. Retaining the 3nt PAM sequence was found to drastically reduce CRISPR effectiveness as was seen in Results II; optimized sgDNA design requires the sgDNA not having a PAM complement in its sequence.

10. *Acquisition of GPD-CAS9 and sgDNA scaffold vectors.* *GPDp-CAS9* endonuclease was amplified from pXL1-CAS9-HYG while the single guide DNA scaffold (sgDNA) was amplified using plasmid pYF515. These two plasmids were gifts from the Lin lab.[14]

11. *PCR amplification and purification of sgDNA scaffold, CdU6p, sgDNA, and CAS9.* The CRISPR-Cas9 gene editing system was assembled by PCR amplification of the various pieces using Phusion polymerase. All amplicons were visualized on appropriate TAE-agarose ethidium bromide gel electrophoresis with corresponding DNA ladders. PCR reactions had a 5µL negative sample taken from the reaction mixture before template DNA(s) were added. PCR products were purified using the Wizard Plus SV Gel and PCR Clean-Up System.[39]

Reactions for both the 108bp sgDNA scaffold and 275bp *CdU6p* sequences used 2µM dNTP and 200µM primers concentrations (see BLO263/264/265/328/329/330/342/343/344 for sgDNA scaffold forward primers). The *CAS9* reaction was supplemented with 1M Betaine (Sigma B0300-1VL) and sgDNA reaction with 5% DMSO (NEB B0515A) to facilitate proper priming. sgDNAs were assembled by overlap PCR; all others were standard PCRs.[41] The sgDNA scaffold and *CdU6p* reactions used ~2-10ng of pYF515 and 10-30ng of JEC21 gDNA as templates respectively. The *CAS9* reaction used 10-25ng of purified pXL1-CAS9-HYG plasmid as a template. The sgDNA overlap used ~10ng of gel purified *CdU6p* DNA and ~30ng of gel purified sgDNA scaffold, which was a ~1:1 molar ratio, as templates. A temperature gradient program was found to more reliably amplify the sequences relative to a blanket well temperature. The gradient program also allowed the sgDNA scaffold and *CdU6p* PCRs to be run with the same program, hence the Gradient's usage rather than standard temperature setting. 50µL or 100µL reactions were set up depending on the quantity of sgDNA needed; ~1-3µg and 3-5µg were typically purified from each respectively. PCR conditions and primers used are as follows:

Amplicon	Polymerase	1M Betaine + 5% DMSO	Forward and reverse primers (#µM)	Conditions
U6p	Phusion	X	BLO260/261 (200µM)	95°C for 30s, [9t°C for 15s, 58.8°C [50-61°C gradient] for 15s, 72°C for 30s]x34, 72°C for 2', hold at 4°C.
sgDNA scaffold	Phusion	X	[See above]/BLO263 (200µM)	95°C for 30s, [95°C for 15s, 56.7°C [50-61°C gradient] for 15s, 72°C for 30s]x34, 72°C for 2', hold at 4°C.
sgDNA	Phusion	DMSO only	BLO260/263 (200µM)	95°C for 30s, [95°C for 15s, 56.7°C [50-61°C gradient] for 15s, 72°C for 30s]x34, 72°C for 2', hold at 4°C.
CAS9	Phusion	Betaine only	BLO258/259 (250µM)	95°C for 30s, [95°C for 15s, 60°C for 15s, 72°C for 4']x30, 72°C for 10', hold at 4°C..

12. *PCR assembly of C. deneoformans HDR templates.* Phusion overlap PCR was used to assemble the *URA5* disruption, *URA5* excision, and *MIP1p* excision HDR templates. All

amplicons were visualized on appropriate TAE-agarose ethidium bromide gel electrophoresis with corresponding DNA ladders. All PCR reactions had a 5µL negative sample taken from the reaction mixture before template DNA(s) were added. All products were purified using the Wizard Plus SV Gel and PCR Clean-Up System using a modification of the DNA Purification by Centrifugation Quick protocol.[39]

12. a. *Amplifications of homology arm reagents for HDR templates.* The PCRs for the 5' 103bp and 3' 119bp *URA5* CDS, 5' 500bp and 3' 563bp *URA5* CDS, 5' 545bp and 3' 522bp *URA5* UTR, 5' *MIP1* 726bp UTR homology arms used 2µM dNTP and 200-400µM primer concentrations. The *MIP1* arm required 5% DMSO and 1M betaine supplement to properly amplify. ~10-20ng of JEC21 genomic DNA extract was used as a template. PCR conditions and primers were as follows was used:

Amplicon	Polymerase	1M Betaine + 5% DMSO	Forward and reverse primers (#µM)	Conditions
URA5 CDS 103bp 5'	Q5	X	BLO301/306 (400µM)	98°C for 30s, [98°C for 15s, 61.4°C [58-67°C gradient] for 15s, 72°C for 30s]x34, 72°C for 2', hold at 4°C.
URA5 CDS 119bp 3'	Q5	X	BLO302/307 (400µM)	98°C for 30s, [98°C for 15s, 59.8°C [58-67°C gradient] for

				15s, 72°C for 30s]x34, 72°C for 2', hold at 4°C.
URA5 CDS 500bp 5'	Q5	X	BLO301/304 (400µM)	98°C for 30s, [98°C for 15s, 63.5°C [58-67°C gradient] for 15s, 72°C for 30s]x34, 72°C for 2', hold at 4°C.
URA5 CDS 563bp 3'	Q5	X	BLO302/305 (400µM)	Same as 5' 500bp arm above.
URA5 UTR 522bp 5'	Phusion	X	BLO331/333 (200µM)	95°C for 30s, [95°C for 15s, 62°C [60-64°C gradient] for 15s, 72°C for 30s]x34, 72°C for 2', hold at 4°C.
URA5 UTR 545bp 3'	Phusion	X	BLO334/335 (200µM)	Same as 5' 522bp arm above
MIP1p 5' 726bp	Phusion	√	BLO339/341 (200µM)	95°C for 30s, [95°C for 15s, 61.3°C [57-64°C gradient] for 20s, 72°C for 45s]x28, 72°C for 4', hold at 4°C

12. b. *Amplification of cassettes for HDR templates.* The amplifications of 1.895kb NEO^R gene, 3.546kb *NEO^R-CTR4p-GFP-CYC1t*, 3.650kb *NEO^R-CTR4p*-MLS-*GFP-CYC1t*, and 3.635kb *NEO^R-CTR4p-MIP1 Nterm* cassettes used 2µM dNTP and 200-400µM primer

concentrations ~5-10ng of purified plasmids were used as templates: pIBB314 was the template for *NEO*^{R}; pIBB329 and 332 were respective templates for the two +*CYC1t* cassettes; pIBB334 was the template for the *MIP1* Nterm cassette. was used as a template. PCR conditions and primers used were as follows:

Amplicon	Polymerase	1M Betaine + 5% DMSO	Forward and reverse primers (#µM)	Conditions
URA5 CDS cassette	Q5	X	BLO300/303 (200µM)	98°C for 30s, [98°C for 15s, 65°C for 15s, 72°C for 1']x28, 72°C for 4', hold at 4°C
URA5 UTR cassettes	Phusion	X	BLO332/336 (200µM)	95°C for 30s, [95°C for 15s, 62°C [60-64°C gradient] for 15s, 72°C for 80s]x34, 72°C for 6', hold at 4°C
MIP1p cassette	Phusion	√	BLO338/340 (200µM)	95°C for 30s, [95°C for 15s, 62.5°C [60-64°C gradient] for 20s, 72°C for 90s]x30, 72°C for 6', hold at 4°C

12. c. <u>*Overlap PCR to assemble HDR templates.*</u> The amplifications for the 2.117kb and 2.958kb NEO^{R} gene with ~100bp and ~500bp flanks homologous to the *URA5* CDS; 4.543kb *NEO*^{R}*-CTR4p-GFP-CYC1t* and 4.637kb *NEO*^{R}*-CTR4p*-MLS-GFP-*CYC1t* cassettes with flanks homologous to the *URA5* UTRs; and 4.383kb *NEO*^{R}*-CTR4p* cassette with flanks homologous to

the *MIP1* 5' CDS and 5' UTR used 2µM final dNTP and 200µM primer concentrations. ~1-25ng of purified homology arms and ~8-10ng of cassettes were used as templates. PCR conditions and primers are as follows:

Amplicon	Polymerase	1M Betaine + 5% DMSO	Forward and reverse primers (#µM)	Conditions
URA5 CDS disruption 100bp template	Q5	X	BLO306/307 (200µM)	98°C for 30s, [98°C for 15s, 62.3°C for 20s, 72°C for 105s]x28, 72°C for 4', hold at 4°C
URA5 CDS disruption 500bp template	Q5	X	BLO304/305 (200µM)	Same as above
URA5 replacement templates	Phusion	√	BLO331/334 (200µM)	95°C for 30s, [95°C for 15s, 62°C [60-64°C gradient] for 15s, 72°C for 80s]x34, 72°C for 6', hold at 4°C
MIP1p replacement template	Phusion	√	BLO338/339 (200µM)	95°C for 30s, [95°C for 15s, 61°C [60-64°C gradient] for 20s, 72°C for 110s]x30, 72°C for 7', hold at 4°C

13. *Transformation of C. deneoformans via electroporation.* Fresh cultures of JEC21 were grown on YPD from glycerol stocks four days before the day of this protocol; culture freshness was required to minimize the appearance of colonies with spontaneous mutations on nonselective media. Colonies 2 days post-plating were used to inoculate ~15mL (or x3 5mls cultures) of YPD broth; these cultures were then incubated overnight (~17-20hrs). The next morning, cells from this starter culture were used to inoculate a 100mL YPD culture to a density of ~0.2 OD_{600nm}. The culture was incubated for ~4-6hr until an OD of about 0.6-0.7; this correlates to a cell density of $>3.5x10^7$ cells/mL. The 100mL culture was pelleted in an Eppendorf Centrifuge 5810R rotor chilled to 4°C, spinning for 5 minutes at 4000rpm. The pellets were resuspended in ~10mL of chilled ultra-pure H_2O each, pooled, and brought to a wash volume of ~50mL. This wash was pelleted and washed once more as described above. After the second wash, cells were resuspended in ~10mL of Electroporation Buffer ([EB] 10mM Tris-HCl pH7.5, 1mM magnesium chloride, 270mM sucrose), supplemented with 0.2mL of 1M DTT (Fluka Analytical 43816), and then brought to a volume of 50mL with EB buffer. The mixture was incubated on ice for ~10 minutes before being pelleted as described above. The pellet was resuspended in fresh EB before being pelleted a final time. The supernatant was decanted and the pellet was resuspended in the remaining EB into a thick slurry. ~100µL of the slurry was pipetted into UV-sterilized, chilled electroporation 0.2cm gap cuvettes (Bio-Rad 1652082); culture was carefully tapped to the bottom of the cuvette until the entire bottom was coated. 6µL of sample DNA was then added and gently mixed into the culture. Cuvettes were electroporated with a Bio-Rad GenePulser Xcell at 0.5kV, 25µF, and ∞Ω. Time constants of 35-117ms were found to correlate to the best transformations. The cultures were resuspended in 1mL of chilled YPD media and transferred to culture tubes for a 3-hour recovery at 30°C with shaking at 200RPM. Cultures

were then transferred to 1.5mL Eppendorf tubes for pelleting, a 1mL ultra-pure H_2O wash, and resuspended in 0.3mL of ultrapure H_2O. Cells were plated on appropriate selective media and incubated for 2-3 days at 30˚C.

CAS9 and sgDNA PCR products produced in Methods 11 were electroporated into *C. deneoformans*. Quantification was done with the NanoDrop ND-1000 Spectrophotometer and ethidium bromide agarose electrophoresis. Initial trials used 170ng *CAS9* and 100ng sgDNA in ~6µl volumes of ultra-pure water (Appendix 5); all Aim II and III experiments used 1µg and 700ng of *CAS9* and sgDNA, respectively. The DNA was vacuum-dried using an Eppendorf Vacufuge 5301 Concentrator with default conditions at room temperature for 35-60 minutes; dried pellets were then resuspended in 6µL of ultra-pure water. Samples in concentrator were parafilm covered with a small aeration perforation.

For the *URA5* NHEJ experiment, 2µg of the *NEO^R–CTR4p*-GFP-*CYC1t* gene expression cassette was co-transformed with the *CAS9* and sgDNAs for use as a non-homologous drug selection marker. For the *URA5* HDR experiments, 2µg of a 1.895kb NEO^R gene with 5' and a 3' *URA5* homologous sequences and/or *NEO^R-CTR4p-(MLS)-GFP-CYC1t* with 5' 525bp and 3' 502bp *CdURA5* flanks were used as the repair template. For promoter replacement of *MIP1,* 2µg of 4.383kb *NEO^R-CTR4p-CdMIP1 N-term* was used in the electroporation.

14. <u>*PCR Assays of URA5 and MIP1*</u>**.** 5-FOA and NEO resistant colonies were subjected to genomic extraction protocols described in Methods 5 in order to be screened for *URA5* amplicon size. NEO resistant colonies growing on copper-depleted media were similarly extracted from to screen MIP1 amplicon size. This method was used to ascertain successful gene editing using the CRISPR-Cas9 *URA5* and *MIP1p* disruption and excision systems. All amplicons were visualized

on appropriate TAE-agarose ethidium bromide gel electrophoresis with corresponding DNA ladders. All PCR reactions had a 5µL negative sample taken from the reaction mixture before template DNA(s) were added.

The GoTaq PCR kit (Promega catalog M3001) was used to amplify the 1.023kb *URA5* CDS along with some of the 5' UTR to screen for *NEO*^{R} *URA5* disruption template recombination and NHEJ-disrupted locus size. Taq 2x Mastermix PCR kit (NEB catalog M0270L) was used to screen for a variety of targets in *URA5* and *MIP1*: a 383bp *URA5* fragment containing the sg265, 328, 329, and 330 cut sites; a 1.834kb fragment containing the entire *URA5* locus; insertion of *CTR4p* into the *URA5* locus; and insertion of *CTR4p* into the *MIP1* locus. All reactions used 2µM final dNTP and 200µM primer concentrations. ~10-20ng of JEC21 dual-resistance phenotype genomic DNA extract was used as a template. PCR conditions and primers used were as follows:

Amplicon	Taqpol Kit	Forward and reverse primers (#µM)	Conditions
URA5 sgDNA cutsite	NEB 2x	BLO66/67 (200µM)	95°C for 30s, [95°C for 30s, 52°C for 15s, 68°C for 30s (short) and 6.5' (long)]x34, 68°C for 2' (short) and 10' (long), hold at 4°C
URA5 CDS+3' UTR	GoTaq	BLO304/305 (200µM)	95°C for 30s, [95°C for 10s, 56.1°C [50-60°C gradient] for 15s, 72°C for 3']x30, 68°C for 5', hold at 4°C

URA5 locus	NEB 2x	BLO316/317 (200µM)	95°C for 30s, [95°C for 15s, 55.2°C [54-57°C gradient] for 20s, 68°C for 5']x30, 68°C for 8', hold at 4°C
URA5 CTR4p-3' UTR	NEB 2x	BLO293/317 (200µM)	95°C for 30s, [95°C for 15s, 55.2°C [54-57°C gradient] for 20s, 68°C for 3']x30, 68°C for 6', hold at 4°C
MIP1 5' UTR+CDS	NEB 2x	BLO339/345 (200µM)	95°C for 30s, [95°C for 15s, 53°C for 20s, 68°C for 6']x30, 68°C for 8.5', hold at 4°C
MIP1 CTR4p-CDS	NEB 2x	BLO293/345 (200µM)	95°C for 30s, [95°C for 15s, 57°C for 20s, 68°C for 4']x30, 68°C for 6', hold at 4°C

15. *GFP expression tracking with EVOS Widefield fluorescent microscopy.* Assays for GFP signal were done using an EVOS microscope with a GFP light cube filter. These were an attempt to qualify *CTR4p*-GFP-terminator *in vivo* function. Constructs from Methods 7 were transformed into JEC21 using electroporation protocols described in Methods 13. Transformant colonies were inoculated in ~1.5mL YPD-NEO overnight [~18hr]. 500µL of the culture was used to inoculate a 1.5mL YPD-NEO-400µM BCS culture. 1mL of the YPD-NEO-BCS culture was spun down and then resuspended in Complete Minimal Medium-NEO-BCS. Samples were run alongside one wild-type *C. deneoformans* JEC21 negative control.

+*CYC1t* and +*CYC1t,TEL* constructs were linearized with Sca-I and transformed episomally using electroporation. Growth conditions were identical to those described above and were screened at 40x for GFP signal. Samples with presumptive signal were then analyzed at 60x

oil immersion, image captured, and then deconvoluted using the open-source 'Fiji Is Just Imagej' (FIJI) Iterative Deconvolve plug-in software.[42]

To test for differences in chromosomal *GFP* expression, +*CYC1t* constructs assembled in Methods 7 were inserted into the *URA5* locus via HDR. Growth conditions were identical to those described above but were run alongside a YPD-NEO duplicate cultures without BCS. The lack of BCS leaves copper unchelated and theoretically represses the *CTR4* promoter, hence no signal was expected and allowed the duplicates to be run as negatives. Samples with presumptive signal were then analyzed at 60x oil immersion and analyzed as described above.

CHAPTER III. RESULTS

1. *Construction of a series of modular gene cassettes for Cryptococcus.*

Gene expression cassette cloning can be a time-intensive task that scales with the complexity of the cassette. Having more components necessitates more ligation, more cloning, and screening. While useful as vehicles for the expression of various genes and/or fragments *in vivo*, cassettes require careful design and planning to ensure proper assembly. As part of this project, a modular gene expression cassette featuring a selection marker, followed by a promoter, and finalized by an expression tracker was designed. Restriction sites were structured such that orientation and assembly would be streamlined. The unique sites would also allow for each fragment in the cassette to be a potential insertion or excision site, allowing for a stream-lining of cassette design for future experiments (Fig 2).

Figure 2 – Schematic for modular gene expression cassettes designed in this project.

1. a. *Design and assembly of a modular gene cassette for homology-driven recombination*

In order to create a template to insert into the Cas9 cut-site by homology driven DNA repair, a modular gene cassette was designed. This modular cassette contained a neomycin resistance gene (NEO^R) for selection, the copper-repressible *CnCTR4* promoter for regulated transcription, and a cryptococcal codon-optimized *GFP* for tagging a protein of interest (Fig. 3).

Homologous arms to a "gene of interest" (Protein of Interest or POI) could be added to this cassette, making this a versatile system for genetic manipulation.

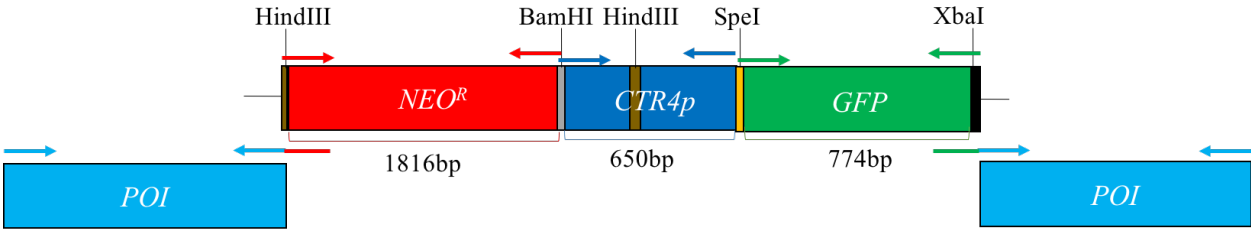

Figure 3 – Schematic for the modular gene cassette showing the position and sizes of the three fragments. The *CTR4p* and *GFP* fragments reside within unique BamHI-SpeI and SpeI-XbaI sites, respectively. The GFP in this cassette does not contain a stop codon so that a gene of interest can be expressed in-frame. This cassette can be used to add 5' and 3' regions homologous to 'Protein of Interest' (POI) by overlap PCR. Arrows denote primers used for amplifying the fragments.

The cassette was synthesized and inserted within the HindIII-XbaI sites of the pCR2.1 TOPO plasmid using a multi-fragment ligation technique. The *NEO*^{R} fragment was amplified from plasmid pIBB314 with primers BLO291 and BLO292 containing HindIII and BamHI sites. The *CTR4p* fragment was amplified from pIBB236 with primers BLO293 and BLO294 containing BamHI and SpeI sites. The GFP fragment was amplified from plasmid pIBB314 using primer BLO295 and BLO296 containing SpeI and XbaI sites. The PCR fragments (Fig. 4) were digested with the appropriate restriction enzymes, purified, and ligated into the HindIII-XbaI digested vector (see Methods 7). Two different vector-to-insert molar ratios, 1:1 and 1:3, were used for the ligations.

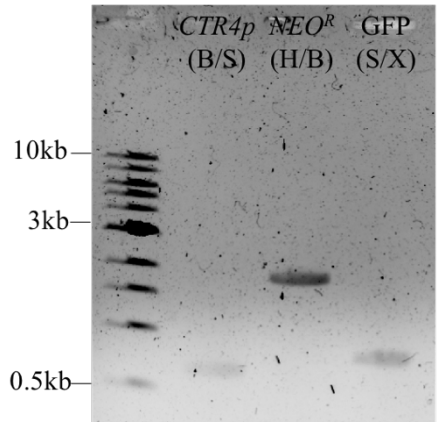

Figure 4 - Purified *CTR4p, NEO*^{R}, and GFP double-digests. Digests using the following enzymes: BamHI/SpeI (B/S), HindIII/BamHI (H/B), and SpeI/XbaI (S/X). Visualized with 1kb NEB DNA ladder on 0.8% TAE-agarose ethidium bromide gel, run at 100V 30min.

10 colonies from each ligation transformation, were analyzed by restriction digests. A HindIII-XbaI digestion should yield three fragments of sizes 3.819kb, 2.236kb, and 1.019kb, as shown by the Virtual Cutter (Fig. 5A). This pattern is found only in colony #5. Similar results were obtained for the HindIII-BamHI, BamHI-SpeI, and SpeI-XbaI digests (see Fig 5 legend for details). Sanger sequencing with primers BLO291-296 confirmed the sequence identity and reading frame of the 1.817kb NEO^R gene, the 0.65kb *CTR4p*, and 0.774kb GFP CDS (see Appendix 3.b-3.i).

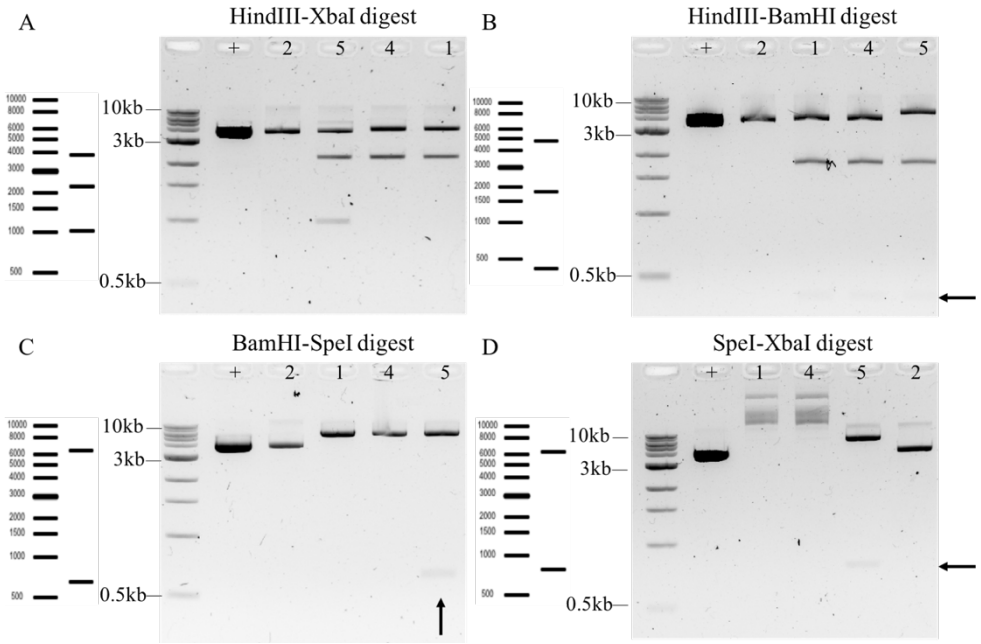

Figure 5 – Double digests of vectors obtained from 1:3 molar ligation transformants with accompanying SerialCloner Virtual Cutter predictions. (A.) HindIII-XbaI. (B). HindIII-BamHI. (C.) BamHI-SpeI. (D.)

SpeI-XbaI. Arrows denote faint bands in Construct #5 well. #5 contained all desired fragments. All visualizations were done using 0.8%TAE- agarose ethidium bromide gels with 1kb NEB DNA ladder.

Electroporation into the wild type *C. deneoformans* JEC21 strain demonstrated that transformation with the construct conferred NEO^R phenotype when using both linearized plasmid and purified whole-cassette amplicon (not shown). This transformant was frozen as pIBB326, and the map of the plasmid containing the complete cassette is shown in Fig 6. This construct was used as a reagent for the assembly of the +MLS and +terminator containing cassette variants.

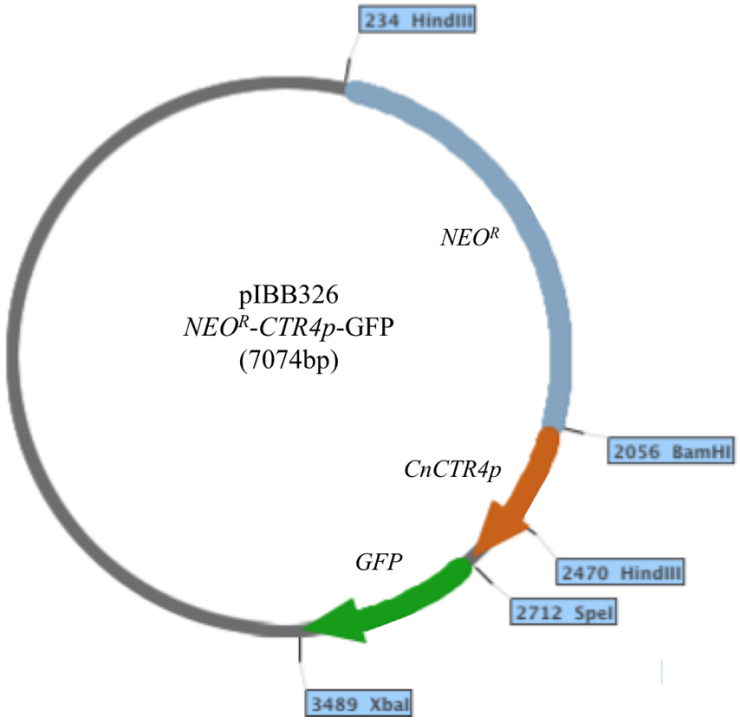

Figure 6 – Plasmid map of the cassette plasmid (pIBB326). The 7074bp plasmid has a pCR2.1 TOPO backbone. The *NEO^R*, *CTR4p*, and *GFP* sequences are shown in blue, orange, and green, respectively. The unique BamHI, SpeI, and XbaI sites, as well as the HindIII restriction site are indicated.

1. b. *Addition of a putative MLS from CnMIP1 into the SpeI site of the modular gene cassette*

The original modular cassette contained no special localization signals for the expressed proteins. To ascertain the necessity of nuclear-encoded mitochondrial proteins like PolG, a Mitochondrial Localization Signal (MLS) needed to be added to the N-terminal of the GFP reading frame (Fig 7).

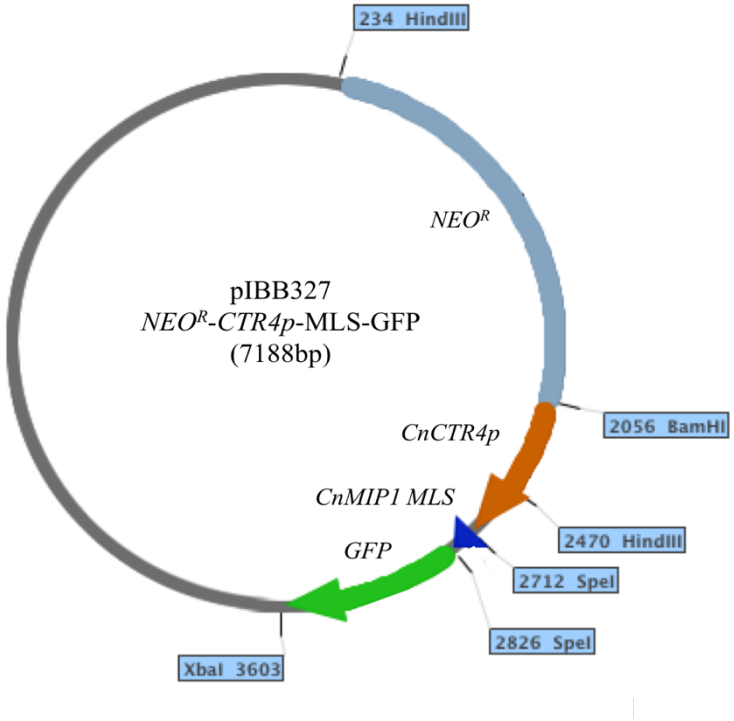

Figure 7 – Plasmid map of the cassette plasmid containing the *MIP1* MLS in-frame with the GFP sequences. The MLS sequence was inserted into the SpeI site in between the *CTR4p* and *GFP*.

The predicted MLS from *C. neoformans MIP1* were amplified with BLO311 and BLO318. These primers contained SpeI restriction sites so that the resulting PCR fragment could be cloned into the SpeI site in-frame with the GFP gene using a 1:4 molar vector-to-insert ligation ratio. Orientation and presence of the *MLS* was confirmed by PCR assays of 15 transformant colonies using two separate reactions: one with the forward *CTR4p* primer (BLO293) and reverse MLS primer (BLO318); the other with the forward MLS (BLO311) and

reverse *GFP* (BLO296, see Appendix 1 for primers). The *CTR4p*-MLS PCR would yield a 776bp amplicon only if the *CTR4p* was 5' to the MLS. Similarly, the MLS-*GFP* PCR would yield an 883bp product only if the MLS was correctly situated and in the proper orientation. All 15 samples were subjected to the *GFP* PCR assay, eight of which yielded amplicons of correct size (Fig 8A). Those eight were then subjected to the *CTR4p*-MLS PCR assay, and all eight yielded a PCR product of the expected size (Fig 8B).

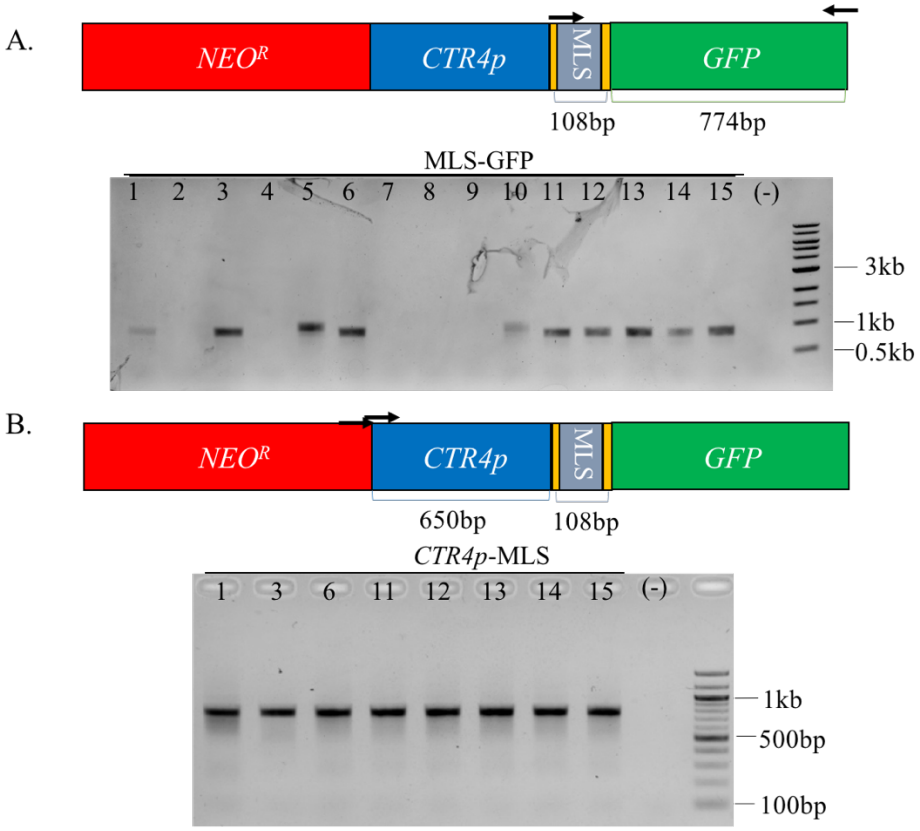

Figure 8 – MLS orientation PCR assays. (A) 0.8% TAE-agarose ethidium bromide gel visualization of MLS-*GFP* PCR using MLS forward primer and reverse *GFP* primer. Expected product size was 883bp. Visualized with 1kb NEB DNA ladder run at 100V for 30min. Cassette schematic included for reference; yellow boxes flanking the MLS denote the SpeI sites used for ligation. (B) 2% TAE-agarose ethidium bromide gel visualization *CTR4p*-MLS PCR using *CTR4p* forward primer and reverse MLS primer. Expected product size was 776bp. Visualized with 100bp Tridye DNA ladder run at 100V for 27min.

Two colonies, #13 and #15, were sequenced with primers BLO293, BLO311, and BLO318 to confirm sequence identity and orientation of the MLS (Appendix 3.h,i).
Colony #13 that was confirmed to have the correct insert by PCR and sequencing was saved as pIBB327. pIBB327 was later used to assemble the terminator-containing cassette variants.

1. c. *Creating modular gene cassettes with terminator fragments*

The original modular cassette featured a *GFP* reading frame without a stop codon or a downstream terminator so that it could be used to tag the N-terminal of a protein of interest (Fig 3). However, in order to test for conditional expression of *GFP* with the *CTR4p* copper-repressible promoter, terminators and a stop-codon needed to be added for proper GFP expression. A literature search for terminator sequences used in yeast molecular biology revealed that the *CYC1* terminator (*CYC1t*) had previously been utilized to drive transcription of modified genes in *S. cerevisiae*.[43,44] A *URA5* terminator (*CnURA5t*) had been used in an algae model but seemingly not in yeast models.[45] To see if the *CnURA5* 3' UTR could be used as a short transcription terminator, a 215bp fragment was captured by primers that inserted flanking XbaI sites. *CnURA5* is ~500bp upstream from the next gene in the KN99 chromosome, accordingly we went with a fairly limited fragment to screen for sufficiency with GFP expression. The 3' UTR of *CnCYC1* is less crowded but small fragments had been shown to be sufficient in *S. cerevisiae*; a 229bp fragment of the *CnCYC1* 3' UTR was accordingly amplified with primers that also added XbaI sites to the flanks.[44] The XbaI sites would allow for insertion of the UTR fragments into the corresponding site in the pIBB326 and 327 cassettes. A TAA stop codon for GFP was also introduced via the forward primers (BLO319 and BLO321, see

Appendix 1) for the two terminators. The *CnCYC1* and *CnURA5* terminators (*CnCYC1t* and *CnURA5t*) were added to both the no-MLS and +MLS cassettes as seen Figure 9.

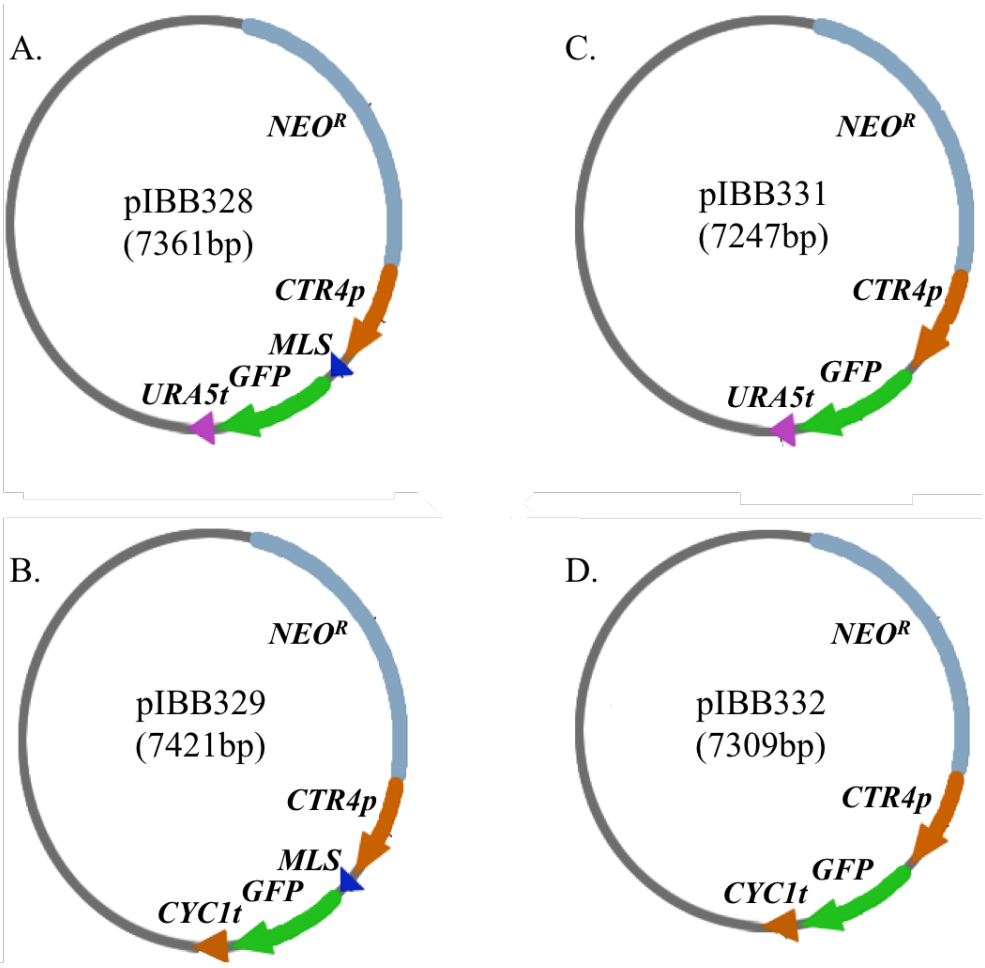

Figure 9 – Plasmid maps of terminator-containing cassette plasmids. (A) pIBB328 +MLS,+*URA5t* cassette (B) pIBB329 +MLS,+*CYC1t* cassette. (C) pIBB331 +*URA5t* cassette (D) pIBB332 +*CYC1t* cassette. The terminators were inserted into the unique XbaI site of the cassette, and contained a 5'-TAA stop codon for GFP.

Amplicons were gel purified and digested with XbaI alongside appropriate cassette plasmids. Ligation conditions described in Methods 7 were used to assemble the constructs. 24 colonies, 12 transformed with pIBB329, 12 with pIBB332, were sampled for NdeI digest and PCR assays. *CnCYC1t* contains a unique NdeI site that was used to show construct size and confirm *CYC1t* presence in the 12 pIBB339 transformants (Fig 10). PCR was used to confirm

fragment presence and orientation in 5 pIBB329 and 1 pIBB332 constructs (Fig 11). Issues with XbaI ligation in the no-MLS cassette-terminator constructs, pIBB331 and 332, led to the use of SpeI to excise the *CnMIP1* MLS from the +MLS,+terminator cassette plasmids. Products were transformed into an *E. coli* expression system. SalI-NdeI restriction digests were used to show excision of MLS (Fig 14B). The *CnMIP1* predicted MLS contained a unique SalI site, allowing us to show that non-linearized constructs lacked the MLS. PCR was used to show that the pIBB331 and 332 constructs retained the correctly oriented terminator sequences (Fig 12C).

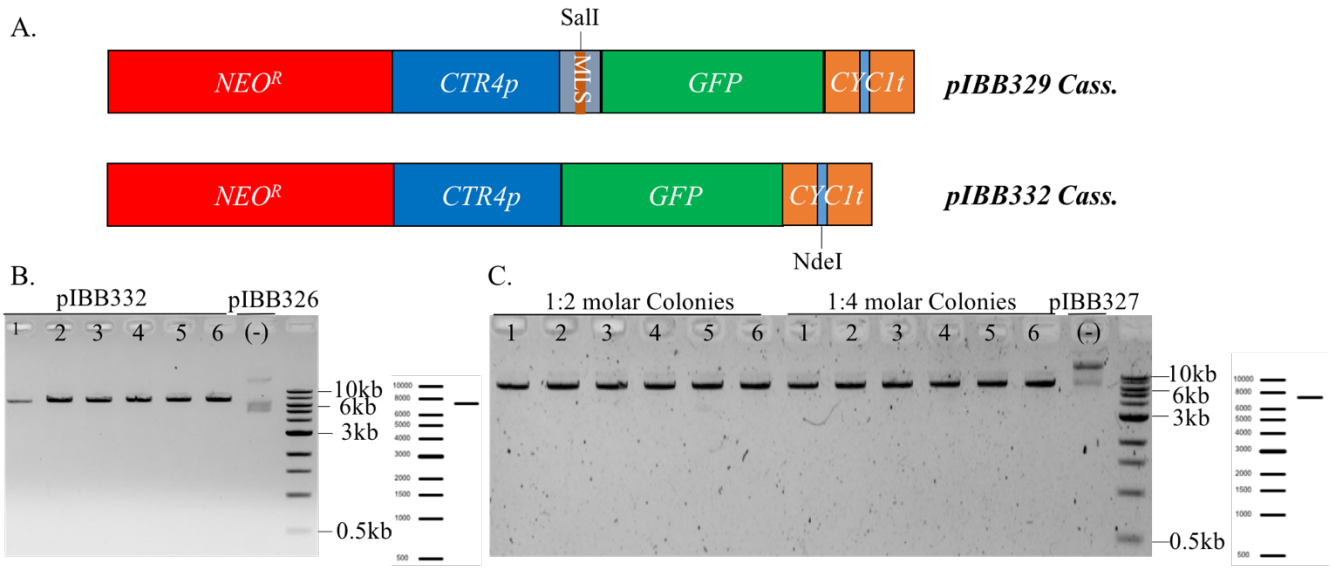

Figure 10 – NdeI digests of pIBB329 and pIBB332 transformants. (A) Cassette schematics with the unique NdeI site highlighted in the *CnCYC1t* sequence. (B) pIBB332 extracts visualized on 0.8% TAE-agarose ethidium bromide gel with digest product run for 30min. at 100V. 1kb NEB DNA ladder used for size comparison. Serial Cloner Virtual Cutter NdeI digest prediction to right of the ladder well. (C) pIBB329 extracts visualized on 0.8% TAE-agarose ethidium bromide gel with digest product run for 30min. at 100V. 1kb NEB DNA ladder used for size comparison. Serial Cloner NdeI digest prediction next to ladder well.

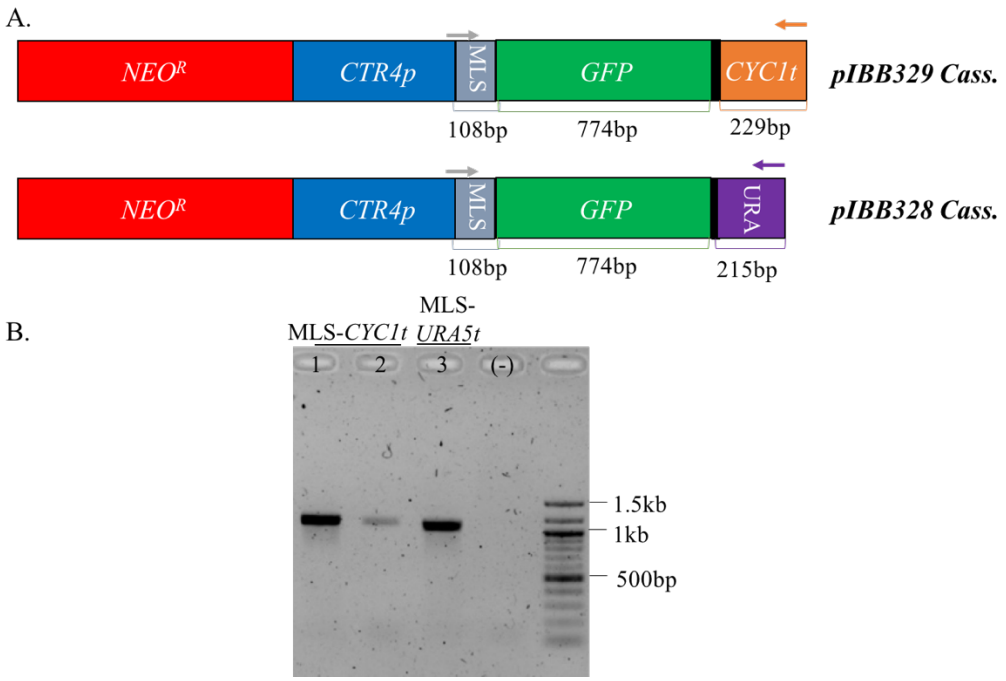

Figure 11 – PCR assay to determine the insertion, and orientation of insertion, of the +MLS,+terminator cassette constructs. (A) Schematics of the pIBB329 +MLS,+*CYC1t* and pIBB332 +MLS,+*URA5t* constructs with primer arrows indicating those used for the orientation test. (B) 3 transformants each from the 1:2 and 1:4 vector-to-*CYC1t* molar ratio ligations, and one transformant from the *URA5t* ligation were analyzed. MLS forward (BLO318) and terminator reverse (BLO320 for *CnURA5t* and 322 for *CnCYC1t*) primers were used and produced the expected 1.114kb MLS-GFP-*CYC1t* and 1.100kb MLS-GFP-*URA5t* bands. PCR product was visualized on a 2% TAE-agarose ethidium bromide gel run at 100V for 30min.

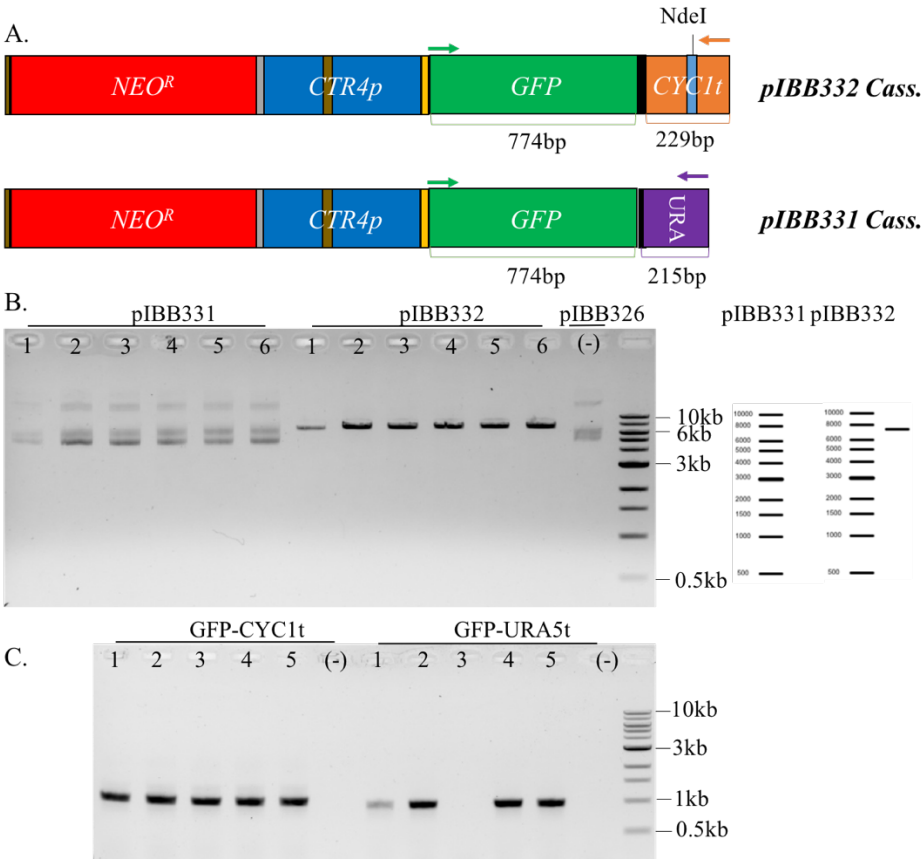

Figure 12 – Confirming constructs pIBB331 and pIBB332. (A) Schematics of the pIBB331 +*URA5t* and pIBB332 +*CYC1t* constructs with primer arrows indicating those used for the orientation test and the NdeI site in *CYC1t*. (B) SalI-NdeI digest assay of MLS-excised +terminator cassette plasmids extracted from *E. coli*. Visualized on 0.8% TAE-agarose ethidium bromide gel using 1kb NEB DNA ladder as a size reference. Run at 100V for 30min. NdeI-SalI Virtual Cutter predictions from Serial Cloner to right of ladder. (C) PCR assay to determine the insertion and orientation of insertion of the GFP-terminator cassette constructs with no MLS. SpeI-GFP forward (BLO295) and XbaI-terminator reverse (BLO320 for *CnURA5t* and BLO322 for *CnCYC1t*) primers were used and expected to produce 1.018kb and 0.956kb bands for the *GFP-CYC1t* and *GFP-URA5t* amplifications respectively. Run at 100V for 30min. Visualized with a 0.8% TAE-agarose ethidium bromide gel using 1kb NEB DNA ladder.

Confirmed constructs from the +MLS,+*URA5t* 1:2 molar colony #3 [pIBB328], +MLS,+*CYC1t* 1:2 molar colony #1 [pIBB329,330], +*URA5t* subclone colony #4 [pIBB331], and +*CYC1t* subclone colony #4 [pIBB332] were saved in bacterial glycerol stocks and later used as a reagent for telomeric-cassette-terminator assembly and *URA5* repair template assembly for CRISPR-Cas9 excision tests.

1. d. *Creating a NEO^R-CTR4p-CdMIP1 N-terminal fragment cassette.*

As was mentioned previously, the original modular cassette featured a *GFP* reading frame without a stop codon or a downstream terminator so that it could be used to tag the N-terminal of a protein of interest (Fig 3). However, *in vivo* tests for *GFP* expression using the terminator constructs did not yield evidence suggestive of a functional GFP gene. There was a need to trouble-shoot; additionally, concern arose that the *GFP* product may interfere with the functionality of promoter-edited genes down the line. A gene of promoter-editing interest in this project was *MIP1*. Editing and manipulation of this gene has been troublesome in previous studies (Walters [46]), hence the decision to remove the *GFP* fragment of pIBB326 for a test of conditional *MIP1* expression using the *CTR4p* copper-repressible promoter.[46] Primers were designed to amplify a 1105bp fragment of the *MIP1* CDS starting at the ATG start codon and SpeI and XbaI at the 5' and 3' ends of the fragment (BLO337 and 338 in Appendix 1). This would allow for ligation into the pIBB326 plasmid. SpeI-XbaI digest was used to excise the *GFP* fragment and replace it with the *MIP1* N-terminus following gel purification of the reagents (see Fig 13 for construct).

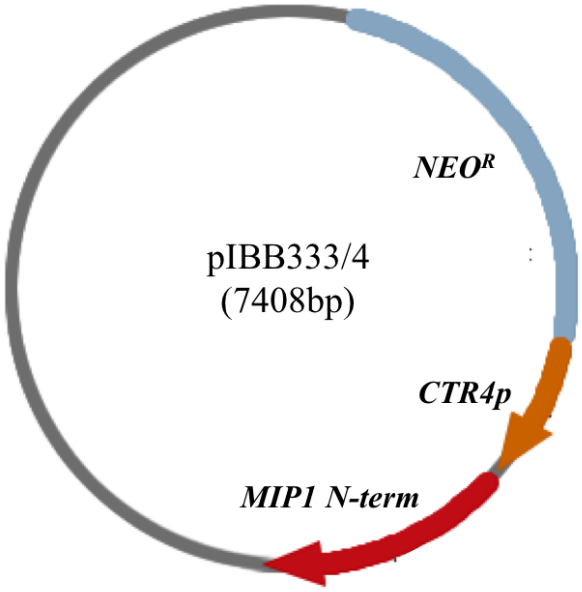

Figure 13 – Plasmid Map of pIBB333 and 334; pIBB334 is an extract from a different colony from the same transformation plate with pIBB333.

Ligation of the SAP-treated pIBB326 vector with the digested *MIP1* fragment yielded three bacterial colonies with a kanamycin-resistant phenotype. All colonies were sampled for ScaI digest and PCR assays. The *MIP1* fragment and pIBB326 plasmid both contain a ScaI site (Fig 14); digest with ScaI would produce two bands: One 5.155kb and one 2.253kb. pIBB326 conversely would linearize into a singular 7.074kb product Accordingly, ScaI digest was used to show evidence for *MIP1* presence in the transformants (Fig 14B). Two extracts gave the correct digest products while a third gave an expected pattern likely due to the relative homology between the SpeI and XbaI-recognized sequences. That unexpected pattern was indicative of an incorrect ligation product, hence we did not investigate it further. The digest product from colonies #1 and 2 were subjected to a PCR using primers that would confirm *MIP1* fragment presence in the construct and show a correct orientation in the constructs (Fig 14C).

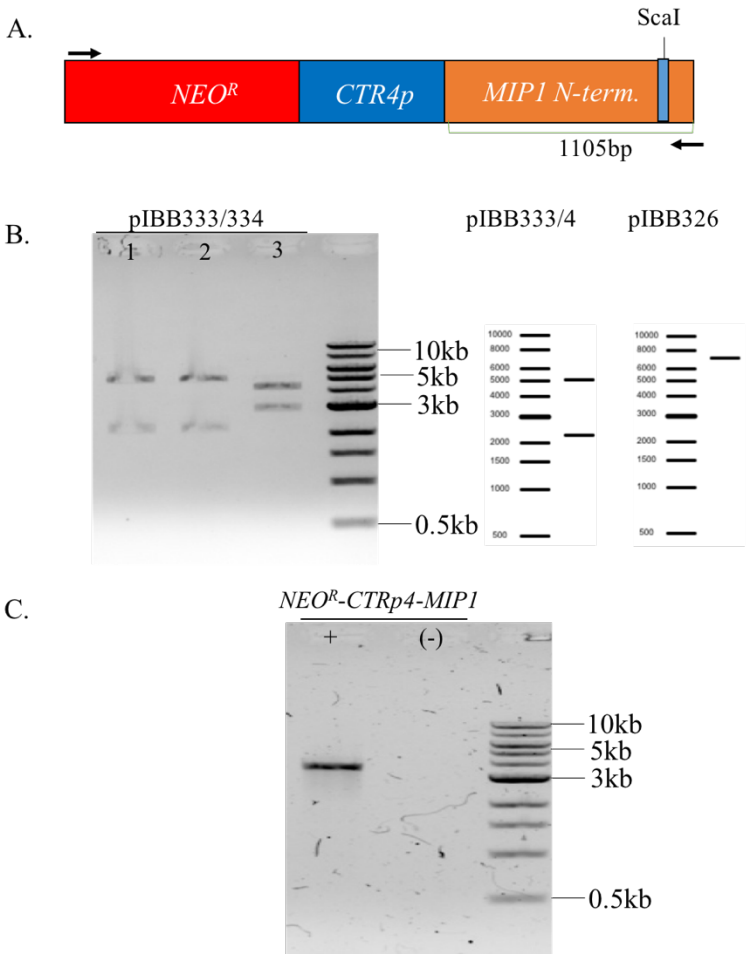

Figure 14 – Confirming the presence of the *MIP1* fragment in plasmids pIBB333/334. (A) Schematic of cassette with annotated ScaI site and relevant primers for PCR confirmation. (B) Plasmids digested with ScaI. (C) PCR amplification targeting the *NEO*^{R} 5' to the MIP1 fragment; expected size of cassette is 3.635kb. Both (B) and (C) were visualized on a 0.8% TAE-agarose ethidium bromide gel with the 1kb NEB DNA ladder used for size visualization.

The two correct plasmids with the *NEO*^{R}*-CTR4p-MIP1* N-terminal fragment were frozen down at -80˚C in bacterial glycerol stocks as pIBB333 (Fig 14B #1) and pIBB334 (Fig 14B #2). pIBB334 was later used as a reagent for assembly of the *MIP1p* repair template assembly for CRISPR-Cas9 promoter recombination tests.

2. *CRISPR-Cas9 in the yeast, C. deneoformans*

CRISPR-Cas9 is an RNA-guided endonuclease system used to induce precise double-stranded DNA breaks and has been adapted for use in a variety of organisms.[27] These cuts compromise eukaryotic chromosome integrity, forcing DNA repair and/or cell death. *C. neoformans* and its sister species are haploid yeasts with single-copy, linear chromosomes.[3] Fan and Lin developed a transient CRISPR-Cas9 protocol for the *C. neoformans* species complex that targets chromosomal sites in *Cryptococcus* with a single RNA guide sequence (sgRNA) allowing for a double-stranded cut to be induced in precise locations.[14] This damage can facilitate reliable insertion of constructs with long stretches of homology to the damaged locus. Alternatively, erroneous DNA repair can catalyze gene knock-out via frame-shift mutagenesis. CRISPR-Cas9 can, therefore, be very useful for editing genomic sequences.[16]

2. a. *Design and assembly of cryptococcal CAS9* and *URA5*-targeting sgRNAs

CRISPR-Cas9 systems require the expression of the Cas9 protein and an sgRNA to affect site-directed DNA-damage *in vivo.* To express the Cas9 protein transiently in *Cryptococcus*, a PCR fragment containing a constitutive *GPD* promoter and the *CAS9* gene with a C-terminal *SV40* nuclear localization signal (NLS) was amplified from the pXL1-HYG-CAS9 plasmid[14] using primers BLO258 and BLO259 as shown in Fig 15C.

The sgRNAs used in this project were expressed from DNA fragments amplified from the plasmid, pYF515.[14] This plasmid contains a small tracrDNA-terminator fusion sequence that serves as a scaffold for *in vitro* sgDNA assembly. The sgDNA construct is expressed via a cryptococcal 5' *U6* promoter (*CdU6p*) that over-expresses the fused crDNA-tracrDNA sequence. Target-specific sequences were added in between the promoter and tracrDNA by overlap PCR

using bridge primers BLO264, 265, 328, 329, and 330 to produce the desired sgDNAs (Fig 15B). These bridge primers contained three parts: a 5' ~20nt fragment that overlapped with the end of *U6p*, a middle portion that was specific to the target gene (crDNA in Fig 15), and 3' 20nt that corresponded to the beginning of the tracrDNA scaffold sequence (Fig 15B). Five different sgDNAs, sg264, 265, 328, 329, and 330, were used in this project that targeted different sections of the metabolic gene, *URA5*. The different bridge primers contained crDNA sequences that targeted different cut sites in the *URA5* gene. The *URA5* cut sites were designed to be in the exonic regions to improve the chances of disruption. Two of the bridge primers (BLO264 and BLO265) contained the PAM sequence in the primer itself. This had an important consequence for the activity of Cas9, as will be shown in later sections.

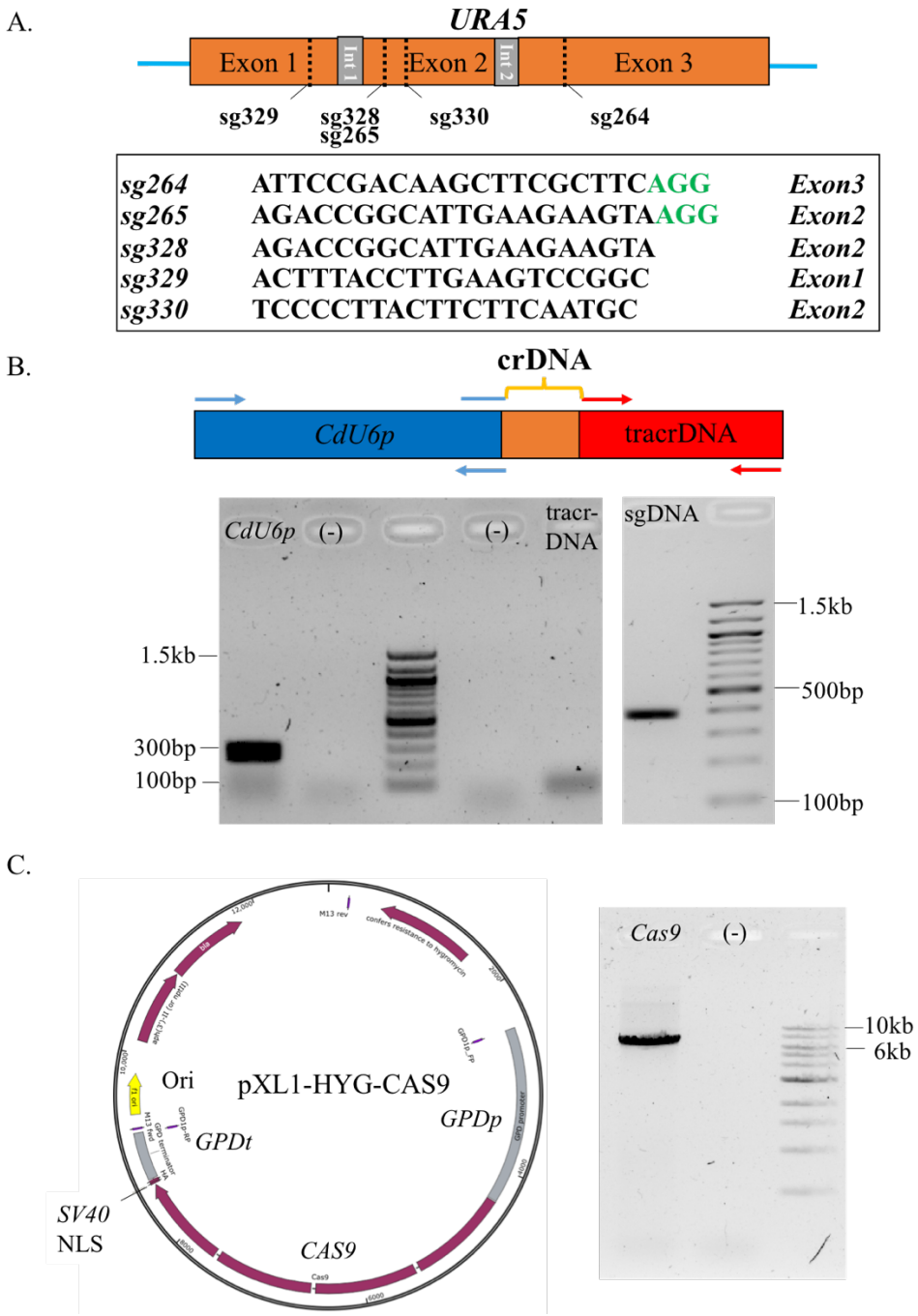

Figure 15 – *URA5* CRISPR-Cas9 system used in this project. (A) Diagram of *URA5* with annotated cut sites for the sgDNAs used to target damage to the gene. Green sequence in sgDNA box denotes the Protospacer Adjacent Motif complement included in the crDNA sequence. (B) Schematic of the 383bp cryptococcal sgDNA sequence. Arrows denote primers. 275bp *CdU6p* and 108bp tracrDNA (Left) and 383bp sgDNA (right) PCR products visualized with 100bp Tridye Ladder DNA ladder on 2% TAE-agarose ethidium bromid gels/ (C) pXL1 plasmid map with annotated 6.985kb *CAS9* gene with *GPD* promoter (*GPDp*) and terminator (*GPDt*). 0.8% TAE-agarose ethidium bromide gel used to visualize amplified gene with 1kb NEB DNA ladder.

The two initial *URA5*-targeting sgDNAs, assembled with bridge primers BLO264 and BLO265 (Fig 15), resulted in poor recombination in preliminary recombination experiments (Appendix 5). They contained 23nt crDNA sequences complementary to sites in exon3 and exon2 of the *URA5* reading frame, respectively. Importantly, the BLO264 and 265 crDNA sequences included a 3nt NCC PAM complement that would bind to the NGG PAM sequence in the chromosome (BLO265 in Fig 16). The PAM is recognized by the Cas9 endonuclease and facilitates nuclease activity.[27] If the PAM is not present or not able to be bound, Cas9 cannot induce a double-stranded DNA break. Due to the poor effectiveness of the initial two sgDNAs, three new bridge primers, BLO328, 329, and 330, were designed that lacked the PAM complements in BLO264 and 265. The motivation for this was that removing the PAM compliment would make the chromosomal PAM accessible to Cas9 (BLO328 in Fig 16). One of the new bridge primers, BLO328, had the same sequence as that of BLO265, only lacking the three PAM nucleotides. This allowed for head-to-head comparison of the effect of the PAM sequence in the sgRNA towards Cas9 activity.

Figure 16 – Sequence comparison of the crDNA sequences in the bridge primers, BLO265 and BLO328. Green nucleotides denote the PAM targeted by each sgDNA sequence. Both are designed to guide Cas9 to the same sequence in *URA5* exon2. BLO265 and BLO328 differ only in the presence of the PAM within the sgDNA itself.

The 383bp sgDNA sequences were assembled by overlap PCR, integrating the BLO264, 265, 328, 329, and 330 crDNA sequences between *U6p* and the tracrDNA scaffold sequence in plasmid pYF515.[14] The amplified and purified *CAS9* and sgRNA gene expression cassettes were electroporated into *C. deneoformans* to show *in vivo* functionality of the CRISPR-Cas9 system in the presence or absence of a homologous template for repair of the DNA damage.

2. b. *Disruption of URA5 with CRISPR-Cas9 mediated NHEJ.*

When lacking a homologous allele, double-stranded DNA damage in chromosomal targets cannot undergo homology directed repair. This forces haploid cells like *C. deneoformans* to undergo nonhomologous end-joining repair (NHEJ). NHEJ is an error-prone pathway that tends to introduce frame-shift mutations into break sites. Since CRISPR-Cas9 induces DNA damage, it can be used to drive NHEJ mutagenesis. As a preliminary experiment, a 1.895kb NEO^R fragment flanked by approximately 500bp of sequence homologous to the *URA5* CDS was used to test homology-directed recombination via CRISPR-Cas9. The sgRNAs used for that experiment were created using primers BLO264 and BLO265 containing the PAM site in their crDNAs; the preliminary experiment demonstrated at least a viability of the system (Appendix 5). Preliminary results showed some promise of *in vivo* CRISPR activity although with low *URA5* disruption effectiveness. Ultimately, the process required optimization. Optimization of this CRISPR-Cas9 driven recombination system was first done by redesigning the bridge primers. BLO328, 329, and 330 did not contain the PAM were used to construct sgDNA sequences and were found to have a significant difference in conferring CRISPR-Cas9 activity. Accordingly, the sgDNAs guided Cas9 to their respective cut-sites in *URA5*. This was done without a homologous repair template in order to ascertain the accuracy of the system. This

forces *C. deneoformans* to attempt NHEJ, which tends to introduce frameshift mutations into the upstream cutsites. Those frameshifts were expected to knockout *URA5* via misaligning the reading frame.[28]

C. deneoformans JEC21 wild type cells were electroporated with approximately 0.7 pmoles (2μg) of pIBB332 *NEO*^{R}-*CTR4p*-GFP-*CYC1t* cassette along with 0.23 pmoles (1μg) *CAS9* fragment and 3 pmoles (0.7μg) sgDNAs. The cassette was comprised of DNA sequences lacking homology to the *URA5* locus and was used as a *NEO*^{R} selection marker for cells that were successfully transformed. The pIBB332 cassette (c332) was used for this and lacked any meaningful homology to the locus. In theory, the exogenous DNAs encoding for *CAS9*, the sgDNA, or c332 should not recombine with the damaged chromosome. Thereby, nonhomologous end-joining DNA repair would be activated to disrupt the *URA5* reading frame. Transformants were selected for by plating the cultures on YPD-NEO for three days prior to determining growth on 5-FOA media (Fig 17).

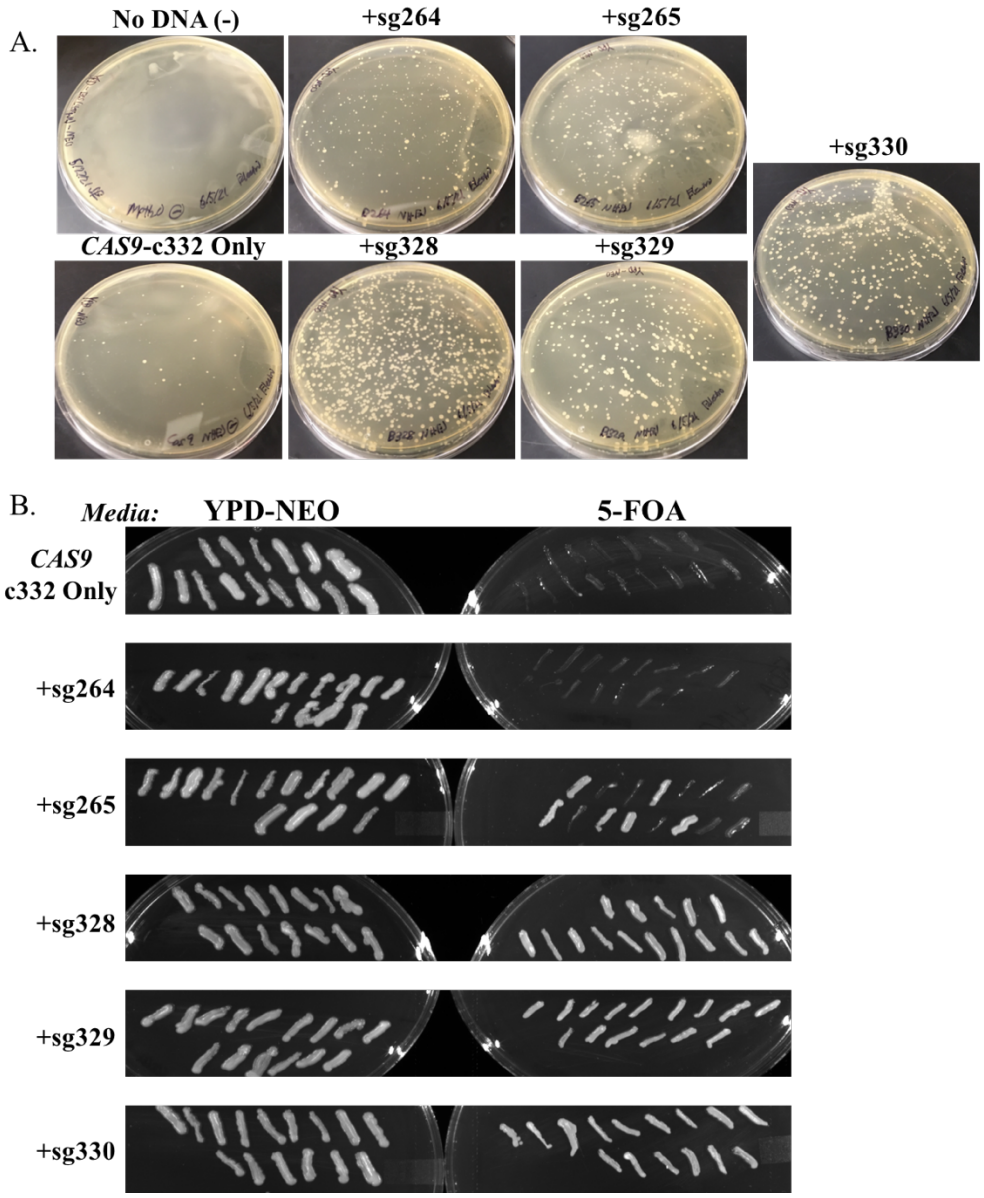

Figure 17 – *URA5* NHEJ CRISPR-Cas9 electroporations and resultant phenotypes. c332 represents the pIBB332 cassette used for NEO^R selection. sg264-330 represent the sgDNAs added to each sample. (A) YPD-NEO plates incubated for three days at 30˚C following plating of 300µL of transformed recovery culture. (B) 5-FOA restreaks of 15 colonies from each YPD-NEO plate incubated for two days at 30˚C.

The NHEJ-driving mutagenesis system tested the accuracy of the five *URA5* sgDNAs used in this project. By not providing a homologous repair template, we aimed to examine the effectiveness of the transient CRISPR-Cas9 system in producing *URA5* knockout mutants by erroneous non-homologous end-joining DNA repair. As a reminder, the bridge primers BLO264

and BLO265 contained the PAM within their sequence, while the bridge primers BLO328, 329, and 330 did not. As seen in the preliminary experiments, sg264 was repeatedly found to be unable to facilitate *URA5* disruption (Appendix 5, Fig 17B). sg265 was somewhat able to disrupt *URA5* using both NHEJ and HDR; in the NHEJ trials, approximately 40% of the sg265 CRISPR transformants demonstrated a dual NEO^R/5-FOA^R phenotype. sg328, 329, and 330 were all capable of high-fidelity conferral of 5-FOA^R phenotype when using the NHEJ system; approximate 100% of the transformants across the +sg328, 329, and 330 electroporations showed the dual NEO^R/5-FOA^R phenotype. Furthermore, an sgDNA was shown to be necessary for inducing the 5-FOA^R phenotype; when electroporating only the *CAS9* and c332 *NEO^R-CTR4p*-GFP-*CYC1t* gene cassettes, samples were not resistant to 5-FOA media, meaning *URA5* and the uracil synthesis pathway was not knocked out in these colonies (Fig 17B). A total of 90 colonies, 15 from each CRISPR-Cas9 NHEJ sample, were assayed for dual NEO^R and 5-FOA^R phenotypes. Colonies transformed with the *CAS9*-pI332-cassette only, or with sg264 added, were not able to grow on 5-FOA media. Six of fifteen +sg265 colonies were able to survive 5-FOA media, while all colonies with sg328, 329, and 330 added survived on 5-FOA (Table 1)

Table 1 – Phenotypes induced by NHEJ repair of CRISPR-Cas9 damage to *URA5*. sg264-330 denote the sgDNAs added to individual samples, all of which contained CAS9 and a *NEO^R* expression cassette.

Sample	Colonies Assayed	NEO^R	5-FOA^R	Dual Resistant
CAS9 + nonhomologous cassette	15	15	0	0%
+ sg264	15	15	0	0%
+ sg265	15	15	6	40%
+ sg328	15	15	15	100%
+ sg329	15	15	15	100%
+ sg330	15	15	15	100%

The discrepancy between sg265 and sg328 was particularly interesting due to their common target in *URA5*; the key difference between the two sgDNAs being a three nucleotide PAM complement in sg265.

In an attempt to screen for indels and confirm each sgDNAs cut site, a 383bp fragment of *URA5* containing the cut sites were amplified from four colonies from each +sg328, 329, and 330 transformation (Fig 18). sg265-transformed colonies were not screened given the common target between sg265 and sg328.

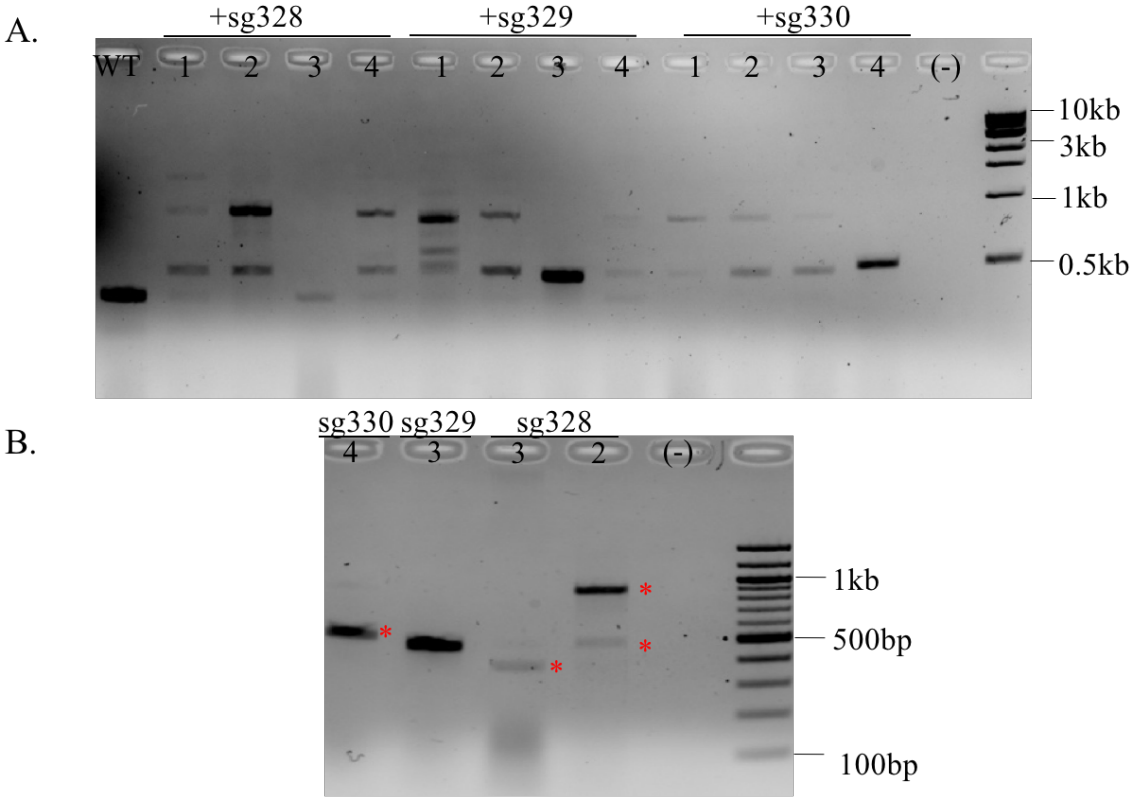

Figure 18 – PCR assay for size of *URA5* Exon 1-Exon 2 fragment containing the sg328, 329, and 330 crDNA targets. sg328-330 denotes the corresponding NHEJ system sgDNAs (A) 2% TAE-agarose ethidium bromide gel with *URA5* fragment PCR visualized with 1kb NEB DNA ladder. WT sample is JEC21 positive control for size reference of wildtype fragment. (B) 2% TAE-agarose ethidium bromide gel with *URA5* fragment PCR products send for sequencing visualized with 100bp Tridye DNA ladder. Red stars denote bands that were extracted for sequencing.

The presence of multiple bands in many samples and elevated bands in all samples was intriguing. It was possible that 11 of the 12 sampled colonies were of mixed origins, although the presence of a clear pattern led us to sequence three of the *URA5* fragments from sg328 #2, sg329 #3, and sg330 #4 (stars in Fig 18B). sg328 #2 was representative of the double-band pattern result seen in eight of the twelve gDNA extracts and was correspondingly gel purified to extract each band. sg329 #3 was ~450bp, a fairly unique band. sg330 #4 was representative of the ~500bp seen in ten of the twelve samples. Sequence alignments showed, within four nucleotides of the targeted PAM for each sgDNA, the chromosome had integrated exogenous DNA. For sg329 #3, this was shown to be the tracrRNA fragment from the BLO329 sgDNA gene (Fig 19).

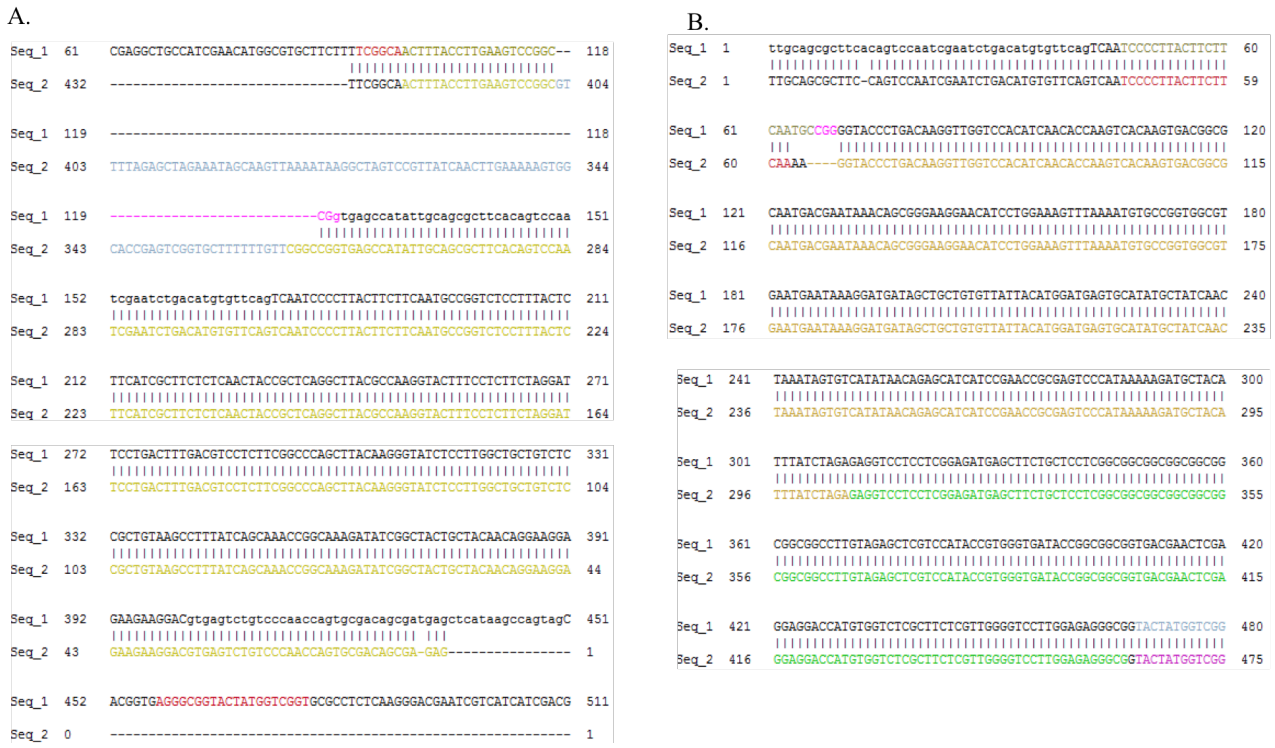

Figure 19– Alignments of sequenced *URA5* CRISPR-cutsites. (A.) Alignment of BLO67 primed sequence from sg329 NHEJ colony #3 (Seq2) with the *URA5* wild type sequence (Seq1). Gold coloration denotes the aligning *URA5* CDS fragment, blue denotes the tracrDNA sequence, red denotes the BLO66 and 67 primer targets, and purple denotes the sg329 PAM. (B.) Alignment of BLO66-primed sequence from sg330 NHEJ colony #2's lower band (Seq2) with a *URA5* sequence (Black) where the *CnCYC1t* construct (Gold) and a fragment of the GFP sequence (Green) had inserted into the sg330 cut site (Red sequence with purple PAM).

For sg328 #2 ‘s lower ~500bp band, which was of similar size, this also occurred. sg328 #2’s ~1kb band was found to be caused by the insertion of the entire sg328 sgDNA gene along with a fragment of the *GFP-CYC1t* sequence from the nonhomologous pIBB332 cassette used as a selection marker. This was an unexpected finding and leaves significant questions as to how NHEJ mechanisms choose blunt fragments for chromosomal repair. Amplification of the *URA5* locus using primers in neighboring genes and those capturing various portions of the CDS yielded results indicative of aberration caused by DNA insertion into the locus (Fig 20).

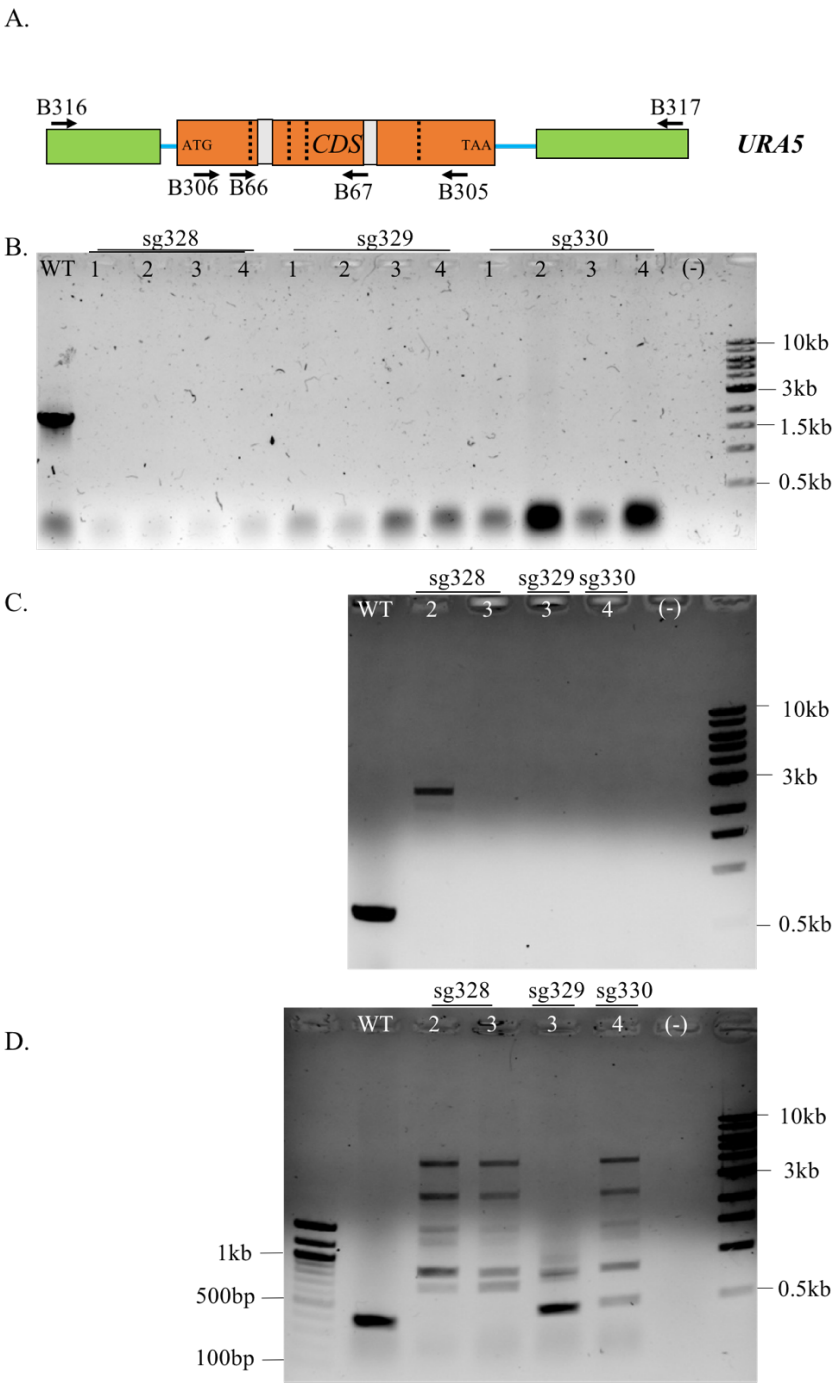

Figure 20 – *URA5* locus size screening for CRISPR-Cas9-driven NHEJ with progressively larger extension times and shorter locus targets. sg328-330 represent sgDNAs used to damage *URA5*. (A) Schematic of the *URA5* locus with annotated primers denoting the areas screened. Green boxes denote neighboring genes. (B) PCR assays of locus from neighboring genes inwards with 2.5min. extensions. 0.8% TAE-agarose ethidium bromide gel visualizing BLO316/BLO317-primed PCR; 1kb NEB DNA ladder used for size reference. WT is wild-type *C. deneoformans* JEC21 genomic DNA sample producing the expected 1.844kb locus product. (C) PCR assays with 4min. extension spanning mid-Exon1 to end of

Exon3. 0.8% TAE-agarose ethidium bromide gel visualizing BLO305/BLO306-primed PCR; 1kb NEB DNA ladder used for size reference. WT is wild-type *C. deneoformans* JEC21 genomic DNA sample producing the expected 689bp locus product. (D) PCR assays with 6.5min. extension spanning end of Exon1 to mid-Exon2. 0.8% TAE-agarose ethidium bromide gel visualizing BLO66/BLO67-primed PCR; visualized with 1kb NEB DNA ladder on right-most well and 100bp Tridye DNA on left-most for size references. WT is wild-type sample producing the expected 383bp locus product.

URA5 NHEJ disruption trials yielded limited evidence for frameshift mutagenesis. Instead of restoring the chromosome with frameshift mutations in or around the sgDNA cut site, JEC21 seemingly integrated exogenous DNA fragment regardless of their nonhomology to the *URA5* locus. The gene was disrupted by the insertion of exogenous DNA, ranging from small tracrDNA fragments and to large regions of the pIBB332 non-homologous cassette. Regardless, the CRISPR-Cas9 developed in this project was capable of inducing targeted DNA damage in desired chromosomal targets *in vivo* such that erroneous DNA repair can knock out a gene.

2. c. *Insertion of the modular gene cassette into URA5 with CRISPR-Cas9 by using sequence homology*

CRISPR-Cas9 has been used in other studies to insert DNA into a targeted cut site in the cryptococcal genome.[14,35] In this project, constructs with arms homologous to the 5' and 3' UTRs of the *URA5* gene were used to insert different exogenous DNAs into a cryptococcal chromosome.

Lin and Fan had demonstrated that while 500bp homologous arms resulted in good rates of CRISPR-Cas9 driven recombination in the *ADE2* gene, short homology arms of about 50bp in length did not.[14] Accordingly, approximately 500bp fragments of the 5' *URA5* UTR ending at -18bp from the ATG, and 3' UTR beginning +28 from the TAA stop codon were amplified and attached to the flanks of the +MLS,+*CYC1t* (c329) and no MLS,+*CYC1t* (c332) modular gene cassettes by overlap PCR (Fig 15). The arm-flanked cassettes served as homologous repair

templates that should drive recombination following CRISPR-Cas9 damage to *URA5*. This would result in the *URA5* CDS being completely excised and replaced with the cassettes, thereby conferring geneticin-resistance due to the NEO^R gene each cassette, as well as 5-fluoroorotic acid (5-FOA) resistance caused by uracil synthesis disruption *(Δura5*). Overlap PCR did, however, produce non-specific products that could not be resolved using a temperature gradient or additives such as betaine and DMSO, and gel purification gave poor yields (Fig 21D).

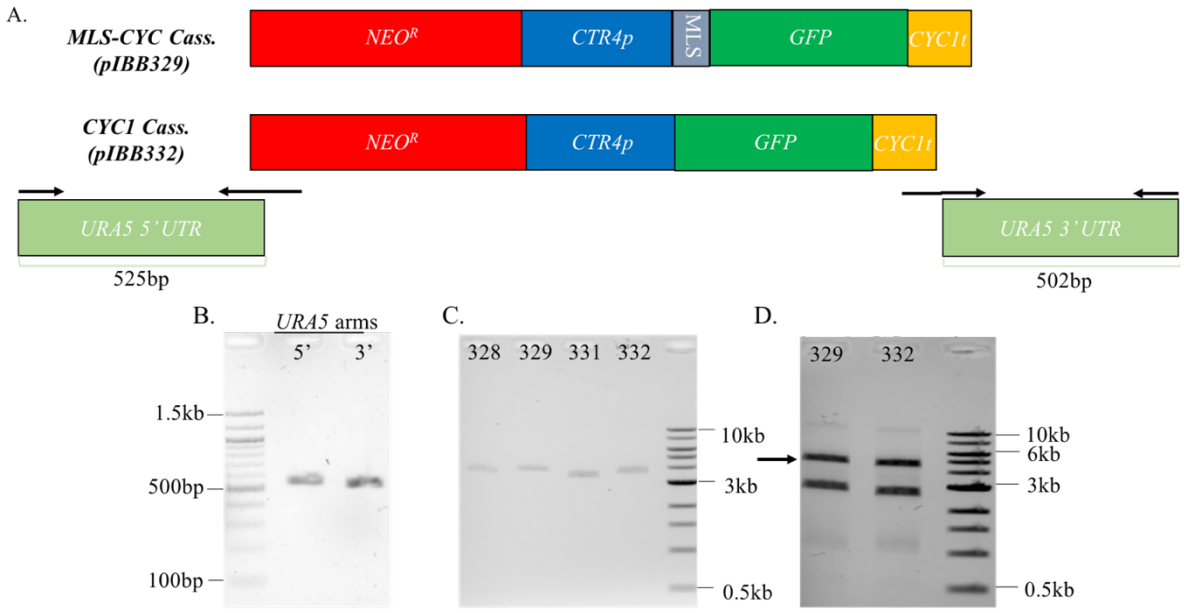

Figure 21 – Construction of the gene cassettes for insertion into *URA5* by homology-driven recombination. (A) Schematic of the 3.61kb c329 (+MLS,+*CYC1t*) and 3.506kb c332 (no MLS,+*CYC1t*) cassettes and the homologous *URA5* flanking sequences. (B) Gel purified *URA5* 5' 525bp and 3' 502bp arms visualized on a 2% TAE-agarose gel. (C) Gel purified cassettes from pIBB328 (3.588kb), pIBB329 (3.650kb), pIBB331 (3.474kb), and pIBB332 (3.546kb) cassettes visualized on a 0.8% TAE-agarose gel. (D) LEFT: Column purified overlap PCR products containing the 4.637kb c329 (+MLS,+*CYC1t*) and 4.543kb c332 (no MLS,+*CYC1t*) cassettes with attached 5' and 3' arms (black arrow indicating desired product) visualized on a 0.8% TAE-agarose gel.

C. deneoformans JEC21 wild type cells were electroporated with approximately 0.70 pmoles (2μg) of column purified overlap PCR products along with 0.23 pmoles (1μg) *CAS9* fragment and 3.0 pmoles (0.7μg) sgDNAs. The transformation cultures were resuspended in ultra

pure water and then divided, with one half being plated onto geneticin-containing (YPD-NEO) media and the other half being plated onto 5-FOA media. This was to determine whether one of the phenotypes was a better *initial* selection than the other. As shown in Figure 22A, plating initially on YPD-NEO resulted in significant quantities of transformant colonies while initially plating on 5-FOA resulted in no significant growth difference from the negative control. The comparable growth between the 5-FOA sample plates and the negative control is suggestive that the colonies likely arose due to spontaneous mutations rather than targeted mutagenesis in *URA5*. Furthermore, none of the colonies assayed from these plates had a NEO^R phenotype. As such, initial selection with NEO was used in all *URA5* mutagenesis experiments in this project. This finding was in-keeping with the preliminary homology-driven recombination experiments using the smaller NEO^R construct (Appendix 5). Seemingly, expression of the CRISPR-Cas9 system, intracellular trafficking, and genomic repair takes a protracted amount of time relative to the expression of NEO^R resistance enzymes.

Transformant colonies from electroporations with all five sgDNAs were screened for dual resistance to Geneticin and 5-FOA. A total of 150 colonies initially plated on YPD-NEO were assayed for 5-FOA resistance, resulting 63 of the 150 exhibiting the desired dual resistance phenotype (Table 2).

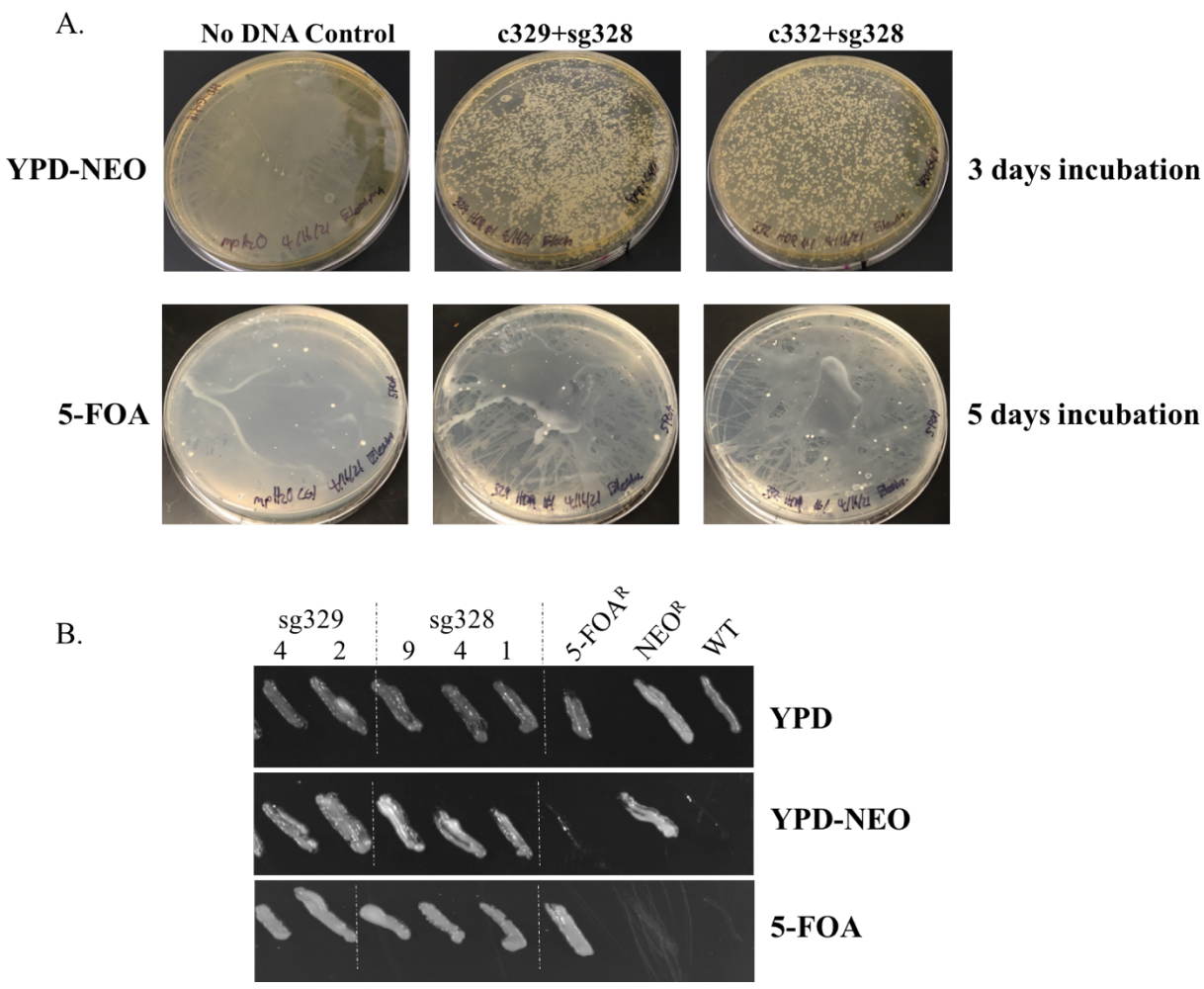

Figure 22 – Selection on YPD-NEO is a better initial selection for homology-directed recombination into *URA5*. (A) YPD-NEO and 5-FOA plates following 3 and 5 days of incubation at 30˚C. c329 is the *NEO*^{R}-*CTR4p-GFP-CYC1t* cassette repair template and c329 is the *NEO*^{R}-*CTR4p*-MLS-*GFP-CYC1t* cassette repair template. sg328 represents the sgDNA used. (B) Restreaks from the *NEO*^{R}-*CTR4p-GFP-CYC1t* repair template NEO plate showing dual resistant phenotypes alongside relevant control strains. WT is JEC21 (IBCN43), 5-FOA^{R} is a uracil synthesis knockout *C. deneoformans* JEC43 strain (IBCN44), and NEO^{R} is a *C. neoformans* KN99 strain that has a *MTW1*-mCherry-*NEO*^{R} cassette (IBCN17).

Table 2 – Growth and phenotypes of the *URA5* HDR excision colonies. sg264-330 denote the sgDNAs added to individual samples, all of which contained *CAS9* and a *NEO*^{R} expression cassette. c329 and 332 denote the +MLS,+*CYC1t* and no MLS,+*CYC1t* repair template cassettes respectively.

Cassette	sgDNA	Transformants	NEO^R	5-FOA^R	Dual Resistant
c329	sg264	25	25	0	0%
	sg265	25	25	2	8%
	sg328	10	10	7	70.0%
	sg329	10	10	9	90.0%
	sg330	35	35	20	57.1%
c332	sg328	15	15	9	60.0%
	sg329	15	15	8	53.3%
	sg330	15	15	8	53.3%

In order to test whether the dual phenotype was due to integration of the cassette into the genome, 49 dual-resistant colonies were tested for NEO^R phenotype stability by passaging them twice on non-selective media, each passage consisting of two days of incubation at 30˚C on YPD before replating them on YPD-NEO. All colonies retained the geneticin-resistance phenotype, suggesting that the exogenous cassettes were integrated into the genome rather than being episomally expressed (not shown).

43 of the dual-resistant phenotype colonies were then screened by PCR for integration of their respective cassette into the *URA5* locus using primers BLO316 and BLO317 that amplified from outside the homologous *URA5* flanking sequence (Fig 23B). Those that did not amplify with those primers were subjected to an internal cassette primer-external genomic amplification using the BLO293 primer (Fig 23C).

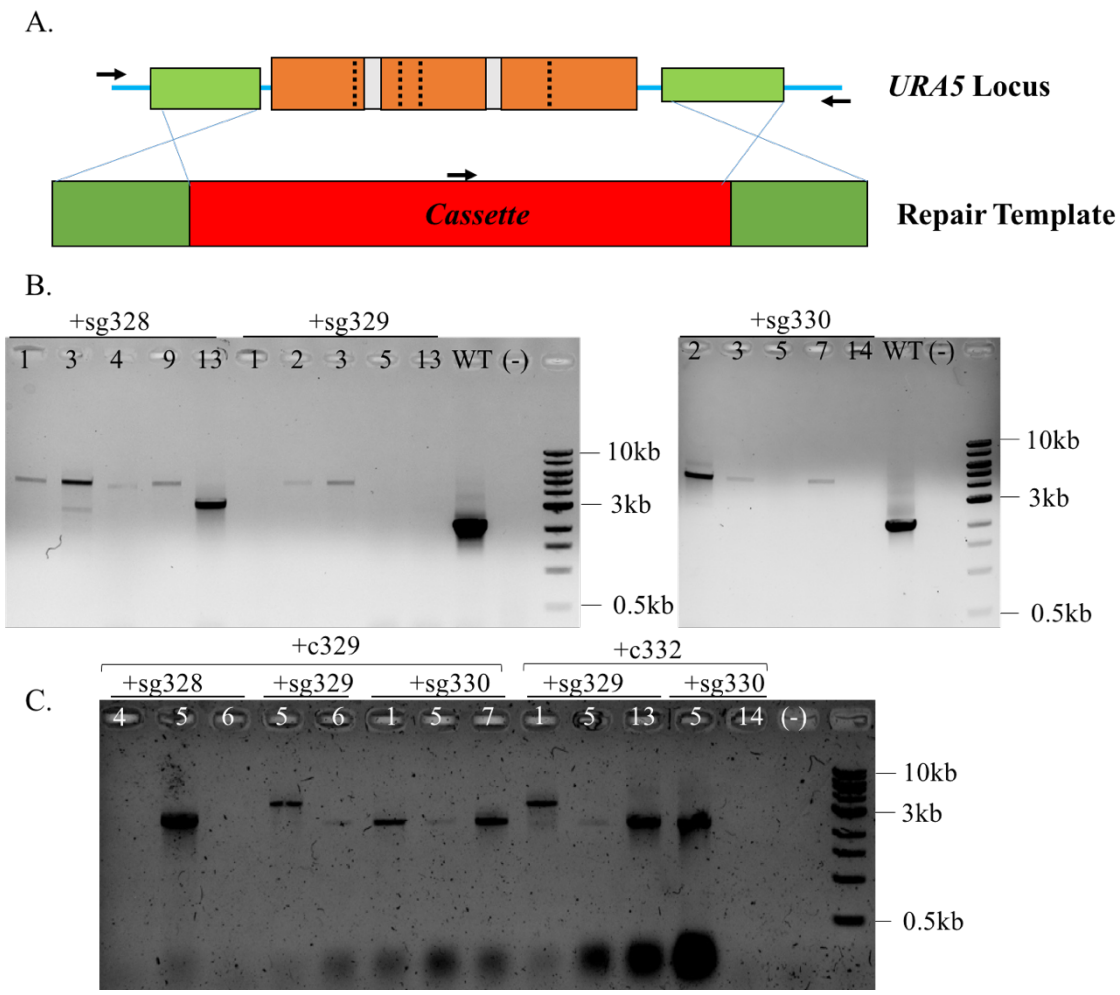

Figure 23 – *URA5* cassette integration assays. sg328-330 represent sgDNAs used to cut *URA5*. (A) Schematic for *URA5* locus homology-driven recombination. Arrows denote primers used to assaying the size of the locus while the line connected the template to the locus represent the regions of homology between repair template and *URA5* UTR. Doted lines represent the sgDNA sites targetting Cas9 to the *URA5* CDS. (B) 0.8% TAE-agarose ethidium bromide gel screening for size of *URA5* locus using primers outside the sites of recombination. All samples are from +c332 repair template transformants. Faithful recombination which should elevate the 1.844kb WT locus to a 4.496kb product. WT is *C. deneoformans* JEC21 genomic DNA sample which produces the non-elevated fragment. 1kb NEB DNA ladder used for sized comparison. (C) Cassette integration assay targeting samples that did not yield amplifications for *URA5* locus. This PCR used the *CTR4p* Forward primer (BLO293) with a reverse primer outside the the recombination site (BLO317) to ascertain if the repair template had been inserted into the *URA5* locus. +c332 corresponds to the no-MLS,+*CYC1t* cassette repair template, which should produce a 2.401kb product. +c329 corresponds to the +MLS,+*CYC1t* cassette repair template, which should produce a 2.511kb product. All samples visualized on 0.8% TAE-agarose ethidium bromide gel with 1kb NEB DNA ladder.

Of the 43 sampled dual resistant colonies, 30 yielded genomic samples positive for *URA5* excision and faithful cassette replacement. Targeting the *URA5* CDS with sg328 yielded 60%

recombination (6/10), sg329 yielded 70% (7/10), and sg330 yielded 74% (17/23) across both templates. See Table 3 for a breakdown of recombination data across each sgDNA and template used.

Table 3– Genotypes of the *URA5* HDR excision colonies. c332 corresponds to the pIBB332 cassette repair template. c329 corresponds to the pIBB329 cassette repair template. sg265-330 represent the sgDNAs used to induce damage in the *URA5* CDS.

Sample		Total Assayed	No Recombination	Abnormal Recombination	Faithful Recombination	%
c329	sg265	2	1	0	1	50.0%
	sg328	5	0	0	3	60.0%
	sg329	5	1	1	3	60.0%
	sg330	18	1	4	13	72.2%
c332	sg328	5	1	1	3	60.0%
	sg329	5	0	1	4	80.0%
	sg330	5	0	0	4	80.0%

Altogether, editing *URA5* using CRISPR-Cas9 was shown to be highly effective. Non-homologous end joining repair, while chaotic, was shown to be readily able to knock out the gene via an error-prone mechanism. Homology-driven DNA repair was also able to knock out *URA5* in a reliable manner; however, it was also able to precisely insert exogenous DNA fragments with homologous flanking sequences. The CRISPR-Cas9 reagent plasmids and strains with chromosomal cassette insertions were saved as glycerol stocks at -80˚C.

3. *Conditional regulation of CdMIP1 via CRISPR-Cas9-mediated promoter replacement.*

Gene manipulation can be accomplished by a variety of mechanisms. Novel genes can be knocked in, endogenous genes can be knocked out, and or the endogenous regulatory elements of a gene changed by knocking-in elements from other genes. Promoter editing is a form of regulatory element alteration where the coding domain of a gene is untouched but its upstream

UTR is changed.[18,19,20] Thereby, the endogenous promoter in that UTR can be knocked out and a new promoter knocked in via recombination. The replacement promoter can be constitutive or conditional, driving *de novo* regulation of the gene without actually editing the encoded protein. To that end, three sgDNAs targeting the promoter of *MIP1* (*MIP1p*) were designed in order to facilitate homology-driven replacement of the endogenous promoter with the conditional *CnCTR4* promoter.

3. a. *Design and assembly of CRISPR-Cas9 reagents targeting the MIP1 5' UTR*

In order to test the CRISPR-Cas9 system developed in this project for the capacity to facilitate promoter replacement, three bridging primers, BLO342, 343, and 344, were designed to make sgDNAs that would cut within a 200bp fragment of the 5'-UTR of *MIP1* (*MIP1p*). Homology-directed DNA repair would then excise and replace that fragment with a *CnCTR4p* conditional promoter while a NEO^R gene would disconnect the regulatory remnants of *MIP1p* from the CDS (Fig 24). The pIBB334 *NEO^R-CTR4p-MIP1 Nterm* cassette (c334) was used as the basis for the repair template. A 726bp sequence homologous to a portion of the *MIP1* 5'-UTR and a 1106bp sequence homologous to a portion of the *MIP1* CDS were added to the flanks of the cassette by overlap PCR (not shown).

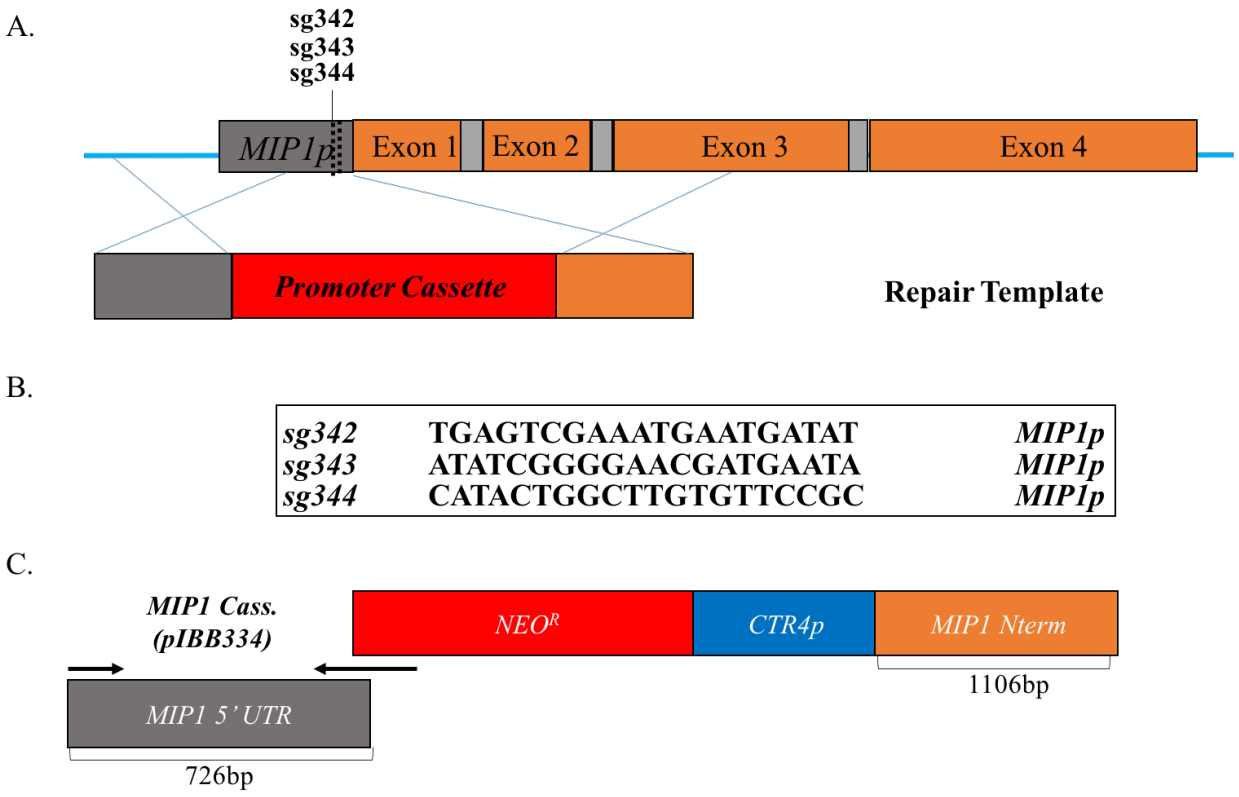

Figure 24 – Homology-driven recombination between a replacement promoter cassette and *MIP1*. (A) Schematic for recombination where blue lines denote strand-crossover between a construct and the genomic target. (B) crDNA sequences for sgDNAs constructed from the BLO342, 343, and 344 primers. (C) Schematic for the pIBB334 promoter cassette repair template. Arrows denote primers used for overlap PCR.

Much like the *URA5* CDS excision experiments, recombination was expected to occur such that approximately 200bp of the *MIP1* 5'-UTR was excised and replaced by the c334 cassette, putting *MIP1* gene expression under the control of the copper-repressible *CnCTR4* promoter.

3. b. *Insertion of a modular gene cassette into the MIP1 5' UTR.*

MIP1 is a putative, essential mitochondrial polymerase whose transcript was shown to be necessary for phenotype viability in *C. deneoformans* by RNA interference (RNAi).[46] RNAi interference is a means of silencing transcription, thereby shutting down translation.[38] In theory,

replacing the endogenous *MIP1* promoter with *CTR4p* would also provide a means of knocking down the *MIP1* transcript. Since the *CTR4p* is strongly down-regulated by elevated copper bioavailability, increasing copper concentrations could be expected to strongly decrease *MIP1* expression. Bathrocuproinedisulfonic acid (BCS) is a copper chelator that is used to deplete copper such that *CTR4p* upregulates genes.[24,47] Conversely, 25μM $CuSO_4$ with 1mM ascorbic acid has been previously used for optimal *CTR4p* down-regulation.[18] If *MIP1* expression is essential for mitochondrial viability, excessive down-regulation by $CuSO_4$ media would result in cell death via respiratory dysfunction while BCS media would maintain sufficient levels of transcript.

C. deneoformans JEC21 wild type cells electroporated with the repair template (2μg, 0.74pmole), *CAS9* fragment (1μg, 0.23pmole), and sgDNA (0.7μg, 3.0pmole) and plated initially on geneticin and BCS-containing YPD media. 105 colonies total, 35 from each +sgDNA sample, were then restreaked on YPD containing $CuSO_4$ and ascorbic acid (Fig 25B) to screen for copper-repressible phenotype. Despite the RNAi results for *MIP1* transcript knock-down, all colonies grew reliably under elevated copper conditions. Albeit, certain colonies had a distinctively lobate appearance (Fig 25B). The lobular pattern is often seen in acapsular strains and contrasts with the normal growth of JEC21, which has a shiny colony appearance as seen in Figure 25C.

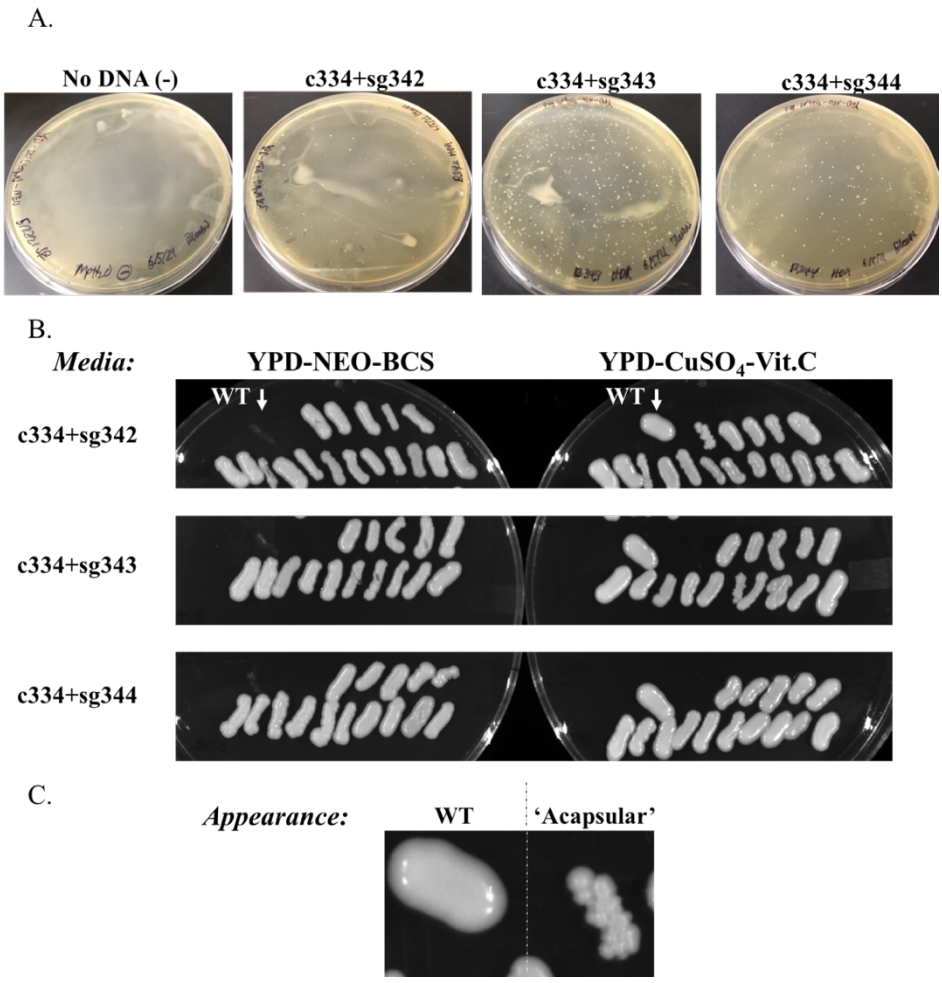

Figure 25 – Replacement of *MIP1* endogenous promoter with the conditional *CTR4p* promoter (A) Transformations on YPD-NEO-BCS plates incubated for three days at 30˚C. (B) Growth of 15 colonies from each transformation on YPD-NEO-BCS and YPD-$CuSO_4$-Ascrobic Acid (Vitamin C) plates incubated for three days at 30˚C. JEC21 was used as a wild type (WT) control. (C) A magnified "acapsular" colony from the c334+sg342 YPD-$CuSO_4$-Ascorbic Acid plate compared to the wild type.

Table 4 – Growth and phenotypes of the *CTR4p-MIP1* colonies.

Sample	Colonies Assayed	NEO^R	Cu^+ Repressed	Irregular Restreaks
+ sg342	35	35	0	7
+ sg343	35	35	0	9
+ sg344	35	35	0	8

To determine whether the survival of the *CTR4p-MIP1* recombination transformants was in spite of endogenous promoter replacement, the genomes of 15 colonies, 5 from each +sgDNA transformation, were screened by PCR. This was biased towards the irregular colonies with four of the five genomes tested being from the "acapsular"-appearing colonies.

One PCR was done using a primer in the *MIP1* 5'-UTR homology arm (BLO339) and another at the 3' end of exon3 well outside the recombination site for the 3' arm (BLO345). Nine of fifteen assayed colonies yielded elevated loci size indicative of recombination (Fig 26B). To confirm that the repair cassette was inserted via faithful homology-driven recombination, a PCR that amplified from the beginning of the *CnCTR4p* sequence in the repair template (BLO293) to the 3' end of *MIP1* exon3 (BLO345) was done as a follow-up. Reactions that did not give a result with 5' arm, exon3 primers were subjected to a second PCR with the *CTR4p*, exon 3 primers (Fig 26C).

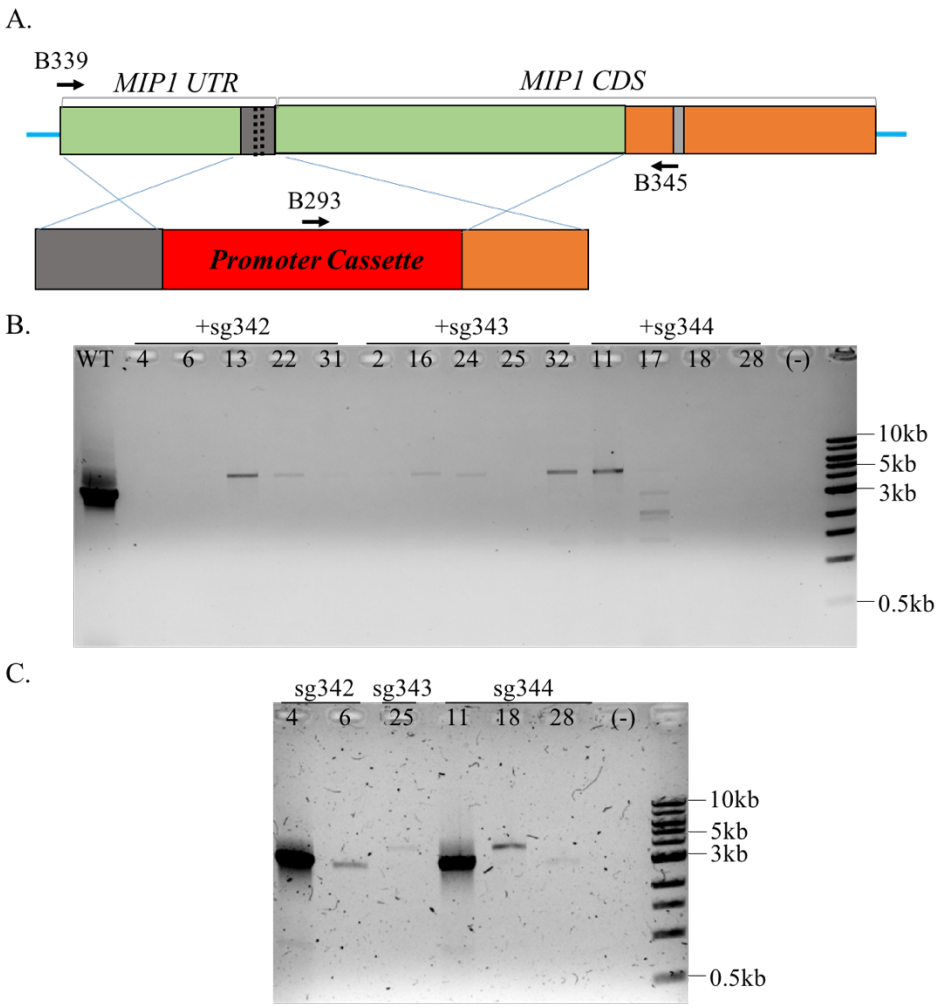

Figure 26 - PCR assays for edited *MIP1* locus. sg342-344 denotes the BLO342-344 sgDNAs. (A) Schematic of the *MIP1* recombination system. Green boxes denote the homologous sequences flanking the pIBB334 *NEO*^{R}*-CTR4p* cassette shown in red. Blue lines indicate how crossing over should occur between the repair template and damaged chromosomal *MIP1* locus. (B) 0.8% TAE-agarose ethidium bromide gel with *MIP1* BLO339,345 amplicon assays visualized with 1kb NEB DNA ladder. WT sample is wild type JEC21 positive control for size reference of the 3.479kb wildtype fragment. Correct insertion of cassette via recombination produces a 5.735kb product. (C) 0.8% TAE-agarose ethidium bromide gel with *CTR4p-MIP1* exon3 amplicon assays visualized with 1kb NEB DNA ladder. Expected band size for correctly inserted cassette is 3.215kb.

Table 5 –Genotypes for *MIP1* promoter replacement colonies. c334 corresponds to the pIBB334 cassette repair template. sg342-344 represent the sgDNAs used to induce damage in the *MIP1* UTR.

Sample		Total Assayed	No Recombination	Abnormal Recombination	Faithful Recombination	%
c334	sg342	5	0	0	5	100%
	sg343	5	0	2	3	60%
	sg344	5	1	0	4	80%

The CRISPR-Cas9 system again facilitated high-fidelity, homology-driven recombination following damage to the *MIP1* 5' UTR (Table 5). Replacement of the endogenous *MIP1* promoter was highly likely given the *CTR4p*-integrated genotypes that were shown via PCR. However, elevated copper conditions did not induce a nonviable phenotype via downregulation of *MIP1*.

CHAPTER IV. DISCUSSION AND FUTURE DIRECTIONS

1. *The URA5 gene was edited in vivo via CRISPR-Cas9 induced damage followed by NHEJ mutagenesis and HDR-mediated recombination.*

The *URA5* gene in *Cryptococcus* encodes the enzyme, orotidine 5' phosphate decarboxylase, which plays a necessary role in the yeast's uracil synthesis pathway. Knockout of this gene is sufficient to disrupt uracil synthesis in these yeasts.[48] 5-fluoroorotic acid is a negative selection agent against cells actively synthesizing uracil and is a common reagent in fungal genetics.[49] *URA5* was used in this project as a CRISPR-Cas9 target to ascertain the ability of the system for precision gene editing. Disruption of the reading frame and excision of the full *URA5* gene was accomplished reliably; transformations with CRISPR-Cas9 constructs induced resistance to 5-FOA in repeatable experiments. *URA5* knock-out by homology-driven recombination and non-homologous end joining DNA repair were both viable editing techniques, though with the interesting nuance that NHEJ-driven disruption results in the random insertion of DNA into damage sites. Seemingly, there is no discrimination in insertion of certain DNAs over others, though this finding requires further study to replicate and validate. Altogether, a robust RNA-guided gene editing system was developed and has been shown to accurately edit the cryptococcal genome on-demand.

The expression of both an sgRNA and *CAS9* was shown to be necessary for *in vivo* genome editing. When an sgDNA construct is not present, uracil knock-out was shown to not occur (Fig 17). This demonstrated that CRISPR-Cas9 will not randomly cut DNA within the genes encoding for enzymes catalyzing the uracil synthesis pathway. Conversely, when sgRNA was present, mutagenesis-driving damage was clearly targeted to the uracil synthesis pathway (Fig 17, 22). Five individual sgDNAs were designed to guide Cas9 to cut in *URA5*; three produced sgRNAs targeting *URA5* Exon 2 (sg265, 328, and 330), one targeted Exon 1 (sg329),

and one targeted Exon 3 (sg265). Additionally, two *URA5* HDR-driving constructs were transformed into *C. deneoformans* with different combinations of sgDNAs to knock-in a NEO^R cassette with a conditionally regulated GFP gene. Three of the sgRNAs, sg328, 329, and 330, were shown to reliably target DNA damage capable of NHEJ-disruption and/or homology-driven recombination when in the presence of homologous repair templates. sg265 was capable of low-efficiency *URA5* knock-out while sg264 was comparable to negative controls in all experiments. The NEO^R-conditional GFP repair templates were shown to accurately recombine when *URA5* was damaged; conversely, constructs lacking homologous flanks became fragmented and were haphazardly inserted into damage sites (Fig 19,23). Seemingly, the difference in targeted-mutagenesis between the sgDNAs was due to PAM design. sg264 and 265 contained 23bp crDNAs containing a 3bp PAM complement while sg328-330 contained 20bp crDNAs lacking the aforementioned PAM complement (Fig 16).

In transformations where *URA5* was targeted, generation of robust resistance to 5-FOA required more than three days of incubation. Initial selection on NEO-containing media appeared to function well, allowing us to select for cells that were successfully transformed during the elongated incubation. Initial selection on 5-FOA following 45 minutes, three hours, and overnight recovery times did not yield significant growth on 5-FOA media relative to negative controls. Accordingly, Δ*ura5* phenotype assays were most effective when using NEO selection first, followed by 5-FOA selection. This is presumably due to a multiday time requirement for the sgDNA and *CAS9* constructs to express, localize, and induce DNA repair *in vivo*. Time trials could be organized in the future to find the necessary time required, though this project found that approximately three days was sufficient for CRISPR-Cas9 induced *URA5* knock-out.

NHEJ trials with sgDNAs sg328, 329, and 330 co-transformed with a NEO^R episomal selection marker with no intrinsic homology to the target were used to try and confirm the 3-4 bp cut sites upstream from the targeted PAMs. These trials found perplexing, yet consistent results; random exogenous DNAs were found to insert within 3-4 bp of the cut sites with no discernible pattern or discrimination. Perhaps most interestingly, restoration of the chromosome with frame-shift mutations was found to not occur what-so-ever; recombination with an exogenous DNA was the clear preference *in vivo* over a direct end-joining repair with the separated chromosomal fragment. The *C. deneoformans* non-homologous end joining DNA repair mechanism appears to take a 'plug the hole with any means necessary' approach to restoring chromosomal integrity and seems to be 'blind' in doing so. The organism appears to just 'grab' any DNA in the nucleus and stitch into a bluntly-cut, double-stranded damage site. This may help to explain a phenomenon found in literature regarding the *C. neoformans* species complex.

Previous studies in the *Cryptococcus* had described a common issue, or at least the perception thereof, when using biolistics for homology-driven insertion experiments. Those experiments were described as frequently suffering from high rates of off-target construct insertions.[31] As was discussed in the Introduction, biolistic transformation has been the traditional means of transforming *C. deneoformans*. This approach involves the violent insertion of DNA via high energy, coated gold pellets.[15] The energy involved in forcing the DNA into the cytoplasm poses the risk of damaging the nucleus and/or DNA within it as the kinetic energy transfers into cytoplasmic as well. While it has been shown that there is a low background rate of mutagenesis caused by biolistically-induced DNA damage, the finding that *C. deneoformans* exhibits a chaotic NHEJ repair mechanism favoring the insertion of exogenous DNA fragments over endogenous chromosomes is well described in literature and defended by this project's

URA5 NHEJ mutagenesis results.[31] It should be noted that NHEJ is the preferred DNA repair mechanism of species in the *C. neoformans* species complex given their primarily haploid nature; the integration of exogenous DNA via NHEJ into chromosomal breaks could explain how studies using biolistic transformation suffered from off-target integrations. The relatively 'gentle' approach of electroporation paired with CRISPR-Cas9 likely mitigates this risk. That being said, this project did not screen for off-target insertions of exogenous DNA; such screening would require the use of some form of Southern Blotting protocol to ascertain the presence of unintended insertions.[50]

More evidence and experimentation with the CRISPR-Cas9 system is desirable. Multiplexing experiments could be done to ascertain the viability of multiple gene edits. Experiments screening for potential off-target mutagenesis are also needed as follow-ups to this project. Despite the questions on off-target insertion and cryptococcal DNA repair that were left unsatisfied by Aim II, it was shown that transformed populations containing >40% recombination positive colonies are reliably obtainable when using a transient electroporation protocol targeting the *URA5* gene.

2. *CRISPR-Cas9 crDNAs must be 20nt and not have a complement covering targeted PAM.*

Cas9 endonuclease requires a network of RNAs to guide the protein towards a DNA target.[26,27] Cas9 additionally requires a three nucleotide sequence, a Protospacer Adjacent Motif [PAM], immediately adjacent to the targeted DNA sequence in order to catalyze a double-stranded DNA break. To that end, constructs containing a *U6* promoter and an encoded sgRNA capable of guiding and activating Cas9 were designed in this project. The initial sgDNAs, sg264 and 265, were designed to incorporate a 20nt DNA complement with a 3nt PAM complement,

meaning that the entire crDNA sequence was 23nt long and covered the targeted chromosomal PAM when binding. sg328, 329, and 330 were designed later and contained 20bp crDNA sequences that did not contain the 3nt PAM complement like their sg264 and 265 analogs; the sg328-330 sgDNAs made a canonical 20nt crRNA element when transcribed. It was shown that sg264 and 265 did not reliably induce high levels of *URA5* knockout while sg328, 329, and 330 readily did across nonhomologous end-joining, homology-driven recombination, and transformed DNA quantity trials (Fig 17, Table 2). Experiments with various DNA concentrations were only done in preliminary trials and should be replicated with sg328, 329, and 330; the high effectiveness of their sgRNAs in inducing chromosomal damage may not necessitate the high DNA concentrations used for obtaining CRISPR-Cas9 activity with sg264 and sg265.

As per Table 1, 60-80% of dual resistant strains transformed with the 20nt complement sgDNAs were shown to have edited genotypes. When using identical recombination templates, dual resistance conferral was 52% in a culture transformed with the sg330 20nt crDNA while transformants containing the sg264 and 265 23nt crDNAs averaged out to a 4% dual resistance. CRISPR-Cas9 activity is seemingly much higher when using 20nt complementary sgDNAs that do not contain a 3nt PAM complement. Presumably, the PAM compliment alters binding between the Cas9 endonuclease and targeted DNA. The PAM is absolutely necessary for Cas9 activity. If the crRNA NCC complement obfuscates binding between Cas9 and the target's NGG PAM, this could explain why sg264 resulted in no detectable *URA5* knockout and sg265 resulted in limited effectiveness.

3. *A modular gene cassette was assembled and tested.*

A gene expression cassette containing a *NEO*^{R} selection marker, a *CnCTR4* promoter, and a *GFP* coding frame with no stop codon or terminator was assembled for use as a reagent for CRISPR-Cas9 gene editing. The cassette was ligated into a pCR2.1 TOPO plasmid, making a final 7.074kb construct. By inserting unique sites between the fragments, the cassette was readily modified by inserting a variety of fragments into the construct. Altogether, the cassette made in Figure 19 was shown to be readily modifiable.

11 vectors containing the core cassette or modified variants thereof were made over the course of this project. The 7.074kb core cassette plasmid [*NEO*^{R}-*CTR4p*-*GFP*-no stop codon] was assembled and the orientation of its fragment sequences confirmed using restriction digests (Fig 5). This initial vector was then modified by inserting a predicted MLS from *CnMIP1* between the *CTR4p* and *GFP* fragments. Four additional constructs were made by attaching a stop-terminator fragment to the MLS and no MLS vectors by attaching a *CYC1* and a *URA5* terminator to the 3' end of GFP. The core cassette was also used to make another construct, a 7.408kb *NEO*^{R}-*CTR4p*-*CdMIP1* N-terminus vector, to serve as a repair construct for the *MIP1* endogenous promoter.

NEO^R phenotype was conferred when transforming of *C. neoformans* KN99 and *C. deneoformans* JEC21 with these various vectors, thereby demonstrating expression of the 1.816kb *NEO*^{R} fragment. Transformation of those same strains with constructs containing complete GFP genes (*CTR4p*-(MLS)-*GFP*-*CYC1t*) did not produce fluorescent signal that was discernible over background autofluorescence (Appendix 6). It is unclear whether this is an

expression issue with the *CTR4p* promoter, the 3' UTRs used as terminators, or a protein stability and/or folding issue with GFP; Western blotting should be used to confirm expression since fluorescent imaging experiments were inconclusive. In addition, it may be a good idea to try synthesizing cassettes with more traditional cryptococcal terminators: *GPD1t*, *TPS1t*, etc. The *CnURA5* and *CnCYC1t* 3' UTR fragments used in this study may not be sufficient to terminate transcription and could possibly be producing aberrated transcripts.

4. *MIP1 might not be a necessary gene or the CnCTR4p construct may be 'leaky.'*

CdMIP1 is a gene in the nucleus that is thought to encode for the enzyme, DNA Polymerase Gamma [PolG]. Mitochondria rely on the import of nuclear gene products like PolG despite retaining some key metabolic enzymes in an attenuated genome in the matrix.[51] Mip1p is presumed to be one such imported product and is assumed to play an essential role in maintaining the yeast's mitochondria. Mitochondria are the organelles responsible for catalyzing cellular respiration and have rightfully been given the metaphor, 'the powerhouse of the cell.' For aerobic organisms like *Cryptococcus*, the role mitochondria play in respiration dictates a necessity for mitochondrial maintenance. Thereby, deleting a gene essential for mitochondrial upkeep would likely result in a nonviable phenotype. In *S. cerevisiae*, knockout of its *MIP1* ortholog is sufficient to abolish respiration by destabilizing the mitochondrial genome.[52] Therefore, knocking out *MIP1* in *Cryptococcus* may induce a similar, yet deleterious disruption of respiration.

MIP1 was used in this project as a CRISPR-Cas9 target to determine the viability of the system for promoter-replacement for a putative essential gene. To that end, disruption and

excision of a fragment of the *MIP1* 5' UTR was accomplished via homology-directed DNA repair. A *NEO*^{R}*-CnCTR4p* cassette was inserted in place of the excised UTR. The NEO^{R} gene was autonomous and served as a regulatory disconnect between the remains of the endogenous *MIP1* promoter and its CDS. This presumably made the *CTR4* promoter the primary regulatory element for the *MIP1* CDS. *CTR4p* is down-regulated in *Cryptococcus* when subjected to high copper environments; this ideally would have allowed the recombinant *MIP1* gene to be knocked-down by a similar mechanism. Minimal media containing 25μM $CuSO_4$ and 1mM Ascorbic Acid was found to be sufficient for *CTR4p* repression in Ory *et al.*; however, in this project those conditions did not result in a non-viable phenotype via *MIP1* knockdown (Fig 25).[18] Genotypic screening was able to confirm high-fidelity promoter replacement using the CRISPR-Cas9 in the *MIP1* 5' UTR (Fig 26). As such, the transient CRISPR system developed in this project has been shown to accurately edit the cryptococcal genome in both the CDS and UTRs of at least two genes. However, evidence for *MIP1*'s essentiality was not found.

As was mentioned above, knock-out of *MIP1* in *S. cerevisiae* is known to confer a respiration-deficient phenotype.[52] This deficiency is not fatal due to the species' capacity to meet its energetic needs via fermentation. *C. deneoformans* is an obligate aerobe that requires respiration to meet its needs and therefore cannot survive without functional mitochondria.[3,46] Growth on copper-depleted YPD-NEO-400μM BCS was used to cultivate transformants for approximately three days before using a negative selection assay with YPD-25μM $CuSO_4$-1mM Ascorbic Acid. YPD with elevated copper was shown to not be sufficient for the abolition of growth using both solid and liquid media. This perplexing finding requires further investigation; the viable phenotype on elevated-copper media possibly suggests issues with the *CTR4p* sequence; *CdMIP1* translation may still be viable with low transcript copy numbers leaking

'through' the down-regulation induced by this promoter. There is also the possibility that the NEO^R gene in the inserted cassette did not fully disconnect the endogenous regulatory elements from the *MIP1* CDS, thereby hampering repression by *CTR4p*. Alternatively, it is possible that *CdMIP1* is simply not an essential gene and its knock-out does not abolish respiration.

The *CTR4p* sequence integrated in the pIBB326-334 constructs was shown to contain a minimum of two canonical CuSEs known to respond to Cuf1 regulation along with a canonical TATA box (See Appendix 3.e, 3.h).[24] Ory *et al.* was able to show that similar *CTR4p* fragments containing at least two CuSEs were responsive to up-regulation by copper chelation and responsive to down-regulation by copper-elevation.[18] That being said, the Ory *et al.* study did detect a limited amount of reporter activity suggestive of promoter 'leakage.' Conditional promoters undergoing repression may not entirely knock-down transcription, meaning that some transcript is still available for translation.[53] Mitochondrial proteins' transcription and translation are highly dynamic, highly regulated processes.[54] It would not be surprising if a leaky *CTR4p* promoter allows for sufficient transcription of *MIP1* to avert complete mitochondrial dysfunction

More investigation into the status of Mip1p protein and mRNA content in these transformed lines is certainly needed. A repair template with an alternative protein-tag to GFP, like say a His-tag, could easily be assembled and inserted into the chromosome to enable Mip1p quantification.[55] Analysis of growth rates and respiration rates would also be useful experiments for determining the relative health of the transformants' mitochondria. Furthermore, optimization of the *GFP* sequence in our pIBB328-332 constructs could also be an avenue for investigating Mip1p status in these cultures while undergoing elevated-copper selection.

References:

1. Hagan, F. et. Al. "Recognition of seven species in the *Cryptococcus gatti*/*Cryptococcus neoformans* species complex." *Fungal Genetic Biology*, Vol. 78. Pg. 16-48. 2015. 09/25/2020. DOI: 10.1016/j.fgb.2015.02.009
2. Hagen, F. et. al. "Importance of Resolving Fungal Nomenclature: the Case of Multiple Pathogenic Species in the *Cryptococcus* Genus." *America Society for Microbiology*| mSphere, Vol. 2, Issue. 08/30/2017. 06/08/2021. DOI: 10.1128/mSphere.00238-17
3. Alexander, B. D. et al. Heitman, J. et al. ed. *Cryptococcus:* From Human Pathogen to Model Yeast. ASM Press, Washington D.C. Pg. 17-23. 2011. 10/15/2019. Print.
4. Cuomo, C. A., Rhodes, J., and Desjardins, C. A. "Advances in *Cryptococcus* genomics: insights into the evolution of pathogenesis." *Memorias Do Instituto Oswaldo Cruz*, Vol. 113, Issue 7. 02/19/2018. 01/29/2021. DOI: 10.1590/0074-02760170473
5. Cherniak, R. and Sundstrom, J. B. "Polysaccharide Antigens of the Capsule of *Cryptococcus neoformans*." *Infection and Immunity*, Vol. 62, Issue 5. Pg. 1507-1512. 05/1994. 06/20/2021. PMID: 8168912
6. Bovers, M., Hagen, F., and Boekhout, T. "Diversity of the *Cryptococcus neoformans-Cryptococcus gattii* species complex." *Revista Iberoamericana de Micologia*, Vol. 25, Issue 1. 2008. 10/15/2019.
7. Li, J. et al. "The 14-3-3 Gene Function of *Cryptococcus neoformans* Is Required for its Growth and Virulence." *Journal of Microbiology and Biotechnology*, Vol. 26, Issue 5. 2016. 10/15/2019. DOI: 10.4014/jmb.1508.08051
8. Perfect, J. R. et. al. "Clinical Practice Guidelines for the Management of Cryptococcal Disease: 2010 Update by the Infectious Diseases Society of America." *Clinical Infectious Diseases*, Vol. 50, Issue 3. 02/01/2010. 11/05/2020. DOI: 10.1086/649858

9. Weete, J. D., Abril, M., and Blackwell M. "Phylogenetic Distrigution of Fungal Sterols." *PLOS One*. 05/28/2010. 06/15/2021. DOI: 10.1371/journal.pone.0010899.

10. Moen, M. D. et. al. "Liposomal Amphotericin B – A review of its Use as Empirical Therapy in Febrile Neutropenia and in the Treatment of Invasive Fungal Infections." *Drugs*, Vol. 69, Issue 3. Pg. 361-392. 02/2009. 12/02/2019. DOI: 10.2165/00003495-200969030-00010.

11. Laniado-Laborin, R. and Cabrales-Vargas, M. N. "Amphotericin B: side effects and toxicity." *Revista Iberoamericana de Micologia*, Vol. 26, Issue 4. 10/2009. 06/15/2021. DOI: 10.1016/j.riam.2009.06.003

12. Fu, J., Hettler, E., and Wickes B. L. "Split marker transformation increases homologous integration frequency in *Cryptococcus neoformans*." *Fungal Genetics and Biology*, Vol. 43, Issue 3. Pg. 200-212. 03/2006. 06/09/2021. DOI: 10.1016/j.fgb.2005.09.007

13. du Plooy, L. M. et. al. "Functional Characterization of Cryptococcal Genes: Then and Now." *Frontiers in Microbiology*, Vol. 9. 09/20/2018. 01/29/2021. DOI: 10.3389/fmicb.2018.02263

14. Fan, Y. and Lin, X. "Multiple Applications of a Transient CRISPR-Cas9 Coupled with Electroporation (TRACE) Systemin the *Cryptococcus neoformans* Species Complex." *Genetics|Investigation*, Vol. 208, Issue 4. Pg. 1357-1372. 04/2018. 11/09/2019. DOI: 10.1534/genetics.117.300656

15. Toffaletti, D. L. et. al. "Gene transfer in *Cryptococcus neoformans* by use of biolistic delivery of DNA." *Journal of Bacteriology*, Vol. 175, Issue 5. 03/1993. 06/09/2021. DOI: 10.1128/jb.175.5.1405-1411.1993

16. Wang, P. Mitchell, A. P. ed. "Two Distinct Approaches for CRISPR-Cas9-Mediated Gene Editing in *Cryptococcus neoformans* and Related Species." *Host-Microbe Biology*, Vol. 3, Issue 3. 06/2018. 01/29/2021. DOI:10.1128/mSphereDirect.00208-18

17. Edman, J. C. and Kwon-Chung, K. J."Isolation of the *URA5* gene from *Cryptococcus neoformans var. neoformans* and its use as a selective marker for transformation." *Molecular*

and Cellular Biology, Vol. 10, Issue 9. Pg 4538-4544. 09/1990. 06/30/2021. DOI: 10.1128/mcb.10.9.4538

18. Ory, J. J. et al. "An efficiently regulated promoter system for *Cryptococcus neoformans* utilizing the *CTR4* promoter." *Yeast*, Vol. 21, Issue 11. 08/05/2004. 10/20/2019. DOI: 10.1002/yea.1139

19. Del Poeta, M. et al. "*Cryptococcus neoformans* Differential Gene Expression Detected *In Vitro* and *In Vivo* with Green Fluorescent Protein." *Infection and Immunity*, Vol. 67, Issue 4. Pg. 1812-1820. 04/1999. 06/15/2021. PMID: 10085022

20. Wickes, B. L. and Edman, J. C. "The *Cryptococcus neoformans GAL7* gene and its use as an inducible promoter." *Molecular Microbiology*, Vol. 16, Issue 6. 06/1995. 06/09/2021. DOI: 10.1111/j.1365-2958.1995.tb02335

21. Matharu, N. et al. "CRISPR-mediated activation of a promoter or enhancer rescues obesity caused by haploinsufficiency." *Science*, Vol. 363, issue 6424. 12/13/2019. 06/15/2021. DOI: 10.1126/science.aau0629

22. Ormerod, K. L. et al. "Comparative Genomics of Serial Isolates of *Cryptococcus neoformans* Reveals Gene Associated with Carbon Utilization and Virulence." *G3: Genes, Genomes, Genetics*, Vol. 3, Issue 4. 4/1/2013. 10/15/2019. DOI: 10.1534/g3.113.005660

23. Waterman, S. R. et al. "Role of *CTR4* in the Virulence of *Cryptococcus neoformans*." *American Society for Microbiology*, Vol. 3, Issue 5. 10/2/2012. 10/20/2019. DOI: 10.1128/mBio.00285-12

24. Waterman, S. R. et al. "Role of a CUF1/CTR4 copper regulatory axis in the virulence of *Cryptococcus neoformans*." *The Journal of Clinical Investigation*, Vol. 117, Issue 3. Pg. 794-802. 03/01/2007. 06/22/2021. DOI: 10.1172/JCI30006

25. Beaudoin, J. and Labbe, S. "The fission yeast copper-sensing transcription factor Cuf1 regulates the copper transporter gene expression through an Ace1/Amt1-like recognition

sequence." *Journal of Biological Chemistry*, Vol. 276, Issue 18. 05/04/2001. 06/09/2021. DOI: 10.1074/jbc.M011256200

26. Jinek, M. et al. "A programmable dual-RNA-guided DNA endonuclease in adaptive bacterial immunity." *Science*. Vol. 337, Issue 6096. Pg. 816-821. 08/17/2012. 06/30/2021. DOI: 10.1126/science.1225829

27. Doudna, J. A. and Charpentier, E. "Genome editing. The new frontier of genome engineering with CRISPR-Cas9." *Science*, Vol. 346, Issue 6212. 2014. 05/19/2021. DOI: 10.1126/science.1258096

28. Xiao-Jie, L. et. al. "CRISPR-Cas9: a new and promising player in gene therapy." *Journal of Medical Genetics*, Vol. 52, Issue 5.04/16/2015. 11/20/2019. DOI: 10.1136/jmedgenet-2014-102968

29. Taxis, C. and Knop, M. "System of centromeric, episomal, and integrative vectors based on drug resistance markers for *Saccharomyces cerevisiae*." *Biotechniques*, Vol. 40, Issue 1. 05/21/2018. 06/20/2021. DOI: 10.2144/000112040

30. Janbon, G. et. al. "Analysis of the Genome and Transcriptome of *Cryptococcus neoformans var. grubii* Reveals Complex RNA Expression and Microevolution Leading to Virulence Attenuation." *PLoS Genetics*, Vol. 10, Issue 4. 04/17/2014. 06/09/2021. DOI: 10.1371/journal.pgen.1004261

31. Friedman, R. Z. et al. "Unintended Side Effects of Transformation Are Very Rare in *Cryptococcus neoformans*." *G3: Genes, Genomes, Genetics*, Vol. 8, Issue 3. Pg. 815-822. 03/01/2018. 06/19/2021. DOI: 10.1534/g3.117.300357

32. Goins, C. L., Gerik, K. J., and Lodge, J. K. "Improvements to gene deletion in the fungal pathogen *Cryptococcus neoformans*: Absence of Ku proteins increases homologous recombination, and co-transformation of independent DNA molecules allows rapid complementation of deletion phenotypes." *Fungal Genetics and Biology*, Vol. 43, Issue 8. Pg. 531-544. 08/2006. 06/09/2021. DOI: 10.1016/j.fgb.2006.02.007

33. Yadav, V. et al. “Centromere scission drives chromosome shuffling and reproductive isolation.” *Proceedings of the National Academy of Sciences of the United States of America*, Vol. 117, Issue 14. Pg. 7917-7928. 04/07/2020. 06/20/2021. DOI: 10.1073/pnas.1918659117

34. Min, K. et al. “Candida albicans Gene Deletion with a Transient CRISPR-Cas9 System.” *mSphere*, Vol. 1, Issue 3. 2016. 06/30/2021. DOI: 10.1128/mSphere.00130-16

35. Wang, Y. et. Al. “A ‘suicide’ CRISPR-Cas9 system to promote gene deletion and restoration by electroporation in *Cryptococcus neoformans*.” *Scientific Reports*. 08/09/2016. 05/08/2020. DOI: 10.1038/srep31145

36. WizardPlus SV MiniPreps DNA Purification System Quick Protocol. Promega.com. https://www.promega.com/-/media/files/resources/protcards/wizard-plus-sv-minipreps-dna-purification-system-quick-protocol.pdf?la=en

37. Boggs, J. E. and Bose, I. “Characterizing the Role of DNA Polymerase Gamma in the Yeast, *Cryptococcus neoformans*.” Unpublished Thesis. WCU. 11/7/2017. 10/15/2019.

38. Bose, I. and Doering, T. L. “Efficient implementation of RNA interference in the pathogenic yeast *Cryptococcus neoformans*.” *Journal of Microbiological Methods*, Vol. 86, Issue 2. 04/29/2011. 11/09/2019. DOI: 10.1016/j.mimet. 2011.04.014

39. WizardSV Gel and PCR Clean-Up System Quick Protocol. Promega.com. https://www.promega.com/-/media/files/resources/protcards/wizard-sv-gel-and-pcr-clean-up-system-quick-protocol.pdf?la=en

40. Duo Peng and Rick Tarleton. “EuPaGDT: a we tool tailored to design CRISPR guide RANs for eukaryotic pathogens.” *Microbial Genomics*. 2015. 07/06/2021. DOI: 10.1099/mgen.0.000033

41. Guo, W. et al. “An improved overlap extension PCR for simultaneous multiple sites large fragments, insertion, deletion and substitution.” *Scientific Reports*, Vol. 9 10/30/2019. 11/09/2019. DOI: 10.1038/s41598-019-52122-8

42. Schindelin, J. et al. “Fiji: an open-source platform for biological-image analysis.” *Nature Methods*, Vol. 9, Issue 7. Pg. 676-682. 2012. 07/06/2021. DOI: 10.1038/nmeth.2019.

43. Zaret, K. S. and Sherman, F. “DNA sequence required for efficient transcription termination in yeast.” *Cell*, Vol. 28, Issue 3. 03/1982. 06/20/2021. Pg. 563-573. DOI: 10.1016/0092-8674(82)90211-2

44. Ito, Y. et al. “Exchange of endogenous and heterogeneous yeast terminators in *Pichia pastoris* to tune mRNA stability and gene express.” *Nucleic Acids Research*, Vol. 48, Issue 22. 12/16/2020. 6/20/2021. DOI: 10.1093/nar/gkaa1066

45. Takemura, T. et al. “Construction of a Selectrable Marker Recycling System and the Use in Epitope Tagging of Multiple Nuclear Genes in the Unicellular Red Alga *Cyanidioschyzon merolae*.” *Plant and Cell Physiology*, Vol. 59, Issue 11. Pg. 2308-2316. 11/2018. 06/20/2021. DOI: 10.1093/pcp/pcy156

46. Walter, S. R. and Bose, I. “Characterization of DNA Polymerase Gamma in the basidiomycetous yeast, *Cryptococcus neoformans*.” Unpublished Thesis. WCU. 04/2020. 07/09/2021.

47. Gordge, M. P. et al. “Copper chelation-induced reduction of the biological activity of S-nitrosothiols.” *British Journal of Pharmacology*, Vol. 114, Issue 5. Pg 1083-1089. 03/1995. 06/30/2021. DOI: 10.1111/j.1476-5381.1995.tb13317.x

48. Kwon-Chung, K. J. et al. “Selection of ura5 and ura3 mutants from the two varieties of *Cryptococcus neoformans* on 5-fluoroorotic acid medium.” *Journal of Medical and Veterinary Mycology*. Vol. 30, Issue 1. 1992. 5/28/21 PMID: 1573522.

49. Boekke, J. d. et al. “5-fluoroorotic acid as a selective agent in yeast molecular genetics.” *Methods in Enzymology*, Vol. 154. Pg. 164-175. 1987. 5/28/2021. DOI: 10.1016/0076-6879(87)54076-9.

50. Yang, Z. et al. “Molecular and genetic analysis of the *Cryptococcus neoformans MET3* gene and a met 3 mutant.” *Microbiology*, Vol. 148, Issue 8. 08/01/2002. 06/19/2021. DOI: 10.1099/00221287-148-8-2617

51. Lodi, T. et al. “DNA polymerase γ and disease: what we have learned from yeast.” *Frontiers in Genetics.* 03/17/2015. 06/29/2021. DOI: 10.3389/fgene.2015.00106

52. Baruffini, E. et al. “Genetic and chemical rescue of the *Saccharomyces cerevisiae* phenotype induced by mitochondrial DNA polymerase mutations associated with progressive external ophthalmoplegia in humans.” *Human Molecular Genetics*, Vol. 15, Issue 19. Pg. 2846-2855. 10/01/2006. 06/29/2021. DOI: 10.1093/hmg/ddl219

53. Huang, L. et al. “Effects of promoter leakage on dynamics of gene expression.” *BMC Systems Biology*, Vol. 9, Issue 16. 03/21/2015. 06/29/2021. DOI: 10.1186/s12918-015-0157-z

54. Barchiesi, A. and Vascotto, C. “Transcription, Processing, and Decay of Mitochondrial RNA in Health and Disease.” *International Journal of Molecular Sciences*, Vol. 20, Issue 9. 05/03/2019. 06/29/2021. DOI: 10.3390/ijms20092221

55. Spelbrink, J. N. “*In vivo* Functional Analysis of the Human Mitochondrial DNA Polyermase PolG Expressed in Cultured Human Cells.” *The Journal of Biological Chemistry*, Vol. 275, Issue 32. Pg. 24818-24828. 08/11/2000. 06/30/2021. DOI: 10.1074/jbc.M000559200

56. Chatterjee, N and Walker, G. C. “Mechanisms of DNA damage, repair, and mutagenesis.” *Environmental Mutagen Society*, Vol. 58, Issue 5. 06/2017. 06/20/2021. DOI: 10.1002/em.22087

57. Caza, M. et. al. “The Sec1/Munc18 (SM) protein Vps45 is involved in iron uptake, mitochondrial function and virulence in the pathogenic fungus *Cryptococcus neoformans*.” *PLOS Pathogens*. 08/2/2018. 05/18/2021. DOI: 10.1371/journal.ppath.1007220

APPENDIX

1. *Primers used in project:*

Name:	Description	Sequence	Restriction Sites
BLO66	*Cd/CnURA5* Intron1-Exon2 F Sequencing primer	TCGGCAACTTTACCTTGAAGTC	
BLO67	*Cd/CnURA5* Intron1-Exon2 R Sequencing primer	ACCGAccatagtaccgccct	
BLO258	*GDP-CAS9* F	CATGCATCTAGGTCTAGAAACC	
BLO259	*GPD-CAS9* R	CCTCTTCACGTGGACGCTCC	
BLO260	*CdU6p* F	TTTGCATTAGAACTAAAAACAAAGCA	
BLO261	*CdU6p* R	CAACAGTATACCCTGCCGGTG	
BLO262	sgDNA scaffold F	GTTTTAGAGCTAGAAATAGCAAG	
BLO263	sgDNA scaffold R	TAAAACAAAAAAGCACCGACTCGGTGCC	
BLO264	*Cd/CnURA5* sgDNA #1 bridging primer; closed PAM Exon3	ACCGGCAGGGTATACTGTTGATTCCGACAAGCTTC GCTTCAGGGTTTTAGAGCTAGAAATAGC	HindIII
BLO265	*Cd/CnURA5* sgDNA #2 bridging primer; closed PAM Exon2	ACCGGCAGGGTATACTGTTGAGACCGGCATTGAAG AAGTAAGGGTTTTAGAGCTAGAAATAGC	
BLO291	Short *NEO*^{R} pCR2.1 Cloning F	gggAAGCTTTGCACTGAGTGTATGGTTG	HindIII
BLO292	Short *NEO*^{R} pCR2.1 Cloning R	aaaGGATCCGGTTTATCTGTATTAACACGGAAG	BamHI
BLO293	*CnCTR4p* pCR2.1 Cloning F	aaaGGATCCGACCAATTGGATATTGCTGTTTC	BamHI
BLO294	*CnCTR4p* pCR2.1 Cloning R	aaaACTAGTCCTAGGGATTGGTGAAGTCGTTGTCG	AvrII,SpeI
BLO295	*GFP* codon opt. pCR2.1 Cloning F	cccACTAGTATGTCCAAGGGTGAGGAG	SpeI
BLO296	*GFP* codon opt. pCR2.1 Cloning R	aaaTCTAGAGAGGTCCTCCTCGGAGATG	XbaI
BLO300	*NEO*^{R} 5' *CdURA5* sg265 disruption overlap F	CTGACATGTGTTCAGTCAATCCCTTGCTGCGAGGAT GTGAG	
BLO301	*NEO*^{R} 5' *CdURA5* sg265 disruption overlap R	CTCACATCCTCGCAGCAAGGGATTGACTGAACACA TGTCAG	
BLO302	*NEO*^{R} 3' *Cd/CnURA5* sg265 disruption overlap F	GTGTTAATACAGATAAACCAAGGGCGCCTTTACTC TTCATCGCTTCTC	
BLO303	*NEO*^{R} 3' *Cd/CnURA5* sg265 disruption overlap R	GAGAAGCGATGAAGAGTAAAGGCGCCCTTGGTTTA TCTGTATTAACAC	
BLO304	5' 500bp sg265 *CdURA5* arm F	GTTGTTTCTGAAGAGGTGAGG	
BLO305	3' 563bp sg265 *Cd/CnURA5* arm R	CTTCCTGACCTCTTGCAG	
BLO306	5' 102bp sg265 *CdURA5* arm F	CATGGCGTGCTTCTTTTCG	
BLO307	3' 119bp sg265 *CdURA5* arm R	CAAGGAGATACCCTTGTAAG	
BLO311	*CnMIP1* put. MLS pCR2.1 Cloning R	gggACTAGTGCTTTGGGAAGCAGATGACGAG	SpeI
BLO312	*NEO*^{R} 5' *CdURA5* BLO264 disruption overlap F	CATGCGCATTCATGATGAGATGCTCCTTGCTGCGAG GATGTGAG	
BLO313	*NEO*^{R} 5' *CdURA5* sg264 disruption overlap R	CTCACATCCTCGCAGCAAGGAGCATCTCATCATGA ATGCGCATG	
BLO314	*NEO*^{R} 3' *CdURA5* sg264 disruption overlap F	GTGTTAATACAGATAAACCAAGGGCGGCTGCAAGA GGTCAGGAAGTAC	
BLO315	*NEO*^{R} 3' *CdURA5* sg264 disruption overlap R	GTACTTCCTGACCTCTTGCAGCCGCCCTTGGTTTAT CTGTATTAACAC	
BLO316	5' 603bp sg264 *CdURA5* arm F	CACTGTCTCTGAAGCAAGACTAGC	
BLO317	3' 623bp sg264 *CdURA5* arm R	GTTTCTCACTTGCGCCAACC	

3LO318	*CnMIP1* put. MLS pCR2.1 Cloning F	gggACTAGTATGCGCAAGGCGCTTGATATTTC	SpeI
3LO319	Stop-*CnURA5t* pCR2.1 Cloning F	aaaTCTAGATAAAGGGTTTTCTTGGATGCAG	XbaI
3LO320	*CnURA5t* pCR2.1 Cloning R	aaaTCTAGACGATTATGAAGATTGACAGCC	XbaI
3LO321	*Stop-CnCYC1t* pCR2.1 Cloning F	aaaTCTAGATAAATGTAGCATCTTTTTATGGGAC	XbaI
3LO322	*CnCYC1t* pCR2.1 Cloning R	aaaTCTAGACTGACAAGGTTGGTCCACATC	XbaI
3LO325	Short *NEO*^{R} pIBB103 Cloning F	aaaGGTACCTGCACTGAGTGTATGGTTG	KpnI
3LO326	*CnURA5t* pIBB103 Cloning R	aaaGGTACCCGATTATGAAGATTGACAGCC	KpnI
3LO327	*CnCYC1t* pIBB103 Cloning R	aaaGGTACCCTGACAAGGTTGGTCCACATC	KpnI
3LO328	*Cd/CnURA5* sgDNA #4 bridging primer; open PAM Exon2	ACCGGCAGGGTATACTGTTGAGACCGGCATTGAAG AAGTAGTTTTAGAGCTAGAAATAGC	
3LO329	*Cd/CnURA5* sgDNA #5 bridging primer; open PAM Exon1	ACCGGCAGGGTATACTGTTGACTTTACCTTGAAGTC CGGCGTTTTAGAGCTAGAAATAGC	
3LO330	*Cd/CnURA5* sgDNA #6 bridging primer; open PAM Exon2	ACCGGCAGGGTATACTGTTGTCCCCTTACTTCTTCAAT GCGTTTTAGAGCTAGAAATAGC	
3LO331	*CdURA5* Excision 5' 525bp arm F	GTTGCGAGAGCTAGCGCATC	
3LO332	*CdURA5* Excision 5' *NEO*^{R}-arm overlap F	GATCTTGTCGACAACGGCGACAAGCTTTGCACTGAGT GTATGG	
3LO333	*CdURA5* Excision 5' *NEO*^{R}-arm overlap R	CCATACACTCAGTGCAAAGCTTGTCGCCGTTGTCGAC AAGATC	
3LO334	*CdURA5* Excision 3' 502bp arm R	GACTACCCGCTCTACGTGTC	
3LO335	*CdURA5* Excision 3' pCR2.1-arm overlap F	TCTAGAGGGCCCAATTCGCCGGTCTAGCTAATCAAGT TCCGAC	
3LO336	*CdURA5* Excision 3' pCR2.1-arm overlap R	GTCGGAACTTGATTAGCTAGACCGGCGAATTGGGCCC TCTAGA	
3LO337	3' 1.106kb *CdMIP1p* excision homology arm pCR2.1 Cloning F	gggACTAGTATGCGCAAGGCGCTCGATA	SpeI
3LO338	3' 1.106kb *CdMIP1p* excision homology arm pCR2.1 Cloning R	aaaTCTAGACTGAAAGATGACAGGAGATAACCAG	XbaI
3LO339	5' 726bp *CdMIP1p* excision homology arm F	CAACGGCGTCGTTAAGATGA	
3LO340	5' *CdMIP1p* Arm-NEO Overlap F	GATTGGCCTGATTAATTGCATGAAGCTTTGCACTGAG TGTATGG	HindIII
3LO341	5' *CdMIP1p* Arm-NEO Overlap R	CCATACACTCAGTGCAAAGCTTCATGCAATTAATCAG GCCAATC	HindIII
3LO342	*CdMIP1p* sgDNA #1 bridging primer; ATG -50bp cut	ACCGGCAGGGTATACTGTTGTGAGTCGAAATGAATGA TATGTTTTAGAGCTAGAAATAGC	
3LO343	*CdMIP1p* sgDNA #2 bridging primer; ATG -68bp cut	ACCGGCAGGGTATACTGTTGATATCGGGGAACGATGA ATAGTTTTAGAGCTAGAAATAGC	
3LO344	*CdMIP1p* sgDNA #3 bridging primer; ATG -25bp cut	ACCGGCAGGGTATACTGTTGCATACTGGCTTGTGTTC CGCGTTTTAGAGCTAGAAATAGC	
3LO345	*CdMIP1 3' Exon3 R*	TCAGTTGCGGGTGTCCAGTC	

2. *Plasmids used in project:*

Name:	Description	Markers	Source
pCR2.1 TOPO	Vector for *NEO*^{R}-*CTR4p*-GFP cassettes; 3.9kb plasmid. Labeled as IBB202.	Amp, Kan	ThermoFisher
pXL1-HYG-CAS9	Gene storage with GDP-CAS9 construct. Labeled as IBB320.	Amp	UGA
pYF515	Gene storage for sgDNA scaffold construct. Labeled as IBB319.	Amp	UGA
pIBB207	Telomeric vector for *NEO*^{R}-*CTR4p*-GFP cassettes; 8.5kb CnMIP1 RNAi construct assembled for Boggs thesis.		Bose lab
pIBB236	Gene storage with cryptococcal *CnCTR4p* fragments.	Amp	Bose lab
pIBB269	Cryptococcal *NEO*^{R} positive transformation control. Also can be used as template for *NEO*^{R}.	Amp	Bose lab
pIBB314	Gene storage with cryptococcal *NEO*^{R} *and GFPcodop*.	Amp	Bose lab
pIBB326	Gene storage for *NEO*^{R}-*CTR4p*-GFP-nostop cassette.	Amp, Kan.	This work
pIBB327	Gene storage for *NEO*^{R}-*CTR4p*-MLS-GFP-nostop cassette.	Amp, Kan.	This work
pIBB328	Gene storage for *NEO*^{R}-*CnCTR4p*-MLS-GFP-*CnURA5t* cassette.	Amp, Kan.	This work
pIBB329	Gene storage for *NEO*^{R}-*CnCTR4p*-MLS-GFP-*CnCYC1t* cassette.	Amp, Kan.	This work
pIBB331	Gene storage for *NEO*^{R}-*CnCTR4p*-GFP-*CnURA5t* cassette.	Amp, Kan.	This work
pIBB332	Gene storage for *NEO*^{R}-*CnCTR4p*-GFP-*CnCYC1t* cassette.	Amp, Kan.	This work
pIBB333	Gene storage for *NEO*^{R}-*CnCTR4p –CdMIP1* 1.105kb Nterm cassette, SAP Colony #1	Amp, Kan.	This work
pIBB334	Gene storage for *NEO*^{R}-*CnCTR4p –CdMIP1* 1.105kb Nterm cassette, SAP Colony #2	Amp, Kan.	This work
pIBB335	Telomeric pIBB207 gene storage with *NEO*^{R}-*CnCTR4p*-GFP-*CnURA5t* cassette.	Amp.	This work
pIBB336	Telomeric pIBB207 gene storage with *NEO*^{R}-*CnCTR4p* -GFP-*CnCYC1t* cassette.	Amp.	This work
pIBB337	Telomeric pIBB207 gene storage with *NEO*^{R}-*CnCTR4p*-MLS -GFP-*CnURA5t* cassette.	Amp.	This work
pIBB338	Telomeric pIBB207 gene storage with *NEO*^{R}-*CnCTR4p*-X -GFP-*CnCYC1t* cassette.	Amp.	This work

3. *Alignment Data:*

```
Similarity : 344/386 (89.12 %)

Seq_1   1     tttgcattagaactaaaaacaaagcatgattattacagttcatttatttttttaaattgat  60
                                                 || |||||||||  |||||||
Seq_2   1     ---------------------------------------TC-TTTATTTTT--AATTGAT  18

Seq_1   61    cggcatgcatgcaaagtatacgtgcaaggacaatggtaacctgcaggtgtgaccgataat  120
              ||||||||||||||||||||||||||||||||||||||||||||||||||||||||||||
Seq_2   19    CGGCATGCATGCAAAGTATACGTGCAAGGACAATGGTAACCTGCAGGTGTGACCGATAAT  78

Seq_1   121   tataaccatttgttgagaatgaagaggtgaggagaaaaacaatggatgacgggaaaaaaa  180
              ||||||||||||||||||||||||||||||||||||||||||||||||||||||||||||
Seq_2   79    TATAACCATTTGTTGAGAATGAAGAGGTGAGGAGAAAAACAATGGATGACGGGAAAAAAA  138

Seq_1   181   taaaaaaacactgagacggcgtggaccgccgtcttatttgcttccgttatccgccaaagt  240
              ||||||||||||||||||||||||||||||||||||||||||||||||||||||||||||
Seq_2   139   TAAAAAAACACTGAGACGGCGTGGACCGCCGTCTTATTTGCTTCCGTTATCCGCCAAAGT  198

Seq_1   241   ggaaattgcacatacaccggcagggtatactgttgAGACCGGCATTGAAGAAGTAAGGgt  300
              ||||||||||||||||||||||||||||||||||||||||||||||||||||||||||||
Seq_2   199   GGAAATTGCACATACACCGGCAGGGTATACTGTTGAGACCGGCATTGAAGAAGTAAGGGT  258

Seq_1   301   tttagagctagaaatagcaagttaaaataaggctagtccgttatcaacttgaaaaagtgg  360
              ||||||||||||||||||||||||||||||||||||||||||||||||||||||||||||
Seq_2   259   TTTAGAGCTAGAAATAGCAAGTTAAAATAAGGCTAGTCCGTTATCAACTTGAAAAAGTGG  318

Seq_1   361   caccgagtcggtgctttttgtttta-  386
              |||||||||||||||||||||||||
Seq_2   319   CACCGAGTCGGTGCTTTTTTGTTTTAA  345
```

Appendix 3.A – Serial Cloner Alignment of forward primed BLO265 sgDNA sequencing reaction (Seq_2) with the BLO265 sgDNA schematic (Seq_1). Green highlighted sequence represented *U6p*, blue is the 20nt crDNA and PAM sequence, red is the tracrDNA.

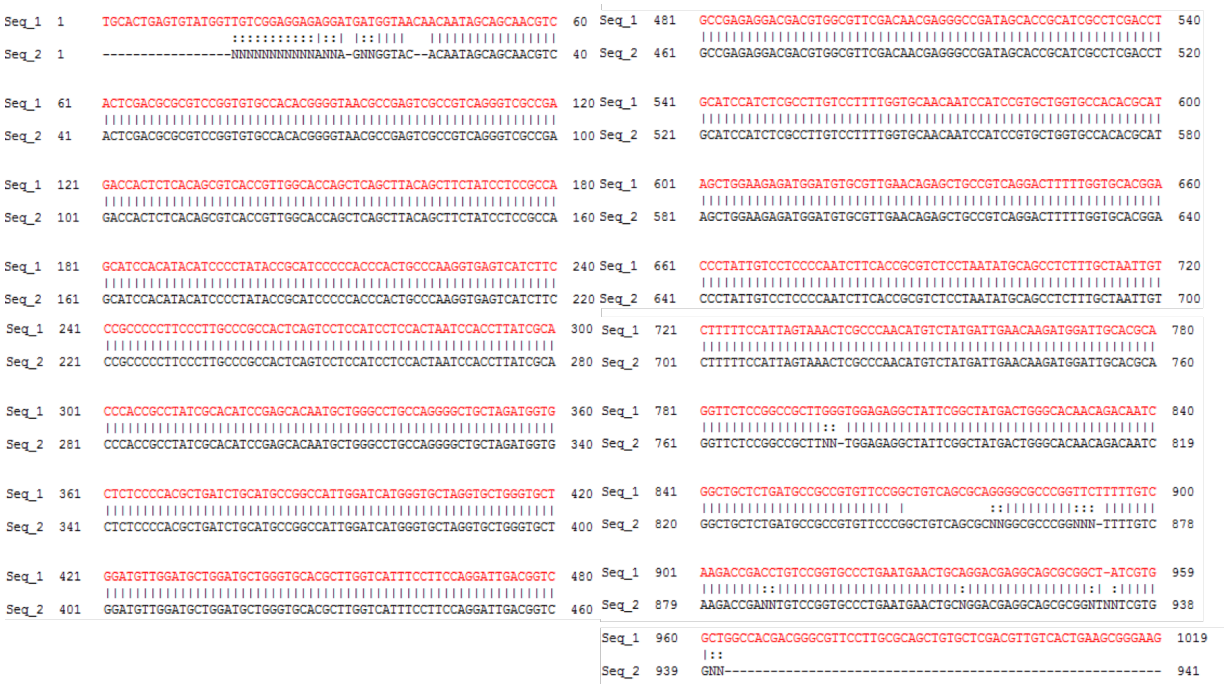

Appendix 3.b – Alignment of sequenced pIBB326 1:3 molar Colony No5 with primer BLO291. Sequence 1 (Seq_1) is the desired/designed sequence. Sequence 2 (Seq_2) is the sequenced No5 construct. 927bp alignment with 1.816kb NEO^R gene. Red sequence denotes the NEO^R gene.

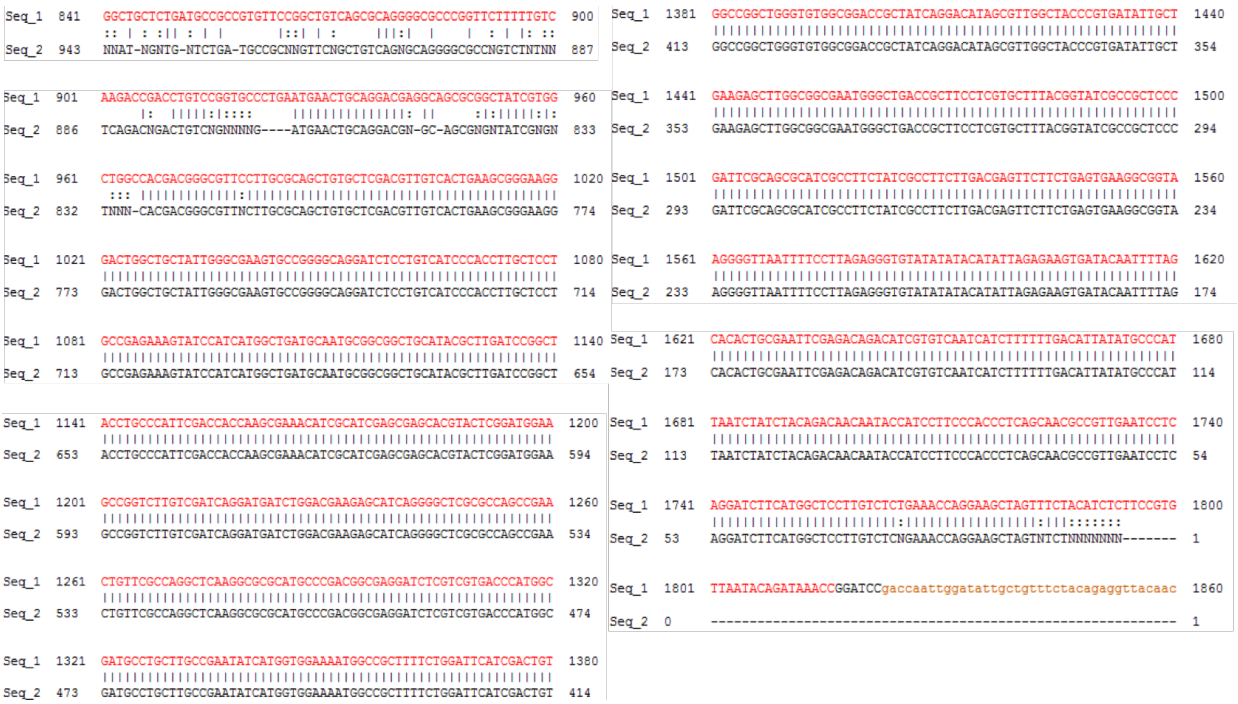

Appendix 3.c – Alignment of sequenced pIBB326 1:3 molar Colony No5 with primer BLO292. Sequence 1 (Seq_1) is the desired/designed sequence. Sequence 2 (Seq_2) is the sequenced No5 construct. 903bp alignment with 1.816kb NEO^{R} gene. Red sequence denotes the NEO^{R} gene.

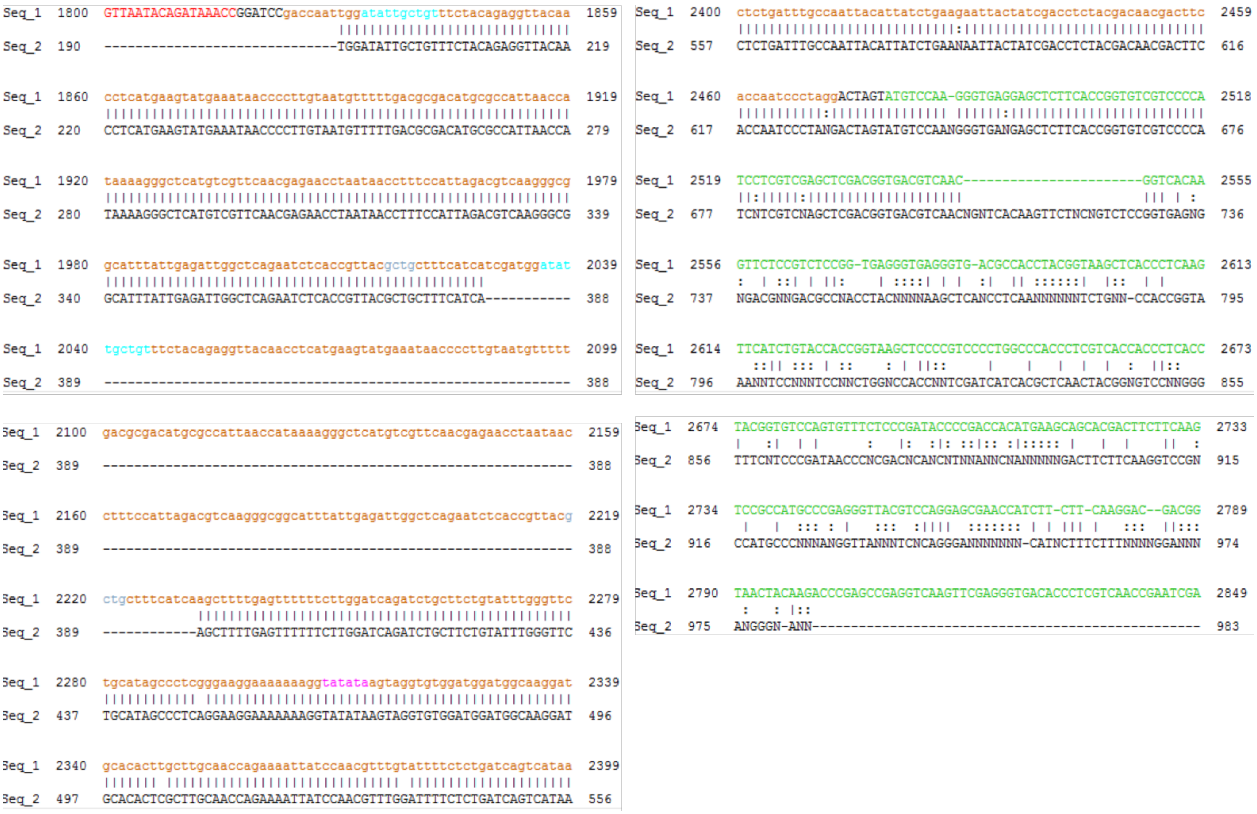

Appendix 3.d – Alignment of sequenced pIBB326 1:3 molar Colony No5 with primer BLO293. Sequence 1 (Seq_1) is the desired/designed sequence. Sequence 2 (Seq_2) is the sequenced No5 construct. 701bp alignment with cassette that spans, but misses a large part of, the 0.65kb *CTR4p* and 0.774kb GFP. Red sequence denotes the NEO^{R} gene, orange is *CTR4p*, and green is GFP. The *CTR4p* canonical TATATA box is highlighted in purple, putative Copper Sensing Elements in cyan, and GCTG metal sensing element core sequences/possible Metal Sensing Elements in light blue.

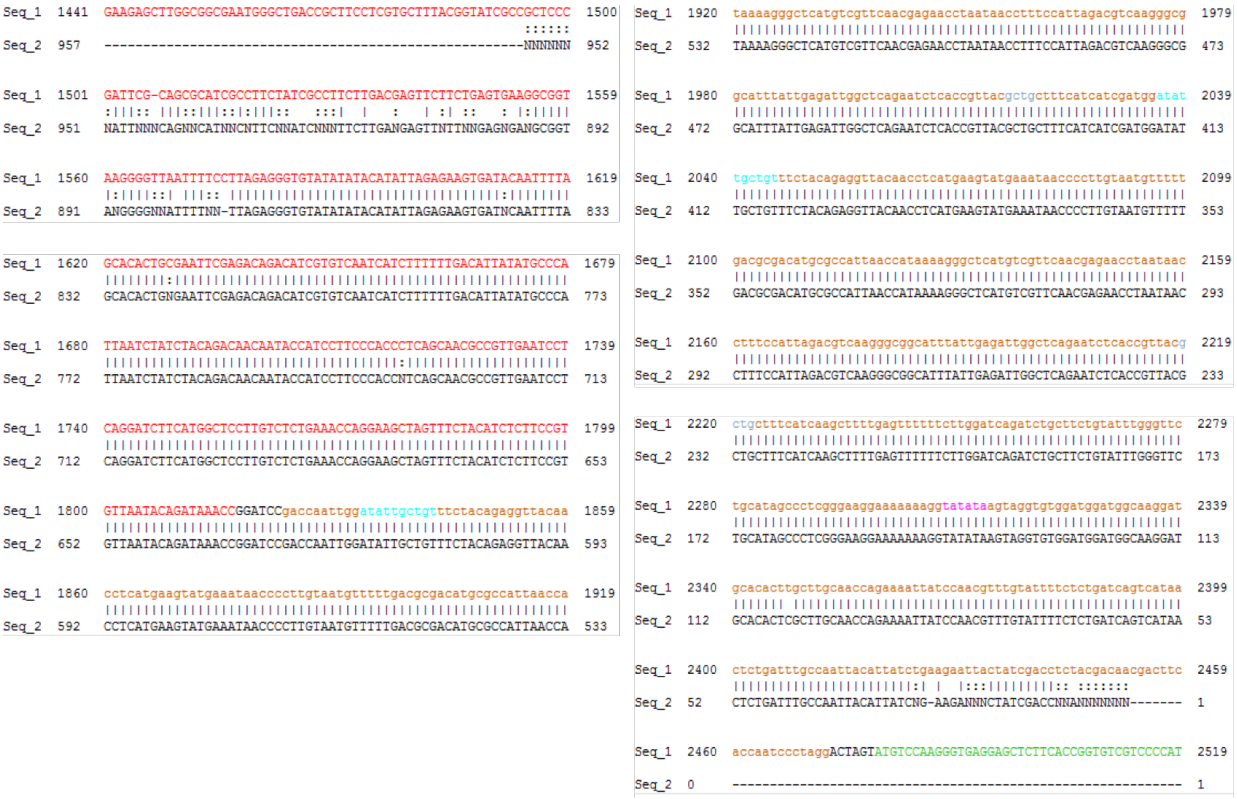

Appendix 3.e – Alignment of sequenced pIBB326 1:3 molar Colony No5 with primer BLO294. Sequence 1 (Seq_1) is the desired/designed sequence. Sequence 2 (Seq_2) is the sequenced No5 construct. 934bp alignment with cassette that spans the 0.65kb CTR4p and the 3' end of the 1.816kb NEO^{R} gene. Red sequence denotes the NEO^{R} gene, orange is *CTR4p*, and green is GFP. The *CTR4p* canonical TATATA box is highlighted in purple, putative Copper Sensing Elements in cyan, and GCTG metal sensing element core sequences/possible Metal Sensing Elements in light blue.

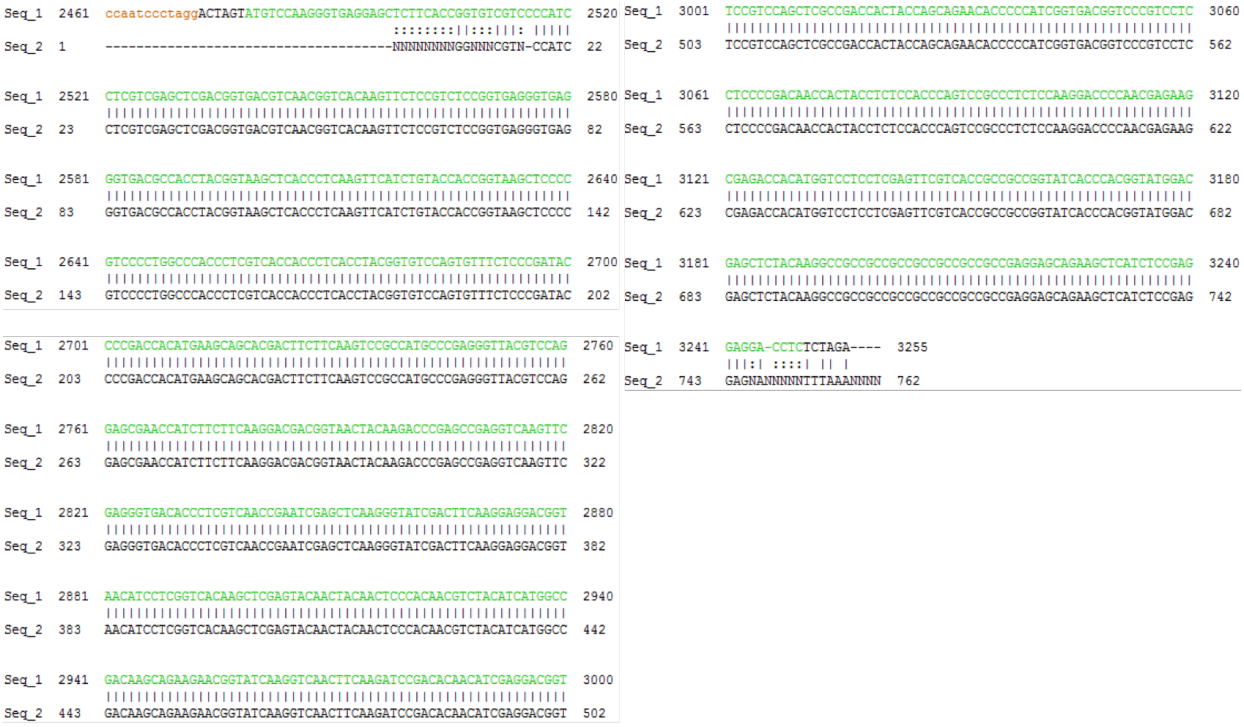

Appendix 3.f = Alignment of sequenced pIBB326 1:3 molar Colony No5 with primer BLO295. Sequence 1 (Seq_1) is the desired/designed sequence. Sequence 2 (Seq_2) is the sequenced No5 construct. Orange denotes the *CTR4p* and green is GFP.

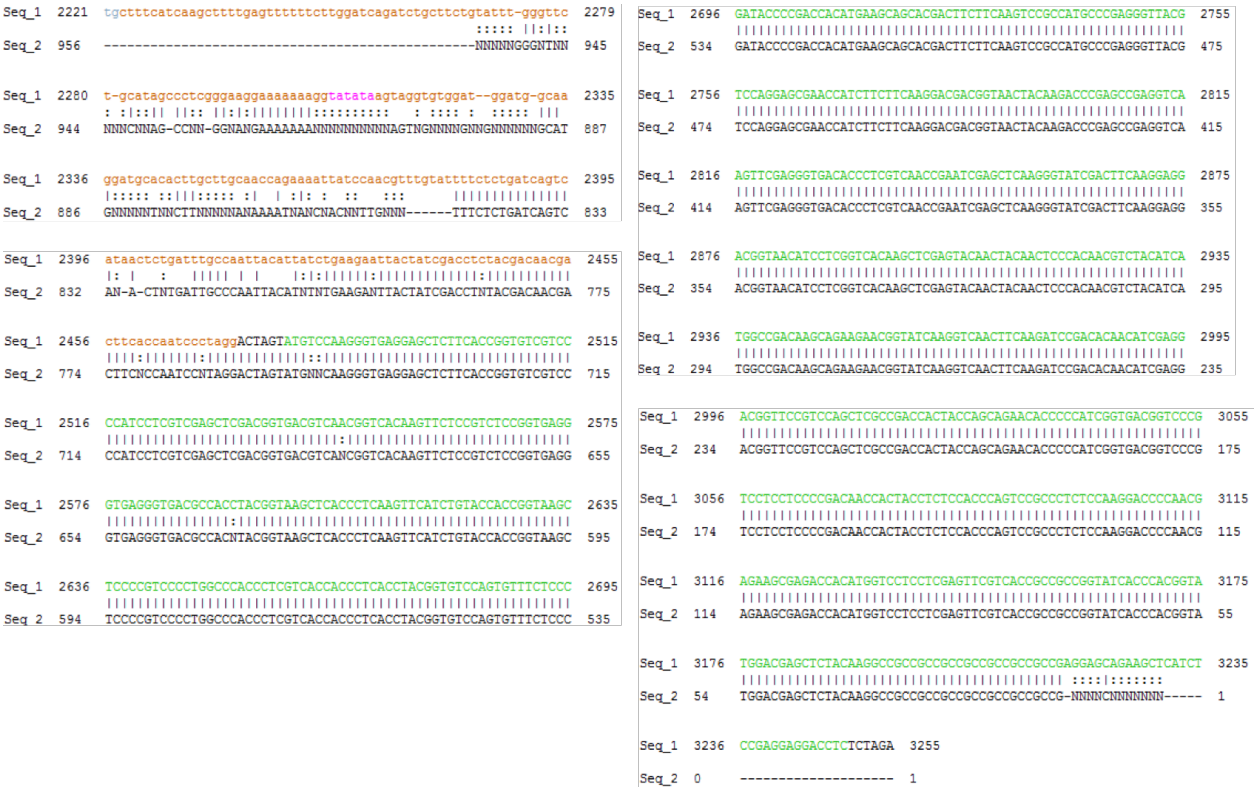

Appendix 3.g – Alignment of sequenced pIBB326 1:3 molar Colony No5 with primer BLO296. Sequence 1 (Seq_1) is the desired/designed sequence. Sequence 2 (Seq_2) is the sequenced No5 construct. Orange denotes the *CTR4p* and green is GFP. The *CTR4p* canonical TATATA box is highlighted in purple, putative Copper Sensing Elements in cyan, and GCTG metal sensing element core sequences/possible Metal Sensing Elements in light blue.

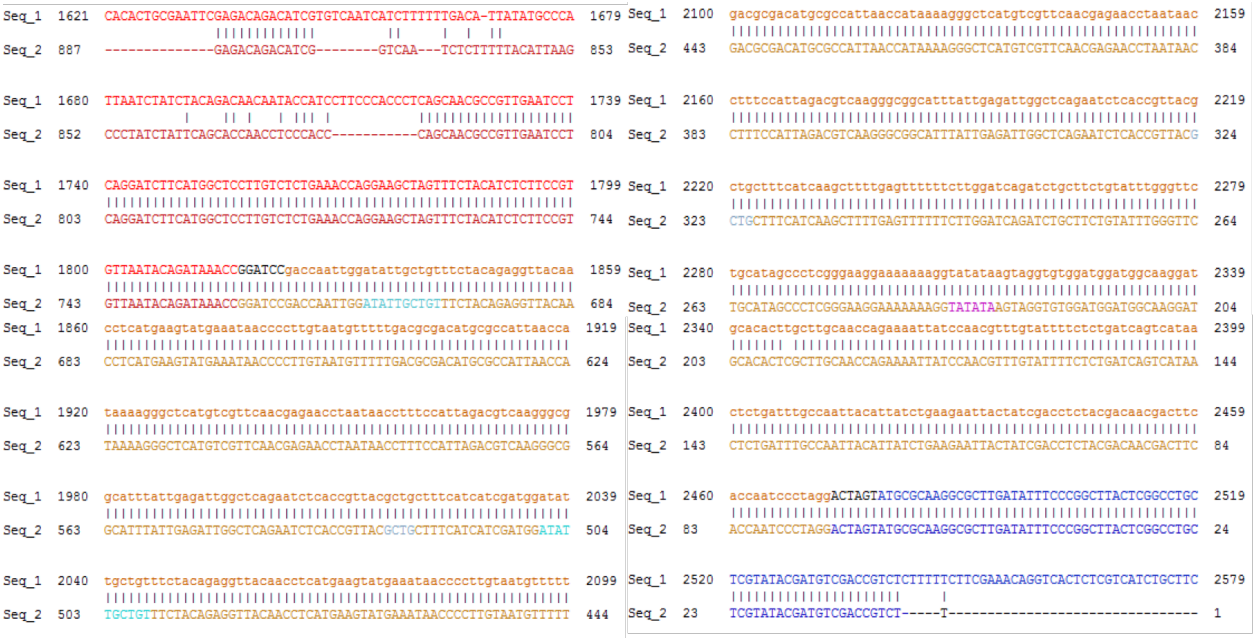

Appendix 3.h – Alignment of sequenced pIBB327 1:3 molar Colony No13 with primer BLO318. Sequence 1 (Seq_1) is the desired/designed sequence. Sequence 2 (Seq_2) is the sequenced No13 construct. Red sequence represents the 1.816kb short NEO^{R} gene, orange is the 0.65kb *CTR4p*, and blue is the 0.108kb *CnMIP1* putative MLS. The *CTR4p* canonical TATATA box is highlighted in purple, putative Copper Sensing Elements in cyan, and GCTG metal sensing element core sequences/possible Metal Sensing Elements in light blue.

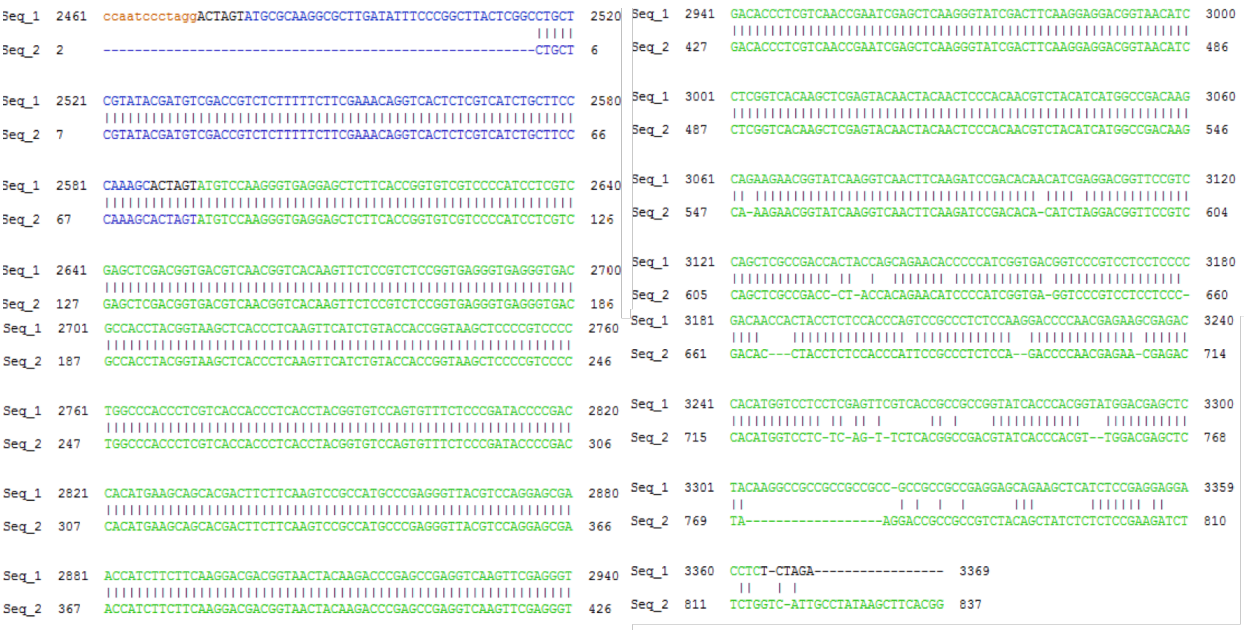

Appendix 3.i - Alignment of sequenced pIBB327 1:3 molar Colony No13 with primer BLO311. Sequence 1 (Seq_1) is the desired/designed sequence. Sequence 2 (Seq_2) is the sequenced No13 construct. Blue sequence represents is the *CnMIP1* putative MLS and green represents the GFP fragment.

Appendix 4 – *Design and assembly of telomeric cassette-terminator constructs*

The cassette constructs described in Results I lacked cryptococcal origins of replication and telomeric termini. Due to the lack of those elements, the constructs were not expected to be maintained nor confer stable phenotypes. To screen for expression improvements in the *CTR4p-GFP*-terminator constructs, all four no MLS and +MLS cassette-terminator constructs were inserted into an RNAi vector, pIBB207 as described in Methods 7. Ligation was used to synthesize four constructs where the RNAi system had been replaced with the no MLS and +MLS cassette-terminator sequences. SalI digests were used to distinguish between cytoplasmic Cassette-terminator (Fig 27A) and KpnI digest was used to show cassette insertion (Figure 27B).

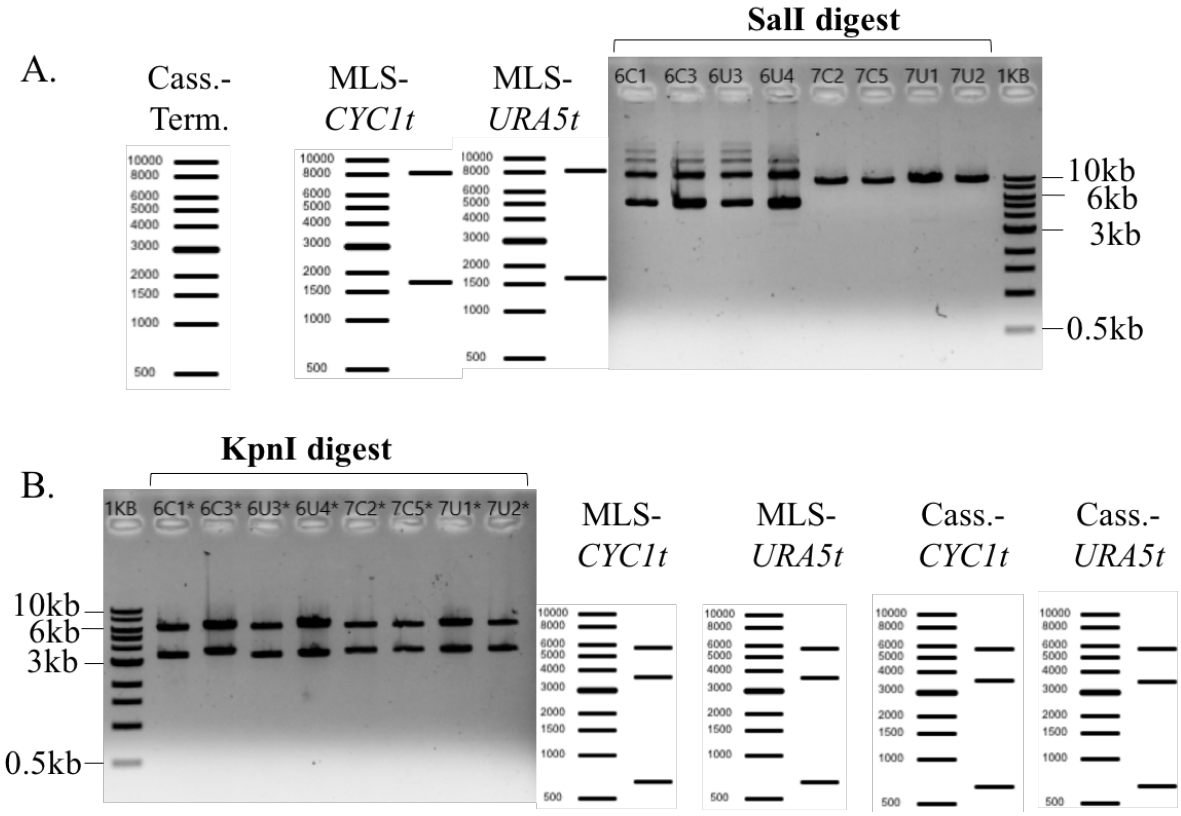

Figure 27– Digests assays of the pIBB207-cassette-terminator constructs. (A) SalI digests of pIBB207-Cassette-terminators to screen for MLS presence verses absence. 6C series are the No MLS,+*CYC1t* constructs. The 6U series are No MLS,+*URA5t*. 7C series is +MLS,+*CYC1t*. 7U series is +MLS,+*URA5t*. Visualized on 0.8% TAE-agarose ethidium bromide gel with 1kb Genewiz Quickload DNA ladder. (B)

KpnI digests of pIBB207-cassttee,+terminators to screen for MLS presence verses absence with identical conditions.

Restriction digests using HindIII were used to screen for insertion and orientation of the cassette (not shown). Confirmed constructs were saved in bacterial glycerol stocks and latter used as a reagent for fluorescent microscopy screening for *GFP* expression

Appendix 5 - *CRISPR-Cas9 targeting URA5 with NEO^R cassette; trial experiment*

As a preliminary experiment to show CRISPR-Cas9 HDR functionality in *in vivo C. deneoformans* JEC21, a 1.895kb Geneticin, AKA Neomycin (NEO), resistance construct derived from pIBB314 plasmid and inserted into the *URA5* reading frame via HDR-driven recombination.

5. a. *Design and assembly of NEO^R HDR reagents*

C. deneoformans requires extensive length of homologous sequence for recombination to occur.[16] It had been shown that 100bp was not enough to trigger recombination, there is some threshold of sequence homology below 1000bp and above 100bp where recombination is prone to occur. Accordingly, a trial with three Homology Directed Repair (HDR) templates were designed, one for sg265 with 222bp of homologous sequence, another for sg265 with 1063bp of homologous sequence (Fig 28A), and a third for sg264 with 1266bp surrounding a *NEO^R* selection marker (not shown). Amplification of the templates went ahead smoothly (Figure 28B). Final overlap assembly was quickly optimized and purified.

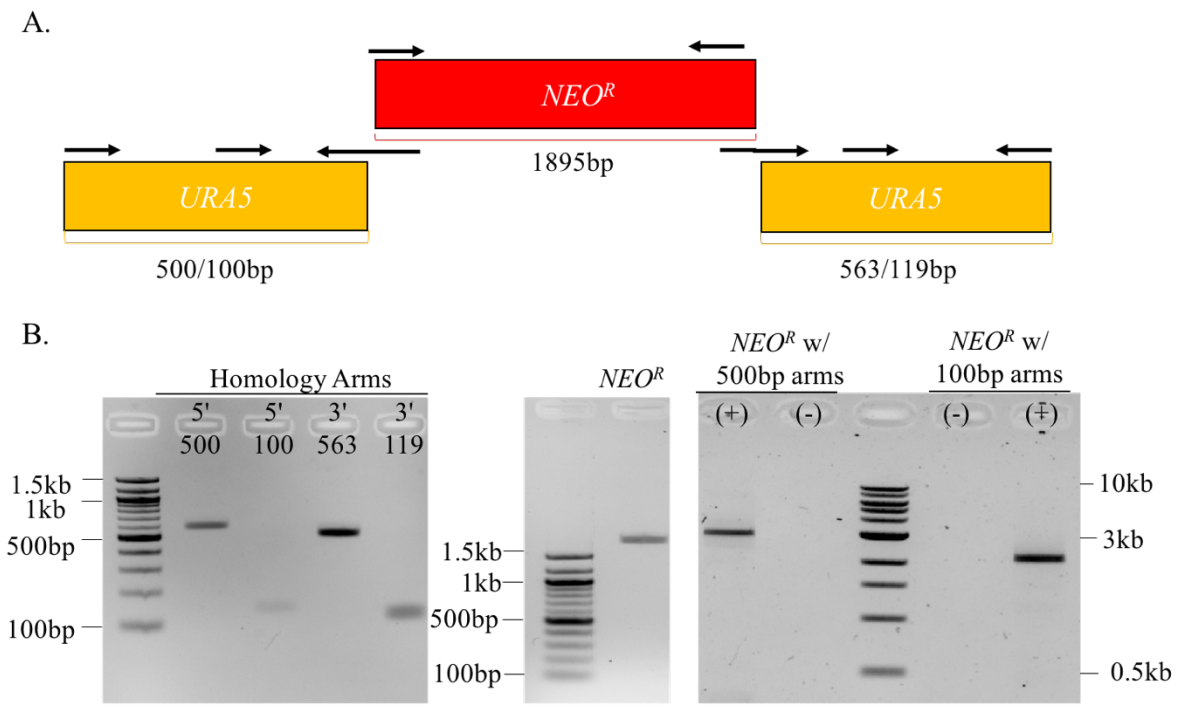

Figure 28 – *URA5* sg265 *NEO*^{R} recombination template. (A) Schematic of NEO^{R} gene with *URA5* homology arms of 103/119bp and 500/563bp. Arrows denote primers and their directionality. (B) Purified *NEO*^{R} HDR template reagents visualized on ethidium bromide agarose gels run at 100V for 30min. (Left) 0.8% gel containing 5' 500, 5' 100, 3' 563, and 3' 119bp homology arm fragments with 100bp Tridye DNA Ladder. (Center) 2% gel containing 1.895bp NEO^{R} gene visualized with 100bp Tridye DNA ladder. (Right) The 2.958kb *NEO*^{R}-500bp/563bp *URA5* flanked and 2.117kb *NEO*^{R}-100bp/163bp *URA5* armed recombination construct run on a 0.8% TAE-agarose ethidium bromide gel for 30min. 1kb NEB DNA Ladder used for visualization of size.

5. b. *HDR disruption of URA5 with CRISPR-Cas9*

When chromosomal DNA is damaged and a double-stranded break (DSB) occurs, the chromosome becomes fragmented. This fragmentation forces cells to repair the damage or risk the chromosome degrading around the break-site due to the instability of the non-telomeric ends.[55] NHEJ can rectify this in an error-prone manner; however, if a homologous allele and or sequence of sufficient homology is present, Homology Directed DNA Repair (HDR) can accurately repair the DSB and restore chromosomal integrity. The mechanism of HDR relies on strand invasion and recombination between the damaged chromosome and the homologous template, thereby allowing cellular proteins to resection and resynthesize the damage site with

high fidelity. In the case of *C. deneoformans*, there are no natural homologous templates for HDR. Synthetic templates can be assembled *in vitro* be transform *in vivo* to induce HDR. The aforementioned templates can contain inserts that the cell will 'repair' into the chromosome, allowing for gene insertion via this pathway. This allows for selection and expression markers to be chromosomally inserted, producing a stable transformed line.

Preliminary NHEJ screening proved to be problematic (not shown); hence, disruption of *URA5* using HDR was used to test CRISPR-Cas9 effectiveness by inducing dual NEO^R and 5-FOA^R phenotypes. This insertion disrupts the *URA5* reading frame, disrupting the uracil synthesis pathway while simultaneously installing a chromosomal NEO^R selection marker. Two *URA5* disruption HDR repair templates were made for specific use with the sg265 and sg264; the sg265 HDR system was the only that reliably gave dual resistance phenotypes, hence the sg264 fell into disuse after one electroporation.

5 separate electroporations were attempted using the preliminary sg265 HDR system in *C. deneoformans* JEC21. Over those electroporations, geneticin resistance was reliably conferred to transformants while transformants plated on 5-FOA after the initial recovery period seemingly were background mutants (Figure 29 and Table 6.).

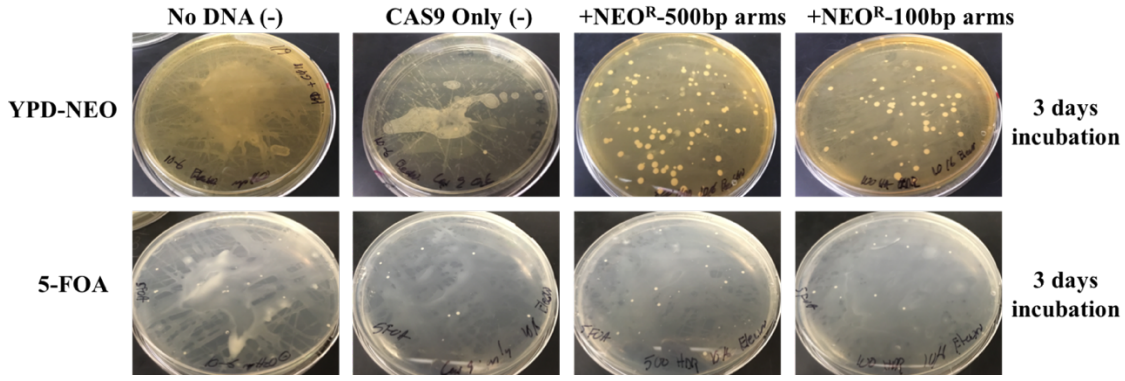

Figure 29 – YPD-NEO and 5-FOA plates inoculated with JEC21 transformed with sgDNA, *CAS9*, and *NEO*^{R} recombination constructs. Plates were inoculated with recovery that was halved to inoculate each plate. 30°C incubation used afterwards.

Over the course of all sg265 CRISPR-Cas9 *URA5* disruption HDR electroporations, 215 transformant colonies were screened for dual resistance to NEO and 5-FOA. 112 of the 215 had been transformed with the 500/563bp armed *NEO*^{R} construct and 103 were transformed with the 100/119bp armed *NEO*^{R} construct. See Table 7 for the breakdowns of the assays. None of the colonies initially plated on 5-FOA had NEO resistance. 96 of the 215 colonies initially plated on YPD-G418 exhibited dual resistance.

Table 6– Growth and phenotypes of the sg264 and 265 *NEO*^{R} repair template electroporations. 100, 500, and 600bp arms denotes the length of homologous flanks surrounding the *NEO*^{R} gene used during in the electroporation.

Cassette	sgDNA	Total Assayed	NEO^R	5-FOA^R	Dual Resistant
NEO^R w/ 500bp arms	sg265	112	112	56	50%
NEO^R w/ 600bp arms	sg264	103	103	3	2.91%
NEO^R w/ 100bp arms	sg265	103	103	40	38.9%

A single electroporation with the sg264 HDR system produced an over-abundance of NEO^R phenotype colonies but similarly poor initial 5-FOA colony totals. 103 colonies from the sg264 HDR YPD-NEO plate were restreaked to assay for dual resistance; of those 103, only three were dual resistant (Not shown).

Genomic samples from dual phenotype colonies derived from each electroporation were subjected to a PCR using primers that amplified the entire *URA5* sequence alongside the NEO^R repair template. Of the 96 sg265 dual resistance colonies, 56 were subjected to genomic extraction and PCR screening. 35 gave expected *URA5* bands while 18 gave negative amplifications. Two elevated *URA5* amplicon sizes were found, another was abnormal but not elevated (Fig 30B), making for two putative recombinations using the preliminary HDR system (Table 7).

Table 7 – Genotypes for *URA5* when using sg265. 500bp and 100bp denotes the lengths of the homologous flanks attached to the NEO^R gene used during in the electroporation.

Construct	Total Assayed	No Recombination	Abnormal Recombination	Faithful Recombination	%
NEO^R/500bp	38	26	1	1	2.63%
NEO^R/100bp	18	9	1	0	0%

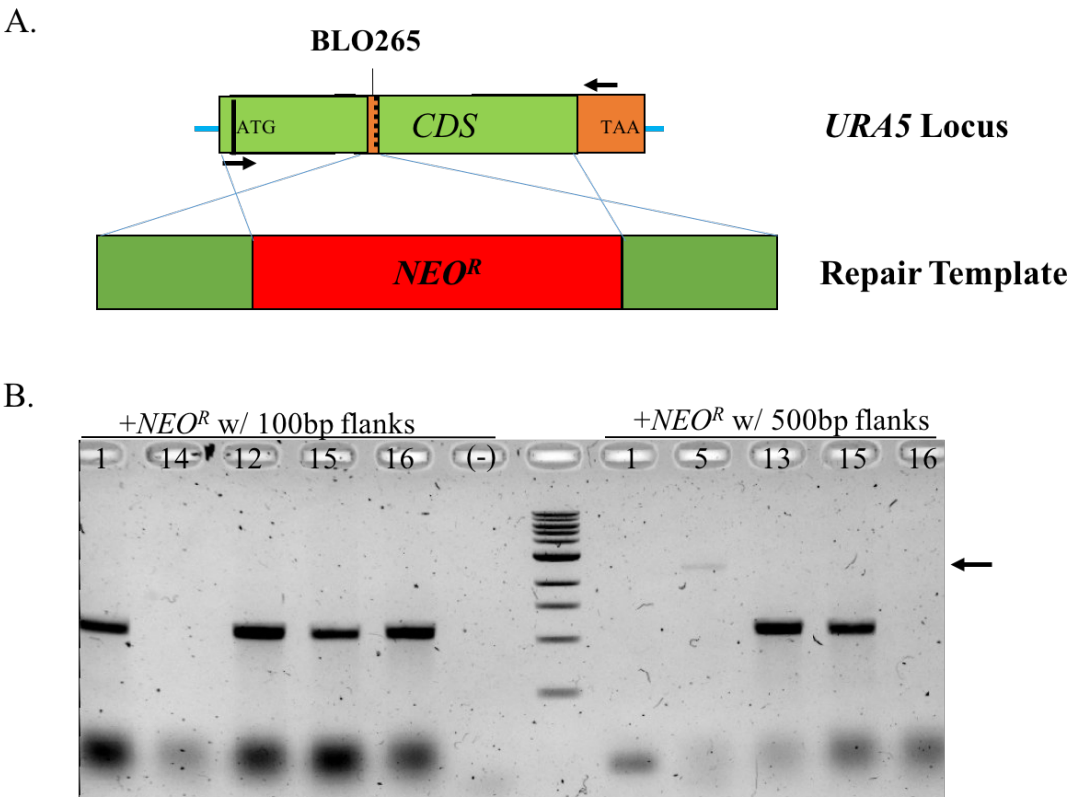

Figure 30 – Loci screening of transformant *URA5*. (A.) Schematic for *NEO*^{R} recombination with the *URA5* CDS. Arrows denote the BLO304 and 306 primers used for screening. (B.) 0.8% TAE-agarose ethidium bromide gels showing amplicon sizes for *URA5*. Arrow denotes sample with elevated *URA5* size suggesting faithful recombination. All samples were run at 100V for 30min. Sizes visualized with 1kb NEB DNA Ladder.

Two of the three dual resistant colonies sampled from the sg264 HDR system genomes sampled and screened for *NEO*^{R} insertion into the *URA5* reading frame. One yielded a negative insertion and the other did not amplify (Not shown).

The sole recombinant strain produced from the sg265 *URA5* disruption experiments was saved in a glycerol stock. Optimization of the CRISPR-Cas9 system was conducted and the reading frame disruption via HDR experiments were not continued.

Appendix 6 – *Fluorescent microscopy of transformed C. deneoformans*

Fluorescent protein fusions allow for visual tracking of targeted protein expression in *Cryptococcus in vivo* via fluorescent microscopy.[57] Accordingly, the episomal transformation and chromosomal insertion of a *Cryptococcus* codon-optimized GFP gene with a terminator and copper-repressible promoter should theoretically allow for *GFP* expression and visualization.

6. a. *Screening for episomal GFP expression*

The *GFP* coding sequence contained in the vectors assembled in Results I. C was complemented with a conditional promoter and two terminators. The promoter specifically was a copper-repressible *CTR4* promoter. The terminators were the KN99 *CnURA5* terminator (*URA5t*) and the KN99 *CnCYC1* terminator (*CYC1t*), of which were added just 3' to the reading frame along with a TAA stop codon. Altogether, these modifications made a complete GFP gene recognizable by cryptococcal transcription and translation machinery. Electroporation was used to transform *C. deneoformans* JEC21 with ScaI-linearized constructs. The vectors lacked replication origin sites and contained no telomeric sequences. This meant that the constructs were not expected to produce stable lines capable of long-term NEO^R or GFP-expression. A fluorescent signal assay of 12 colonies total, 6 from the no MLS,+*URA5t* cassette and no MLS,+*CYC1t* cassette transformations was done. The *URA5t* variants gave no detectable signal at low power and were not screened further. *CYC1t* constructs were screened at higher power with 60x oil immersion for episomal GFP expression (Fig 31).

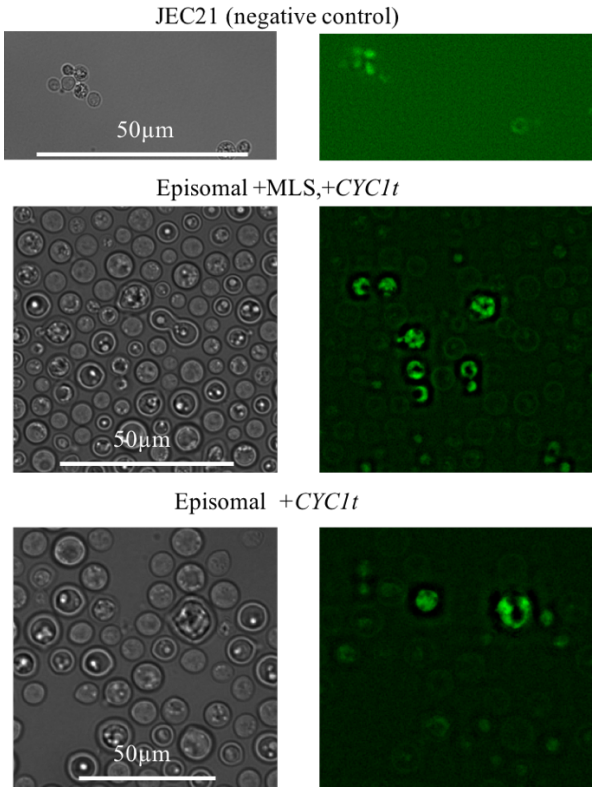

Figure 31 – Episomal GFP screening of *C. deneoformans* transformed with +*CYC1t* constructs at 60x power under oil immersion; deconvolved using FIJI Iterative Deconvolve. (Top) Shows JEC21 negative control. (Middle) Shows +MLS,+*CYC1t*. (Bottom) Shows no MLS,+*CYC1t*. Left images are brightfield; right images are GFP.

6. b. *Screening for chromosomal GFP expression*

With what was thought to be promising data found in transformants with the +*CYC1t* constructs, CRISPR-Cas9 was used insert the +*CYC1t* and +MLS,+*CYC1t* cassettes into the JEC21 genome as was seen in II B. Chromosomal insertion conferred replicative origins, meaning the GFP gene was actively being maintained *in vivo* while also being in a linear sequence with telomeric termini. Phenotype stability was demonstrated, giving evidence for chromosomal recombination. PCR was additionally used to show successful recombination. Samples with confirmed chromosomal insertions were used to screen for *GFP* expression using conditions described in Methods and Materials 15. b. No meaningful signal was found and results were similar to those in Fig 31.

in repressive condition (not shown).

6. c. *Screening for episomal telomeric GFP.*

Data from F.II suggested instability in *GFP* expression using the pCR2.1-cassette-terminator constructs. To attempt to improve episomal, non-maintained stability of transformed constructs, the +MLS,+*URA5t/CYC1t* and no MLS,+*URA5t*/*CYC1t* cassettes were inserted into a construct containing telomeric repeat regions. Linearization produced a construct with telomeric termini but no replicative origins; the construct was transformed using electroporation and screened for episomal GFP expression using conditions specified in Methods and Materials 15 (Fig. 32).

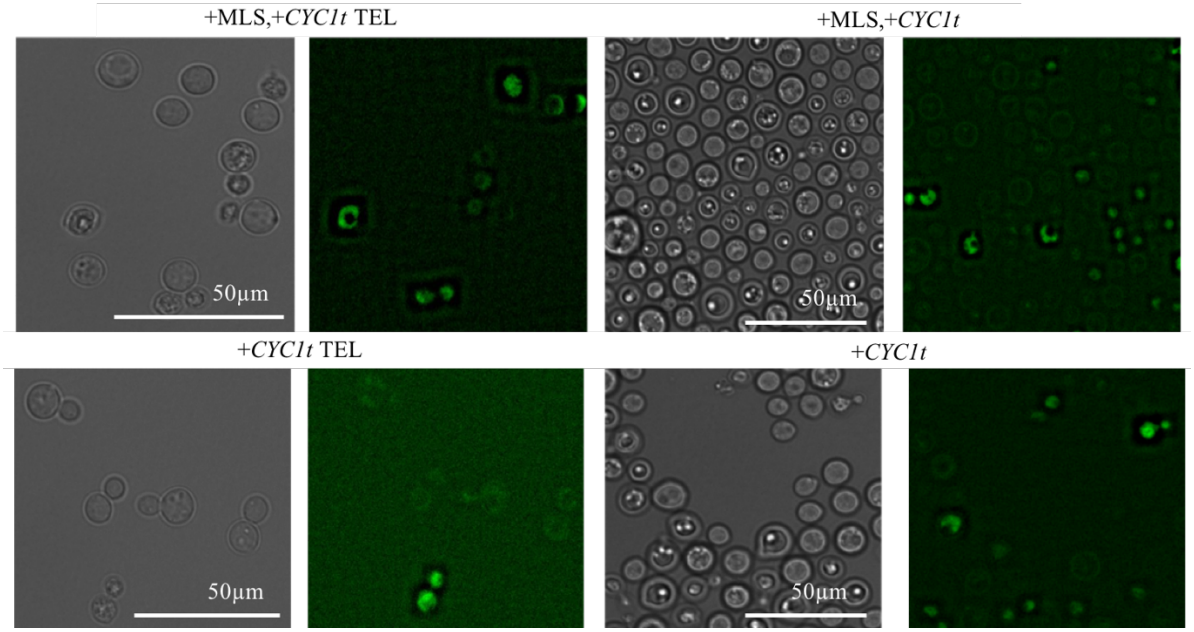

Figure 32 – Episomal GFP in *C. deneoformans* with telomeric construct at 60X power using oil immersion; deconvolved using FIJI Iterative Deconvolve. (Top Left) Shows +MLS,+*CYC1t* cassette in telomeric construct. (Top Right) Shows same construct but in pCR2.1. (Bottom Left) Shows the no MLS,+*CYC1t* in telomeric construct. (Bottom Right) Shows no same construct in pCR2.1. Left images are brightfield; right images are GFP.